เซ็นเซอร์ที่มีเคอร์คูมินโบรอนไดฟลูออไรด์เป็นโครงสร้างพื้นฐาน สำหรับตรวจวัดไซยาไนด์ด้วยตาเปล่า

นายอนุศักดิ์ ไชยแจ่ม

วิทยานิพนธ์นี้เป็นส่วนหนึ่งของการศึกษาตามหลักสูตรปริญญามหาบัณฑิต
สาขาวิชาเคมี ภาควิชาเคมี
คณะวิทยาศาสตร์ จุฬาลงกรณ์มหาวิทยาลัย
ปีการศึกษา 2552

SENSORS BASED ON CURCUMIN BORONDIFLUORIDE FOR NAKED-EYE DETECTION OF CYANIDE

Mr. Anusak Chaicham

A Thesis Submitted in Partial Fulfillment of the Requirements
for the Degree of Master of Science Program in Chemistry

Department of Chemistry

Faculty of Science

Chulalongkorn University

Academic Year 2009

Thesis Title	SENSORS BASED ON CURCUMIN BORONDIFLUORIDE FOR NAKED-EYE DETECTION OF CYANIDE
By	Anusak Chaicham
Field of Study	Chemistry
Thesis Advisor	Assistant Professor Boosayarat Tomapatanaget, Ph.D.
Thesis Co-Advisor	Gamolwan Tumcharern, Ph. D.

Accepted by the Faculty of Science, Chulalongkorn University in Partial Fulfillment of the Requirements for the Master's Degree

S. Hannongbua ..... Dean of the Faculty of Science

(Professor Supot Hannongbua, Ph.D.)

THESIS COMMITTEE

Warinthorn Chavasiri ..... Chairman

(Assistant Professor Warinthorn Chavasiri, Ph.D.)

B. Tomapatanaget ..... Thesis Advisor

(Assistant Professor Boosayarat Tomapatanaget, Ph.D.)

Gamolwan Tumcharern ..... Thesis Co-Advisor

(Gamolwan Tumcharern, Ph.D.)

..... Examiner

(Associate Professor Thawatchai Tuntulani, Ph.D.)

Boon-ek Yingyongnarongkul ..... External Examiner

(Assistant Professor Boon-ek Yingyongnarongkul, Ph.D.)

อนุศักดิ์ ไชยแจ่ม : เซ็นเซอร์ที่มีเคอร์คูมินโบรอนไดฟลูออไรด์เป็นโครงสร้างพื้นฐานสำหรับตรวจวัดไซยาไนด์ด้วยตาเปล่า. (SENSORS BASED ON CURCUMIN BORONDIFLUORIDE FOR NAKED-EYE DETECTION OF CYANIDE) อ. ที่ปรึกษาวิทยานิพนธ์หลัก : ผศ. ดร. บุษยรัตน์ ธรรมพัฒนกิจ , อ. ที่ปรึกษาวิทยานิพนธ์ร่วม: ดร. กมลวรรณ ธรรมเจริญ, 100 หน้า.

ได้สังเคราะห์อนุพันธ์ของเคอร์คูมินโบรอนไดฟลูออไรด์ (**BF_2-CurOH**, **BF_2-CurOMe**, **BF2-CurmonoTs** และ **BF_2-CurdiTs**) และศึกษาสมบัติเชิงแสงของสารประกอบ พบว่าถ้าโมเลกุลประกอบด้วยหมู่ให้อิเล็กตรอนที่วงอะโรมาติกของโมเลกุลจะทำให้การดูดกลืนแสงและการคายแสงเปลี่ยนไปทางความยาวคลื่นมากขึ้น ในทางตรงกันข้ามถ้ามีหมู่ดึงอิเล็กตรอนที่วงอะโรมาติกของโมเลกุล จะทำให้การดูดกลืนแสงและการคายแสงเปลี่ยนไปทางความยาวคลื่นลดลงจากการศึกษาความสามารถในการเรืองแสงของสารประกอบที่สังเคราะห์ขึ้นในตัวทำละลายไดคลอโรมีเทนเป็น 0.62, 0.61, 0.22 และ 0.48 ตามลำดับ ที่น่าสนใจคือ สารประกอบ **BF_2-CurOH** และ **BF_2-CurOMe** มีการเปลี่ยนแปลงคุณสมบัติเชิงแสงในตัวทำละลายต่างชนิดกัน จึงได้ศึกษาอิทธิพลของตัวทำละลายต่อคุณสมบัติของแสงโดยใช้ความ สัมพันธ์ของ คามเลท-ทาฟท์ (Kamlet-Taft) พบว่า ค่าการดูดกลืนแสงและการคายแสงของสาร จะเปลี่ยนไปทางความยาวคลื่นเพิ่มขึ้นเมื่อความเป็นขั้วของตัวทำละลายเพิ่มขึ้นนอก จากนี้ได้ศึกษาการตรวจวัดไซยาไนด์ของสาร **BF_2-CurOH** และ **curcumin** พบว่า **BF_2-CurOH** มีความว่องไวและความจำเพาะเจาะจงกับไซยาไนด์มากกว่า **curcumin** โดยผ่านกระบวนการดึงโปรตรอนของหมู่ไฮดรอกซิลทำให้เกิดประจุลบเกิดขึ้นบนโมเลกุลแล้วเกิดการเคลื่อนที่ของประจุลบผ่านพันธะไพ-คอนจูเกต ส่งผลให้เกิดกระบวนการ ICT ความสามารถในการดึงโปรตรอนของสารประกอบทั้งสองโดยศึกษาด้วยเทคนิคยูวี-วิสิเบิลไทเทรชั่น และฟลูออเรสเซนต์ไทเทรชั่น จะได้ค่า log β เท่ากับ 8.8 และ 7.7 สำหรับโมเลกุล **BF_2-CurOH** และเคอร์คูมินตามลำดับ นอกจากนี้ยังได้ศึกษาถึงอิทธิพลของแอนไอออนชนิดต่าง ๆ ที่มีผลต่อการตรวจวัดไซยาไนด์ของสารประกอบทั้งสองพบว่าในสารประกอบ **BF_2-CurOH** แอนไอออนเกือบทุกชนิดไม่มีผลต่อการตรวจวัดไซยาไนด์ แต่ในสารประกอบ **curcumin** พบว่าแอนไอออนทุกชนิดมีผลต่อการตวจวัดไซยาไนด์ นอกจากนี้พบว่าสารประกอบ **curcumin** และ **BF_2-CurOH** สามารถใช้ตรวจวัดปริมาณของไซยาไนด์ได้ที่ความเข้มข้นต่ำที่สุดคือ 9.33 และ 0.14 ไมโครโมลาร์ ตามลำดับ

ภาควิชา .....เคมี.....	ลายมือชื่อนิสิต ...อนุศักดิ์ ไชยแจ่ม.....
สาขาวิชา .....เคมี.....	ลายมือชื่อ อ.ที่ปรึกษาวิทยานิพนธ์หลัก.....บุษยรัตน์ ธรรมพัฒนกิจ.....
ปีการศึกษา ....2552.....	ลายมือชื่อ อ.ที่ปรึกษาวิทยานิพนธ์ร่วม .....กมลวรรณ ธรรมเจริญ.....

4972561523 : MAJOR CHEMISTRY
KEYWORDS : SOVATOCHROMISM / FLUOROIONOPHORE / QUENCHING / ENHANCEMENT

ANUSAK CHAICHAM : SENSORS BASED ON CURCUMIN BORONDIFLUORIDE FOR NAKED-EYE DETECTION OF CYANIDE. THESIS ADVISOR : ASST. PROF. BOOSAYARAT TOMAPATANAGET, Ph.D., THESIS CO-ADVISOR: PROF. GAMOLWAN TUMCHARERN, PH.D., 100 pp.

Novel **curcumin** derivatives containing BF_2-incorporated **curcumin**, **BF_2-CurOH**, **BF_2-CurOMe**, **BF_2-CurmonoTs** and **BF_2-CurdiTs** have been synthesized. The photophysical properties of all **BF_2-curcumin** derivative revealed that electron donating modified on aromatic ring (**BF_2-CurOMe**) induced the bathochromic shift of the absorption and emission spectra. In contrast, the electron-withdrawing modified on aromatic ring resulted in the hypsochromic shift in both absorptions and emissions. The quantum yields of **BF_2-CurOH**, **BF_2-CurOMe**, **BF_2-CurmonoTs** and **BF_2-CurdiTs** in dichloromethane were 0.62, 0.61, 0.22 and 0.48, respectively. Interestingly, **BF_2**-incoorporated **curcumin** derivatives of **BF_2-CurOH** and **BF_2-CurOMe** exhibited solvent-dependent. The solvent dependent maximum absorption band of both compounds were analyzed using Kamlet-Taft relationship, the result showed that **BF_2-CurOH** and **BF_2-CurOMe** behaved the positive solvatochromism. Concerning on the anion sensing, **BF_2-CurOH** have excellent sensitivity and selectivity toward cyanide ion over **curcumin**. This phenomenon was subjected to deprotonation of hydroxyl group of **BF_2-CurOH** and **curcumin**. The negative charge on oxygen atom which can delocalize through π-conjugated bond. The deprotonation abilities by CN^- to both compounds measured by UV-visible titration and fluorometric titration exhibited the log β values of 8.8 and 7.7 for **BF_2-CurOH** and **curcumin**, respectively. Interestingly, the effect of foreign anions toward cyanide detection for **BF_2-CurOH** was studied and showed that no effect on the determination of CN^- except AcO^-, $H_2PO_4^-$ and F^- while all anions have an effect for cyanide detection of **curcumin** in aqueous solution. Furthermore, the detection limit of CN^- is 9.33 and 0.14 μM for **curcumin** and **BF_2-CurOH,** respectively.

Department : Chemistry	Student's Signature A. Chaicham
Field of Study : Chemistry	Advisor's Signature B. Tomapatanaget
Academic Year : 2009	Co-Advisor's Signature G. Tumcharern

ACKNOLEDGEMENTS

The accomplishment of this thesis could not occur without the kindness, personal friendship, encouragement, suggestions, assistance and the extensive supports throughout my master degree career from my thesis advisor, Assist. Prof. Dr. Boosayarat Tomapatanaget. Particular thanks are given to my thesis co-advisor, Dr. Gamolwan Tumcharern for suggestions, assistance and personal friendship. In addition, I would like to thank Assist. Prof. Dr. Warinthorn Chavasiri, Assoc. Prof. Dr. Thawatchai Tuntulani and Assist. Prof. Dr. Boon-ek Yingyongnarongkul for their input, interest, value suggestions and comments as committee members and thesis examiners.

This thesis would not be successful without kindness and helps of a number of people. First, I am grateful to the Scientific and Technological Research Equipment Center of Chulalongkorn University, particularly, Miss Metinee Jamkatok for NMR results and elemental analysis data. I would like to express my appreciation to former and the current staffs in the Supramolecular Chemistry Research Unit.

Financial supported by National Science and Technology Development Agency (NSTDA) and National of Center of Excellence for Petroleum, Petrochemical, and Advance Materials (NCE-PPAM).

Finally, I would like to express my deepest gratitude to my family for their love, care, kindness, encouragement and other assistance throughout my life.

CONTENTS

	Page
Abstract in Thai……..……	IV
Abstract in English...……	V
Acknowledgements…….....	VI
Contents……	VII
List of Tables ……..	XI
List of Figures……..	XIII
List of Abbreviations and Symbols …….	XVII
CHAPTER I INTRODUCTION……..	1
1.1 Concept of supramolecular chemistry……...	1
1.2 Molecular recognition and molecular recceptors……...	1
1.3 Chromoionophores and fluoroionophores……..	2
1.3.1 Chromoionophores……	2
1.3.2 Fluoroionophore……	2
1.4 Anion receptors……..	5
1.5 Anion sensors…….	6
1.6 Some characteristics of fluoroionophores……..	7
1.6.1 Selectivity……..	7
1.7 Solvatochromism…….....	8
1.7.1 The $\boldsymbol{E_T(30)}$ and $\boldsymbol{E_T^N(30)}$ scale of solvent polarity……...	8
1.8 Multiparameter approaches…….....	9
1.9 Limit of detection……...	11
CHAPTER II LITERATURE REVIEWS……...	12
2.1 Literature reviews……...……	12
2.2 Objective and Scope of this research…….....	22
CHAPTER III EXPERIMENTAL……...	24
3.1 General procedures…….	24
3.1.1 Analytical instrument……	24

Page

3.1.2 Materials……..... 24

3.2 Synthesis…… 25

3.2.1 Preparation of curcumin borondifluoride **(BF_2-CurOH)**……. 25

3.2.2 Preparation of methylation curcumin borondifluoride **(BF_2-CurOMe)**…… 26

3.2.3 Preparation of monotosylation curcumin borondifluoride **(BF_2-CurmonoTs** and **BF_2-CurdiTs)**……..... 27

3.3 UV-visible and fluorescence studies of **BF_2-CurOH**, **BF_2-CurOMe**, **BF_2-CurmonoTs** and **BF_2-CurdiTs**…… 28

3.3.1 UV-visible studies of **BF_2-CurOH**, **BF_2-CurOMe**, **BF_2-CurmonoTs** and **BF_2-CurdiTs**……..... 28

3.3.2 Fluorescence studies of **BF_2-CurOH**, **BF_2-CurOMe**, **BF_2-CurmonoTs** and **BF_2-CurdiTs**……. 29

3.4 Solvatochromism studies of **BF_2-CurOH** and **BF_2-CurOMe**…….. 29

3.4.1 Solvatochromism studies of **BF_2-CurOH** and **BF_2-CurOMe** by UV-visible spectrophotometry……... 30

3.4.2 Solvatochromism studies of **BF_2-CurOH** and **BF_2-CurOMe** by fluorescence spectrophotometry…….. 31

3.5 Complexation studies of ligand **BF_2-CurOH** and **curcumin** by UV-visible spectrophotometry……..... 31

3.5.1 Complexation studies of ligand **BF_2-CurOH** and **curcumin** with various anions: fluoride, chloride, bromide, iodide, acetate, benzoate and cyanide……..... 31

3.5.2 Complexation studies of **curcumin** with various anions: fluoride, chloride, bromide, iodide, acetate, benzoate, cyanide……..... 30

3.5.3 Complexation studies of ligand **BF_2-CurOH** with cyanide ion by UV-visible titration……. 33

3.5.4 Complexation studies of ligand **curcumin** with cyanide ion by UV-visible titration……..... 35

3.6 Complexation studies of ligand **BF_2-CurOH** and **curcumin** by fluorescence spectrophotometry....……..... 38

Page

3.6.1 Complexation studies of ligand **BF_2-CurOH** and **curcumin** with various anions: fluoride, chloride, bromide, iodide, acetate, benzoate and cyanide…..... 38

3.6.2 Complexation studies of ligand **BF_2-CurOH** with cyanide ion by fluorescence titration…….. 39

3.6.3 Complexation studies of ligand **curcumin** with cyanide ion by fluorescence titration…….. 39

3.7 Determination of detection limit of **BF_2-CurOH** with cyanide ion by UV-visible spectroscopy……..…… 40

3.8 Interference studies by fluorescence spectroscopy…….…… 40

3.9 Determination of quantum yields of curcumin, **BF_2-CurOH**, **BF_2-CurOMe**, **BF_2-CurmonoTs** and **BF_2-CurdiTs**……. 41

CHAPTER IV RESULTS AND DISCUSSION…….. 44

4.1 Design concept…..……. 44

4.2 Synthesis and characterization of curcumin borondifluoride (**BF_2-CurOH**)……... 45

4.3 Synthesis and characterization of curcumin borondifluoride methylation (**BF_2-CurOMe**)……... 46

4.4 Synthesis and characterization of curcumin borondifluoride mono-tosylation (**BF_2-CurMonoTs**) and di-tosylation borondifluoride (**BF_2-CurDiTs**)……. 47

4.5 UV-visible and fluorescence spectra of **BF_2-CurOH**, **BF_2-CurOMe**, **BF_2-CurMonoTs** and **BF_2-CurDiTs**…….. 49

4.6 Solvatochromic studies of **BF_2-CurOH** and **BF_2-CurOMe**…….. 51

4.7 The complexation studies by UV-vis technique……. 60

4.8 The complexation studies by fluorescence technique……. 67

4.9 Interference studies…… 76

4.10 Detection limit……. 78

CHAPTER V CONCLUSION……. 83

Refferences……..…… 84

Appendix……... 89

Page

VITA……. 100

LIST OF TABLES

Table		Page
3.1	Amounts of **BF_2-CurOH, BF_2-CurOMe, BF_2-CurmonoTs** and **BF_2-CurdiTs** that used in studies in UV-visible spectrophotometry...	28
3.2	The excitation wavelength that used in studies in fluorescence……	29
3.3	The property parameters of organic solvents HBD ability (α), HBA ability (β), polarity/polarizability (π*) and polarity $E_T(30)$……..	30
3.4	Amounts of **BF_2-CurOH,** CN^-, F^-, Cl^-, Br^-, I^-, BzO^- and AcO^- as tertbutylammonium salt that used in studies in UV-visible spectrophotometry……..	32
3.5	Amounts of anions solutions were used to prepare various anions:ligand ratios……	33
3.6	The concentration of CN^- ion was used in anion complexation studies with ligand **BF_2-CurOH** and the final ratios of guest:host……...	34
3.7	The concentration of CN^- ion was used in anion complexation studies with ligand curcumin and the final ratios of guest:host…….	36
3.8	Amount of CN^- and anions that used in interference studies with ligand **BF_2-CurOH** and **curcumin** for fluorescence studies……	41
3.9	The concentration of **curcumin, BF_2-CurOH, BF_2-OMe, BF_2-monoTs** and **BF_2-CurdiTs** were used to determine quantum yield…..	42
4.1	Maximum absorption and emission of **BF_2-CurOH**, **BF_2-CurOMe**, **BF_2-CurmonoTs** and **BF_2-CurdiTs** at concentration 1.0×10^{-6} M in CH_2Cl_2……	49
4.2	The maximum absorption and emission wavelength of **BF_2-CurOH** in difference solvents……	51
4.3	The correlation coefficients of *a*, *b*, and *c* of the Kamlet-Taft parameters; α, β, and π^*, respectively, and Correlation Coefficient (R^2) for **BF_2-CurOH**……..	54
4.4	The maximum absorption and emission wavelength of **BF_2-CurOMe** in difference solvents…….	55
4.5	Solvent-Independent Correlation Coefficients *a*, *b*, and *c* of the Kamlet-Taft parameters α, β, and π^*, Respectively, and Correlation Coefficient (R^2) for **BF_2-CurOMe**……	58

4.6	Interference of foreign substances with the determination of BF_2-CurOH ($7.5x10^{-6}$M)……..	76
4.7	Interference of foreign substances with the determination of Curcumin ($7.5x10^{-6}$M)……	77
4.8	The absorbance of BF_2-CurOH $7.5x10^{-6}$ M ……	79
4.9	The absorbance of Curcumin $7.5x10^{-6}$ M …….	80
4.10	Summarize of log β and detection limit of Curcumin and BF_2-CurOH in spectrophotometry…….	82

LIST OF FIGURES

Figure		Page
1.1	PET process with the participation of the HOMO and LUMO of the fluorophore and an external molecular orbital……	3
1.2	PET process with the participation of the HOMO and LUMO of the fluorophore and an emply external molecular orbital…….	4
1.3	EET process with the participation of the HOMO and LUMO of the fluorophore and an external molecular orbital……	4
1.4	Schematic diagram of spectral displacement of ADD resulting from interaction of anions with an electron donating group in receptor…..	5
1.5	Schematical illustration of anions sensor…….	6
2.1	Chemical structures of Curcumin in keto–enol tautomeric equilibrium……	12
2.2	Structure of compound 1a-1g……..	14
2.3	(a) Normalized absorption and (b) fluorescence spectra of compound 1a-1g in toluene at 5 mM……..	15
2.4	Key spectroscopic data for the aza-BDP derivatives 1a-g……	15
2.5	Structure of compound 2a-2h……..	16
2.6	Colorimetric changes of compound 3 upon the addition of cyanide ions…….	17
2.7	Suggested Mechanism for ON-OFF switching of compound 3 within the presence of CN^- ions……...	17
2.8	Fluorescence image of poly(methyl methacrylate) polymer sheets doped with chemosensor 3……	18
2.9	Absorbance spectra of compound 4+Cu(II) in the presence of increasing CN^- concentrations (0, 3.3, 6.7, 10.0, 11.7, 13.3, 15.0, 16.7, 18.3 and 20.0 μM)……	18
2.10	Emission spectra of compound 4+Cu(II) in the presence of increasing CN^- concentrations (0, 3.3, 6.7, 10.0, 11.7, 13.3, 15.0, 16.7, 18.3 and 20.0 μM)……	19
2.11	Schematical illustration of synthesis compound **5**……	20

2.12 Spectral changes in the UV–vis absorption of a solution of 5 in THF (1.0×10^{-5} M) upon addition of Bu_4NCN (0–15 μM). The inset shows the absorbance at 330 nm as a function of [CN-]..…….. 20

2.13 Comparison of the fluorescence response of solutions of 5 (right) and borane moiety (left) in THF (λ_{ex} 330 nm; 1.0×10^{-6} M) upon addition of Bu_4NCN (0-2 μM)……. 21

2.14 Polymer synthesis and boron initiator and polymer luminescence (λ_{max} = 365 nm; room temperature in air unless indicated). BF_2dbmOH: (A) solid-state green-yellow fluorescence; (B) red phosphorescence (77 K); (C) blue fluorescent CH_2Cl_2 solution. BF_2dbmPLA: (D) short-lived blue fluorescence and (E) long-lived green phosphorescence for a thin film (N_2); (F) blue fluorescent particle suspension in H_2O after 45 days..... 22

2.15 Molecular structures of **curcumin-BF_2** derivatives were studied in this work..... 23

4.1 Optimized structures of the **curcumin** in enol form and diketone form..... 44

4.2 The ^{1}H-NMR spectrum of **BF_2-CurOH** in d_6- DMSO…….. 46

4.3 The ^{1}H-NMR spectrum of **BF_2-CurOMe** in d_6- DMSO…… 47

4.4 ^{1}H -NMR spectrum of **BF_2-CurMonoTs** in CD_3Cl…… 48

4.5 ^{1}H -NMR spectrum of **BF_2-CurDiTs** in CD_3Cl…… 48

4.6 The normalized UV-visible spectra (a) and fluorescence spectra (b) of **BF_2-CurOH**, **BF_2-CurOMe**, **BF_2-CurmonoTs** and **BF_2-CurdiTs** at concentration 1.0×10^{-6} M in CH_2Cl_2…….. 50

4.7 Absorption (a) and emission (b) spectra of **BF_2-CurOH** in difference solvents……... 52

4.8 The liner plots on plotting λ_{max} (the maximum absorption) versus the solvent parameter $\boldsymbol{E_T^N(30)}$ of **BF_2-CurOH**…… 53

4.9 Relationship between calculated and measured $\tilde{\nu}_{max}$ values for **BF_2-CurOH** dissolved in difference solvent……. 54

4.10 Absorption (a) and emission (b) spectra of **BF_2-CurOMe** in difference solvents…… 56

4.11 The liner plots of λ_{max} (the maximum absorption) of **BF_2-CurOMe** versus the solvent parameter $\boldsymbol{E_T^N(30)}$…… 57

4.12 Relationship between calculated and measured $\tilde{\nu}_{max}$ values for **BF_2-CurOMe** dissolved in difference solvent…….. 58

4.13 The UV-visible absorption spectra of ligand **BF_2-CurOH** and Curcumin at concentration $5.0x10^{-6}$ M in $CH_3CN:H_2O$ (4:1 v/v)…….. 60

4.14 The UV-visible spectra of **BF_2-CurOH** (5 μM) in $CH_3CN:H_2O$ (4:1, v/v) in the presence of 100 equivalent of varies anions……. 61

4.15 UV-visible titration spectra of **BF_2-CurOH** ($7.5x10^{-6}$ M) upon gradual addition of CN^- in $CH_3CN:H_2O$ (4:1, v/v) from 0-100 equivalent…… 62

4.16 Comparing experiment data and calculated data form UV-visible titration of **BF_2-CurOH** and CN^- for stability constant. (a) at 507 nm……... 63

4.17 The UV-visible spectra of **curcumin** (5 μM) in $CH_3CN:H_2O$ (4:1, v/v) in the presence of TBA salts of various anions (F^-, Cl^-, Br^-, I^-, CN^-, AcO^-, $PhCOO^-$ and H_2PO_4, 100 equiv, respectively)…… 64

4.18 UV-visible titration spectra of **curcumin** ($7.5x10^{-6}$ M) upon gradual addition of CN^- in $CH_3CN:H_2O$ (4:1, v/v) from 0-100 equivalent…… 65

4.19 Comparing experiment data and calculated data form UV-visible titration of **curcumin** and CN^- for calculation of stability constant at 510 nm. …….. 66

4.20 The emission spectra of ligand **BF_2-CurOH** (a) and **curcumin** (b) at concentration $5.0x10^{-6}$ M in $CH_3CN:H_2O$ (4:1, v/v)……. 68

4.21 The fluorescence spectra of **BF_2-CurOH** at concentration 5 μM in $CH_3CN:H_2O$ (4:1, v/v) in the presence of 100 equivalent TBA salts of various anions (F^-, Cl^-, Br^-, I^-, CN^-, AcO^-, $PhCOO^-$ and $H_2PO_4^-$). (a) Excitation at 507 nm. (b) Excitation at 649 nm…… 70

4.22 (a)Fluorescence spectra of **BF_2-CurOH** ($7.5x10^{-6}$ M) under excitation at 507 nm in $CH_3CN:H_2O$ (4:1, v/v) upon addition of increasing amount of CN^- ($1.0x10^{-3}$ M). (b) Graph of quenching intensity at 600 nm…….. 71

4.23 Comparing experiment data and calculated data form fluorescence titration of **BF_2-CurOH** and CN^- for calculation of stability constant at emission 600 nm…… 72

4.24 Fluorescence spectra of **BF_2-CurOH** ($7.5x10^{-6}$ M) under excitation at 649 nm in $CH_3CN:H_2O$ (4:1, v/v) upon addition of increasing amount of CN^- ($1.0x10^{-3}$ M)…….. 73

4.25 The fluorescence spectra of **curcumin** at concentration 5 μM in $CH_3CN:H_2O$ (4:1, v/v) in the presence of TBA salts of various anions (F^-, Cl^-, Br^-, I^-, CN^-, AcO^-, $PhCOO^-$ and $H_2PO_4^-$, 100 equiv, respectively) under excitation at 417.1 nm…… 74

4.26 Fluorescence spectra of **curcumin** ($7.5x10^{-6}$ M) under excitation at 417 nm in $CH_3CN:H_2O$ (4:1, v/v) upon addition of increasing amount of CN^- ($1.0x10^{-3}$ M)……... 75

4.27 Comparing experiment data and calculated data form fluorescence titration of **curcumin** and CN^- for calculation of stability constant…. 75

4.28 Effect of foreign substance with determination of CN^-……. 77

4.29 Colorimetric changes of **BF_2-CurOH** (1 x 10-5 M) upon the addition of cyanide in CH3CN:H2O (4:1, v/v) solution. (a. 0, b. 15, c. 22, d. 24, e. 29, f. 36, g. 43, h. 50 and i. 57 µM of CN^-)…… 78

4.30 Linear plot between absorbance and concentration of with CN^-…….. 79

4.31 Linear plot between absorbance and concentration of **curcumin** with CN^-……. 81

4.32 Colorimetric changes of **curcumin** (1×10^{-4} M) upon the addition of cyanide in $CH_3CN:H_2O$ (4:1, v/v) solution. (a. 0, b. 50, c. 75, d. 99, e. 109, f. 124, g. 149 and h. 172 μM of CN^-)…… 82

LIST OF ABBREVIATIONS AND SYMBOLS

A	Absorbance
°C	Degree Celsius
^{13}C-NMR	Carbon nuclear magnetic resonance
^{1}H-NMR	Proton nuclear magnetic resonance
equiv.	Equivalent
g	Gram
Hz	Hertz
J	Coupling constant
mmol	Millimole
mL	Milliliter
M	Molar
M^{-1}	Per molar
δ	Chemicalshift
ppm	Part per million
s, d, t, m	Splitting patterns of 1H-NMR (singlet, doublet, triplet, multiplet)
LSER	Linear Salvation Energy Relationship

CHAPTER I

INTRODUCTION

1.1 Concept of supramolecular chemistry

Supramolecular chemistry becomes one of the most rapidly expanded fields in modern chemistry [1]. The knowledge from this enchanting topic can be applied to enormous diversities of chemical system especially the production of molecular devices and artificial biological systems. The definition of supramolecular chemistry may be expressed in many terms as „chemistry of molecular assemblies and of the intermolecular bond" or „chemistry of the non-covalent bond". Supermolecules consist of two or more species held together by weak intermolecular forces (non-covalent intermolecular bond) such as hydrogen bonding, van der Waals interaction, electrostatic interaction, dipole-dipole interaction or π-π interaction [2]. Construction of any supermolecule are lead to the three important functions: molecular recognition, translocation and transformation [3]. Indeed, molecular recognition has become characteristics of the language of supramolecular chemistry and has been studied more widely than the others.

1.2 Molecular recognition and molecular recceptors

As mentioned above, molecular recognition is defined by the energy and the information involved in the binding and selection of many substrates by a given receptor molecule. It can be implied as the (molecular) storage and (supramolecular) read out of molecular information. High recognition between receptors and substrates was affected by several factors as follows:

a.) steric complemantarity: it depends on shapes and sizes of receptors and substrates;

b.) interactional complementarities, i.e. presence of complementarily binding sites in the suitable disposition on a substrate and a receptor;

c.) large contact area between molecules of a receptor and a substrate;

d.) multiple interaction sites due to weak intermolecular interactions;

e.) strong overall bindings [1].

Studies of molecular recognition require suitable molecular receptors to specifically interact with many substrates. Molecular receptors are clearly defined as organic structures held by covalent bonds, that are able to bind with ionic or molecular substrates by means of intermolecular interactions, leading to an assembly of two or more species. Excellent molecular receptor is one that can bind a particular substrate with high selectivity, high stability and high flexibility [2].

1.3 Chromoionophores and fluoroionophores

A number of direct sensing schemes have been described using colorimetric and fluorescent chemosensor molecules whose optical properties change upon direct binding of the guest (*chromoionophores and fluoroionophores*).

1.3.1 Chromoionophores

Organic compounds became colored by absorbing electromagnetic radiation in the visible range (from 400 to 700 nm approximately), and investigations related with the correlation between chemical structure and color in organic dyes have been carried out extensively. It was soon recognized that many dyes contain systems of conjugated bonds, and it was the energy gap between the highest occupied molecular orbital (HOMO) and the lowest unoccupied molecular orbital (LUMO) that is critical in determining the color of a certain organic dye. Thus, many conjugated systems have HOMO to LUMO differences in energy that correspond to visible light and it is well-established that the larger the conjugated system is, the shorter the difference between fundamental and excited states, resulting in a more bathochromic shift of the absorption band of lesser energy [4]. In addition to that basic conjugated backbone related with the length of the conjugated system, there is a chemical mean of modifying the absorption wavelength by anchoring electron donor or electron acceptor groups to the conjugated system. When both an electron donor and an electron acceptor group are present and are connected through a conjugated system in a certain molecule, a CT band can be observed. This corresponds to a CT transition where, upon excitation with light, there is an important fraction of electronic charge that is transferred from the donor to the acceptor. What is important related to the design of chromogenic reagents is that the interaction of anions with the donor or acceptors groups in those systems can result in a change in color. Thus, for instance, the interaction of an anion with a donor group will make this more donor, pumping more electrons to the conjugated system, enhancing the conjugation, and inducing a bathochromic shift. An important effect also found in many dyes is the solvatochromism. A dye that presents a solvatochromic behavior changes its color in solution on changing the polarity of the solvent in which it was dissolved. This solvatochromic effect has been, for instance, extensively used as an indicator of the polarity of the ground and excited state. For sensing purposes, this effect might have some importance as it would allow one to select the initial and final color of certain designed probes.

1.3.2 Fluoroionophores

Luminescence can be defined as a spontaneous emission of radiation from an excited state. Depending on the mode of excitation, the terms chemoluminescence, electroluminescence, radioluminescence, etc. are used. The luminescence phenomenon can be classified as fluorescence when the excited molecule results in a new molecule with the same multiplicity and as phosphorescence when it involves luminescence with a change in spin multiplicity. An observing in a fluorescence molecule is that absorption of light at a given wavelength results in an almost instantaneous emission of light at a longer wavelength.

In relation to the use of fluorescence for sensing or detecting, the principal advantage over other light-based methods such as absorbance is its high sensibility. This is so because the emission fluorescence signal is proportional to the substance concentration. In absorbance measurements, the substance concentration is proportional to the absorbance which is reated to the ratio between intensities measured before and after the beam passes through the sample. Therefore, in fluorescence, an increase of the intensity of the incident

beam results in a larger fluorescence signal whereas this is not so for absorbance. Fluorescence techniques can measure concentration even one million times smaller than absorbance techniques. It is interesting to understand the basis of the nature of the photoinduced processes that are responsible for the photophysical changes upon anion coordination. These effects are specifically related with the use of the binding site-signaling subunit approach.

1.3.2.1 Fluorescence PET (Photoinduced Electron Transfer)

This photoinduced process has been extensively studied and widely used for sensing purposes of cations and anions [5]. As described above, fluorescence in a molecule is observed when an excited electron, for instance in the LUMO, goes to the HOMO, releasing the excess of energy as light. Over this scheme, it might happen that an orbital from another part of the molecule or from another molecular entity could have energy between that of the HOMO and that of the LUMO of the fluorophore. When this "alien" orbital is full (for instance, if we have a donor group), a PET from this full orbital to the HOMO of the fluorophore can take place. A further electron transfer from the LUMO of the fluorophore to the external orbital retrieves the stable ground state. Following this sequence, fluorescence quenching occurs because the transition from the excited to the ground state takes place following a nonradiative path (see Figure 1.1). What is macroscopically observed is a decrease of the emission intensity or no fluorescence at all. A similar process can take place when there is an empty orbital from another part of the molecule or from another molecular entity between both the HOMO and the LUMO of the fluorophore. In this case, a PET from the excited LUMO to the empty orbital can occur, followed by a further electron transfer from this orbital to the HOMO of the fluorophore. Again, deexcitation occurs without radiation and fluorescence quenching is observed (see Figure 1.2).

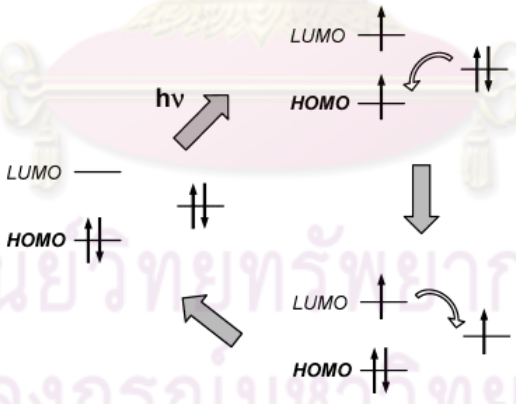

Figure 1.1 PET process with the participation of the HOMO and LUMO of the fluorophore and an external molecular orbital

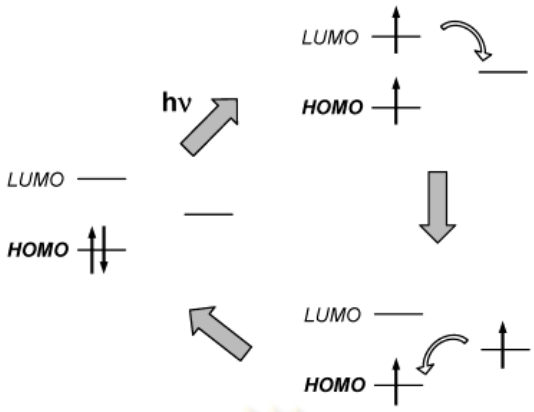

Figure 1.2 PET process with the participation of the HOMO and LUMO of the fluorophore and an emply external molecular orbital

1.3.2.2 Electronic Energy Transfer (EET)

Another mechanism that may be responsible for the fluorescence quenching by certain molecular entities is the EET [5]. When the external molecular group has some empty or half-filled energy levels between the HOMO and the LUMO of the fluorophore, a simultaneous exchange of two electrons (from the LUMO to the foreign orbital and from the foreign orbital to the HOMO) can occur (see Figure 1.3). The double electron exchange restores the fluorophore to its ground state following a nonradiative process therefore resulting in a fluorescence quenching. The occurrence of this double and simultaneous electron transfer requires a close contact between the fluorophore and the molecular group. Thus, flexible linkers may favor the occurrence of an intramolecular energy transfer process of this type.

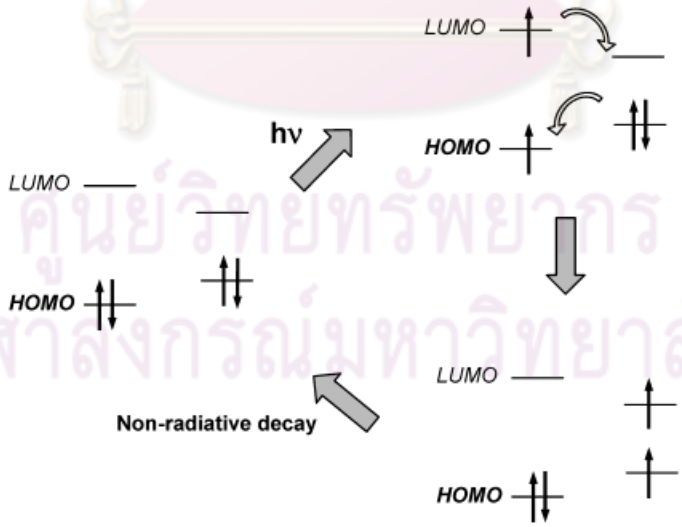

Figure 1.3 EET process with the participation of the HOMO and LUMO of the fluorophore and an external molecular orbital

1.3.2.3 Fluorescence PCT (Photoinduced charge transfer)

This phenomenon can be occurred when a fluorophore contains an electron donating group conjugated to an electron-withdrawing group. It undergoes intramolecular charge transfer from the donor to the acceptor upon excitation by light. The consequent change in dipole moment results in a Stokes shift that depends on the microenvironment of the fluorophore. Notably, the probes have been designed in this basis. It was found from the literature that very few ICT-based fluorescent sensors for anions have been reported due to the weaker binding forces of these guests, which could entail only weak spectroscopic effects upon complexation [6-7]. ICT fluorescent anion receptor relies on the choice of a spacer that links the ICT fluorophore and the anion-binding or anion-recognition site to allow for a highly efficient communication of the anion-recognition messages to the fluorophore. As with the ICT fluorophore, the photophysics and emission of the charge transfer state are subjected to the electron donor/acceptor strength, and the anion-binding site is assumed to be better incorporated in either the electron donor or acceptor moiety. This will change the photophysical properties of fluorophore because the complexed anion affects the efficiency of ICT. An example of this phenomenon showed that anion hydrogen bonding with the donor moiety causes increasing the electron-donating character of the donor group as shown in Figure 1.4. This increase in charge density results in the red shift of absorption and emission together with an increase in the fluorescence intensity.

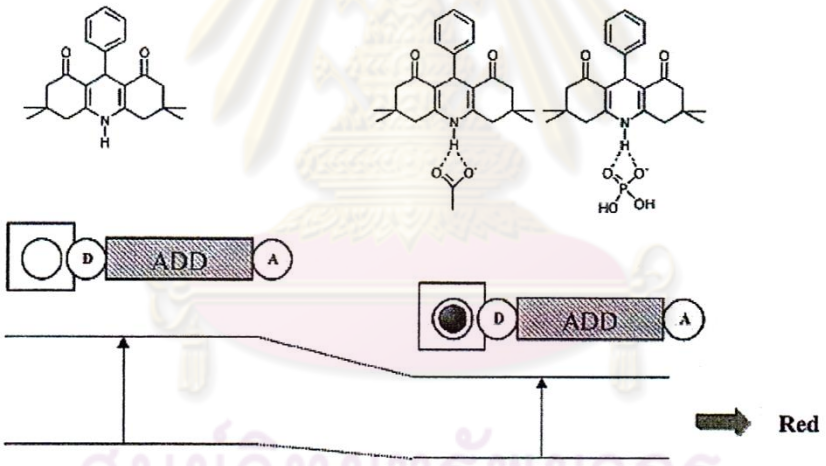

Figure 1.4 Schematic diagram of spectral displacement of ADD resulting from interaction of anions with an electron donating group in receptor

1.4 Anion receptors

The chemistry of anion coordination has some special features that need to be considered [8]. Thus, when making the choice of a receptor for a certain anion, the shape and geometry of the anion (such as spherical, linear, trigonal planar, tetrahedral and octahedral) to coordinate; its charge, which can be varied as a function of the pH; and its hydrophobicity should be taken into account, among other factors [9]. In general, it can be said that abiotic receptors for anions use similar type of interactions as biological receptors. Those can be classified basically in electrostatic interactions, formation of hydrogen bonds, and interactions with metal centers.

Electrostatic interactions with anions are found when using positively charged receptors having for instance guanidinium groups [10-12] or quaternary ammoniums [13]. These two groups have a positive charge that basically does not depend on the pH of the medium. Amines can also give electrostatic interactions with anions as they are usually protonated and therefore charged at neutral and acidic aqueous solutions [14-17].

Hydrogen-bonding groups have been widely used in binding sites for anion recognition. A hydrogen bond can be established when a hydrogen covalently attached to a highly electronegative atom interacts with another electronegative atom (of the same or different molecule) having lone pairs.

Metal complexes have also been used as anion binding sites. Metal complexes can bind anions forming stronger bonds than those generally observed using electrostatic or hydrogen-bonding interactions [18-19].

A certain binding site may combine several of those binding groups in a proper spatial distribution for the selective coordination of target anions. Additional, difference in geometry between anions is an important factor to account for in the design of selective anion receptors, although it is not to synthesize receptor molecules with complementary binding sites in a proper three-dimensional arrangement.

1.5 Anion sensor

The field of molecular recognition association with signaling of reversible anion binding using synthetic sensors has witnessed increasing popularity in recent years [20]. Such systems generally contain some combination of substrate recognition functionality (receptor) and signaling unit, either directly linked [5, 21] or appropriately associated in a noncovalent manner [22-23]. The most common modes of signal transduction typically involve electrochemical or optical changes in the sensor incurred by association of the analyte with the receptor. Figure 1.5 illustrates the mechanism of an anion sensor.

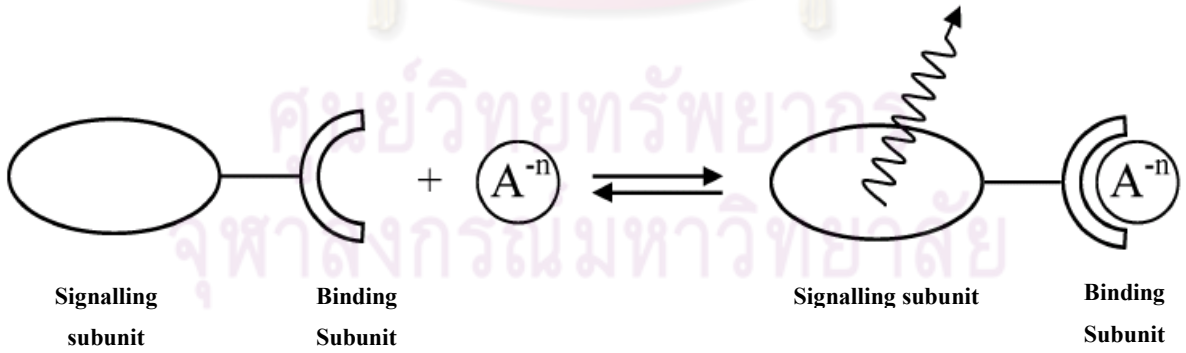

Figure 1.5 Schematical illustration of anions sensor.

Electrochemical-based sensing has proved a popular method for signaling the recognition of analytes. The majority of electrochemical-based sensors employ transition metals or lanthanides for both analyte binding and electrochemical signaling through changes in metal redox potentials upon anion-receptor complexation [24].

Optical signaling of anion recognition typically involves quenching or enchancement of a chromophore‟s absorption [25] or a fluorophore‟s fluorescence emission [26-27] upon proximal association of the analyte. While the utilities of these approaches are becoming increasingly appreciate in term of both qualitative and quantitative analysis, the number of optical signaling sensors available at present for anionic substrates remains quite limited of particular interested in this regard are “colorimetric anion sensors” species that would allow the so-called “naked-eye” detection of anions without resort to any spectroscopy instrumentation [20].

1.6 Some characteristics of fluoronoionophores

1.6.1 Selectivity

A selectivity of a receptor is a preference of that receptor towards a guest. This is customarily estimated from a magnitude of a thermodynamic *stability constant* of a receptor-guest or, in more general terms, a ligand-metal complex. There are several methodologies to determine the binding constant such as NMR spectroscopy, UV-visible spectroscopy, fluorescence and electrochemical techniques depending on the molecular design.

1.6.1.1 Determination of the Stability Constants by UV-visible and Fluorescence Spectroscopy [28]

The stability constant K_s which controls the equilibrium between the free ligand L and the complex ML with the metal may be obtained from the variation of either absorbance or fluorescence intensity at proper observation wavelengths.

$$M + L \rightleftharpoons ML \qquad K_s = [ML]/([L][M])$$

It is easy to derive the following relation involving the absorbance A_0 of the free ligand and the absorbance A of the solution at a given wavelength where ε_L and ε_{ML} are the molar extinction coefficients of the ligand and the complex, respectively. The quantity $A_0/(A_0-A)$ is plotted versus $[M]^{-1}$, and the stability constant is then given by the ratio of intercept/slope.

$$\frac{A_0}{A_0 - A} = \frac{\varepsilon_L}{\varepsilon_L - \varepsilon_{ML}}\left(\frac{1}{K_s[M]} + 1\right)$$

The various methods for determining the stability constants from fluorimetric data were previously discussed [29]. The best of them uses the relation where Φ_L and Φ_{ML} are the quantum yields of the ligand and the complex, respectively. The quantity $IF^0/(IF-IF^0)$ is plotted versus $[M]^{-1}$, and the stability constant is then given by the ratio of intercept/slope.

$$\frac{I_F^0}{I_F^0 - I_F} = \frac{\varepsilon_L \Phi_L}{\varepsilon_L \Phi_L - \varepsilon_{ML} \Phi_{ML}}\left(\frac{1}{K_s[M]} + 1\right)$$

1.7 Solvatochromism

It has long been known that UV/visible/near-IR absorption spectra of chemical compounds may be influenced by the surrounding medium and solvents can bring about a change in the position, intensity, and shape of absorption bands [30, 31]. Hantzschlater termed this phenomenon as *solvatochromism* [32]. A hypsochromic (or blue) shift of the UV/visible/near-IR absorption band with increasing solvent polarity is usually called "negative solvatochromism". The corresponding bathochromic (or red) shift, with increasing solvent polarity is termed "positive solvatochromism". Obviously, solvatochromism is caused by differential solvation of the ground and first excited state of the light-absorbing molecule (or its chromophore). With increasing solvent polarity, the ground-state molecule is better stabilized by solvation than the molecule in the excited state, resulting in negative solvatochromism. Or vice versa, better stabilization of the molecule in the first excited state relative to that in the ground state with increasing solvent polarity will lead to positive solvatochromism. In this context, "first excited state" means the so-called Franck-Condon excited state with the solvation pattern present in the ground state. Since the time required for a molecule to get electronically excited (about 10^{-15} s) is much shorter than that required to execute vibrations or rotations (about 10^{-12} to 10^{-10} s), the nuclei of the absorbing entity (i.e. absorbing molecule + solvation shell) do not appreciably alter their positions during an electronic transition (Franck-Condon principle) [33]. Therefore, the first excited state of a molecule in solution has the same solvation pattern as the corresponding ground state and is called Franck-Condon excited state, whereas the ground state corresponds to an equilibrium ground state. If the lifetime of the excited molecule is large enough, then reorientation of the solvent molecules, according to the new excited situation, takes place, and a relaxed excited state with a solvent shell in equilibrium with this state results. It is from this equilibrium excited state that fluorescence can occur. By analogy, there is a Franck-Condon ground state after emission with the solvation pattern of the equilibrium excited state, which persists briefly until the solvent molecules reorganize to the equilibrium ground state. The differential solvation of these two states is responsible for the solvent influence on emission or fluorescence spectra. The solvent dependence of the position of emission bands in fluorescence spectra has been often included in the term of *so1vatochromism*. The solvent dependence of fluorescence spectra has been sometimes called *solvatofluorochromism* [34] or *fluorosolvatochromism* [35]. However, because of the close connection between spectral absorption and emission, there is no need for special terms for fluorescence-based solvatochromism.

The solvatochromism observed depends on the chemical structure and physical properties of the chromophore and the solvent molecules, which determine the strength of the intermolecular solute/solvent interactions in the equilibrium ground state and the Franck-Condon excited state. In general, dye molecules with a large change in their permanent dipole moment upon excitation exhibit a strong solvatochromism. If the solute dipole moment increases during the electronic transition ($\mu_g<\mu_e$), a positive solvatochromism normally results. In the case of a decrease of the solute dipole moment upon excitation ($\mu_g>\mu_e$), a negative solvatochromism is usually observed.

1.7.1 The $E_T(30)$ and $E_T^N(30)$ scale of solvent polarity

$E_T(30)$ a values are based on the negatively solvatochromic pyridinium N-phenolate betaine dye as probe molecule, and they are simply defined, in analogy to

Kosower's Z values [36, 37], as the molar electronic transition energies $E_T(30)$ of dissolved molecule, measured in kilocalories per mole (kcal/mol) at room temperature (25 °C) and normal pressure (1 bar) [38], according to eq 1.$\tilde{\nu}_{max}$ is the frequency and the wavelength of the maximum of the longest wavelength, intramolecular charge-transfer π-π* absorption band of the dye.

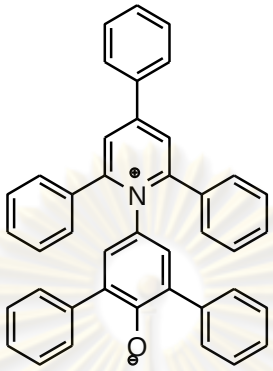

N-phenolate betaine

$$E_T(30)\ (\text{kcal mol}^{-1}) = hc\tilde{\nu}_{max}\,N_A = 28591/\lambda_{max}\ (\text{nm}) \qquad (1)$$

In addition, so-called normalized E_T^N value have been introduced [39]. They are defined according to eq **2** as dimensionless figures, using water and tetramethylsilane (TMS) as extreme polar and nonpolar reference solvents, respectively. Hence, the E_T^N scale ranges from 0.000 for TMS, the least polar solvent, to 1.000 for water, the most polar solvent. Hence, hight $E_T(30)$ or hight E_T^N values correspond to hitgh solvent polarity.

$$E_T^N = \frac{E_T(\text{solvent}) - E_T(\text{TMS})}{E_T(\text{water}) - E_T(\text{TMS})} = \frac{E_T(\text{solvent}) - 30.7}{32.4} \qquad (2)$$

Some of the $E_T(30)$ values were given in deviate somewhat from earlier published values [40]. This is due to recently improved methods for purification and drying of the solvents under consideration. Because of the extreme sensitivity of the indicator pyridinium N-phenolate betaine dye to changes in solvent polarity, traces of polar impurities in less polar solvents can lead to incorrect $E_T(30)$ values, caused by preferential solvation of the betaine molecule with the more polar component of the solvent mixture.

1.8 Multiparameter approaches

In applying the aforementioned, spectroscopically derived empirical parameters to the correlation analysis of solvent effects, it is tacitly assumed that the contribution of the various, nonspecific and specific, intermolecular forces to the overall interaction between solvatochromic probe and solvent molecules is the same as in the interaction between the solute and solvent of interest in the particular solvent-dependent process under investigation. The successful application of the $E_T(30)$ values in correlation

analysis of a great variety of solvent-dependent processes demonstrates that this is often the case. However, according to the chemical structure of the solvatochromic probe N-phenolate betaine**,** this dye is not capable of interacting specifically and significantly with *electron-pair donor* (EPD) solvents. That is, the Lewis basicity of solvents is not registered by this probe, whereas the solvent Lewis acidity is.

Analogous considerations can be made for other empirical solvent polarity parameters derived from solvatochromic dyes. A great variety of multiparameter treatments of solvent effects have been developed, using not only UV/visible/near-IR spectroscopically derived empirical parameters, but also parameters based on equilibrium and kinetic measurements as well as on other spectroscopic methods (e.g. from IR, NMR, and ESR measurements). Multiparameter treatments of solvent solvent effects have been reviewed [41-56]. Multiparameter equations of this kind are still manifestations of linear free-energy relationships [47, 48]. A statistical analysis of the problem how many significant solvent parameters are necessary for a complete quantitative description of solvent effects by means of multiparameter equations has been recently given by Palm et a1 [49]. In the following, only multiparameter treatments based on solvatochromic probe molecules will be mentioned.

The reason for the introduction of multiparameter equations is the observation that solute-solvent interactions, responsible for the solvent influence on equilibria, rates, and absorptions, are caused by a multitude of nonspecific (ion-dipole, dipole/dipole, dipole/induced dipole, instantaneous dipole/induced dipole) and specific (H bonding, EPD/EPA interaction) intermolecular forces between solute and solvent molecules. Is it then possible to develop individual empirical parameters for each of these distinct interaction mechanisms and combine them into a multiparameter master equation such as eq 3:

$$XYZ = (XYZ)_0 + aA + bB + c\mathrm{C} + \ldots \qquad (3)$$

Where the regression coefficients describe the sensitivity of solute property *XYZ* to the different solute/solvent interaction mechanisms and help to unravel the observed overall solvent effect into its various contributions? This appealing concept depends on the possibility of finding solvatochromic (or other) probe molecules which interact with solvents by only one of the existing intermolecular solute-solvent interaction mechanisms and this is not so easy to achieve.

One of the most ambitious, and very successful, quantitative treatments of solvent effects by means of a multiparameter equation such as eq 3 is that introduced by Kamlet and Taft in 1976 [50] and called *linear solvation energy relationship* (LSER) [41,50,51]. Using three UV/visible spectroscopically derived solvatochromic parameters, $\pi^*, \alpha,$ and $\beta,$ eq 4 was established, where y_0, a, b, and c are solvent independent coefficients characteristic of the process under study and indicative of its susceptibility to the solvent properties π^*, α, and β.

$$y = y_0 + a\alpha + b\beta + c\pi^* \qquad (4)$$

The solvatochromic parameter π^* measures the exoergic effects of solute/solvent, dipole/dipole, and dipole/induced dipole interactions. That is, it measures the ability of a solvent to stabilize a neighboring charge or dipole by virtue of nonspecific dielectric interactions. Therefore, π^* values represent a blend of dipolarity and polarizability of the solvent. The solvatochromic parameter a in eq 4 is a quantitative, empirical measure of the ability of a bulk solvent to act as a *hydrogen-bond donor* (HBD) toward a solute [41,55-57]. The solvatochromic parameter β in eq 4 is a quantitative, empirical measure of the ability of a bulk solvent to act as a *hydrogen-bond acceptor* (HBA) or electron-pair donor (EPD) toward a solute, forming a solute-to-solvent hydrogen bond or a solvent-to-solute coordinative bond, respectively [41, 52-56].

1.9 Limit of detection

A limit of detection of an analyte is generally defined as the concentration which gives as instrument signal significantly difference from the blank or background signal. This definition of the detection is quite arbitrary and entirely open to an analyst to provide an alternative definition that for a particular purpose. However, it is required to provide the definition whenever a detection limit is cited in a paper or report.

This is an alternative definition that defines the detection limit as the analyte concentration giving a signal equal to the blank signal, y_B, plus three standard deviations of the blank, S_B [57].

$$\text{Limit of detection} = y_B + 3S_B \qquad (5)$$

According to equation (1), the value of a, the calculated intercept of the calibration plot can be used instead of y_B.

CHEAPTER II

LITERATURE REVIEWS

2.1 Literature reviews

Curcumin, a major polyphenolic pigment of the root turmeric or *Curcuma longa L.*, belonging to the *zingeberacea* family, is widely cultivated in several tropical parts of Asis [58]. About 2–8% of turmeric by weight is **curcumin**. **Curcumin** and some of its analogues are responsible for the bright yellow color of turmeric. **Curcumin** recent success as an anti-tumor agent, has been attracting researchers from wide ranging fields of physics, chemistry, biology and medicine. The chemical structure of **curcumin** has two *o*-methoxy phenols attached symmetrically through α, β-unsaturated β-diketone linker, which also induces keto–enol tautomerism. **curcumin** predominantly exists in the enol form [59]. However, under some special conditions like low pH, the keto form may also exist in equilibrium with the enol form. The keto and enol tautomeric equilibrium in **curcumin** is represented in Figure 2.1. The calculated fully optimized geometry of enolic **curcumin** both in vacuum and in solutions by DFT studies indicated that the enol form is planar and more stable than the diketo form, which is nonplanar [60]. The enolic form, with the dihedral angle of 180° is having perfect resonance between the two phenolic rings and the electron density is distributed on the entire molecule. The keto form on the other hand is twisted.

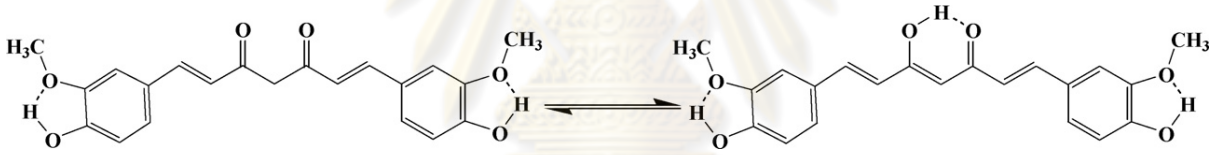

Figure 2.1 Chemical structures of **curcumin** in keto–enol tautomeric equilibrium.

Curcumin is readily soluble in solvents like methanol, ethanol, DMF, DMSO, chloroform, acetonitrile, etc. and is moderately soluble in hexane, cyclohexane, carbon tetrachloride, tetrahydrofuran, dioxane and tert-butanol. Solid **curcumin** is bright yellow in color, and in solution, it exhibits strong absorption in the UV–visible region with absorption maximum in the range from 408 to 434 nm [61-66]. In non-polar solvents, as proposed in simple β-diketones, **curcumin** may exist in keto–enol equilibrium. The keto form being less polar than the enol form, may get stabilized in non-polar solvents, and its contribution may result in blue shifted absorption spectrum. As the polarity of the solvent is increased, the keto–enol equilibrium is shifted towards the enol conformer and the spectral structure is lost. In most of the polar solvents, the absorption maximum is at ~420 nm, while in hydrogen bond acceptor and donor solvents, the absorption maximum is around 430–434 nm, except in methanol where it is ~423–428 nm. In glacial acetic acid, the absorption maximum is at 422 nm and in basic aqueous medium, the yellow color turns bright red, with the absorption maximum shifting to 463 nm due to the ionisation of phenolic OH group and the phenoxide ion is bright red in color [67]. By theoretical studies, Shen and Ji [68] predicted that the **curcumin** anion formed from the deprotonation of the phenolic OH group shows absorption maximum at 531 nm and in one experimental study also, Zsila et al [69] reported absorption maximum at 535 nm in ethanolic-KOH solutions. The strong absorption band observed in

solutions at ~410–430 nm was initially considered to be of n–π^* electronic transition [70], however subsequent studies confirmed it to be of π–π^* nature [66]. The assignment of the absorption band to π–π^* is mainly based on spectral position, spectral shift from non-polar to polar organic solvents and the intensity of the absorption band. The theoretically predicted absorption maximum for the diketo form is 389 nm while those for the enol form are 419 nm. The strong, intense, and experimentally observed absorption maximum at ~420 nm has now been assigned to the π–π^* transitions in the enolic form in solution [68].

Steady state fluorescence spectroscopic investigations of **curcumin** have been reported in organic solvents. The fluorescence spectrum, fluorescence maximum and the fluorescence quantum yield of **curcumin** have been found to be very sensitive to the nature of the solvent. The Stokes' shift varied significantly with the nature of the solvent from 2000 to 6000 cm^{-1} (~30–140 nm) [61-62, 76]. The fluorescence spectrum of **curcumin** in cyclohexane is significantly different from other solvents; with two fluorescence maxima at 446 and 470 nm and the Stokes' shift is 2088 cm^{-1}. In this solvent, the excited state in enol form, has intramolecular hydrogen bonded structure. In non-polar aromatic solvents like toluene and benzene, the fluorescence spectrum is sharp and the maximum is observed at 460–464 nm. Although the polarity of these solvents is similar to that of cyclohexane, interaction between the aromatic π-bonds of the solvent with **curcumin** could disturb the intramolecular hydrogen bonding and induces larger Stokes' shift [61]. In aprotic solvents like chloroform, acetonitrile, ethyl acetate, and acetone the fluorescence intensity and maximum showed variation from 494 to 538 nm. In these solvents, the polarity effects influence the intramolecular hydrogen bonding, and the less rigid structure is more prone to out of plane vibrations [68]. In hydrogen bond donating and accepting solvents, like alcohols, DMF and DMSO, the Stokes' shift is much larger with fluorescence maximum shifting to 535–560 nm. H-bond donating solvents can interact with the keto (C=O) group and H-bond accepting solvents interact with the enolic protons of keto–enol moiety. Alcohols being both H-bond donating and H-bond accepting induce much larger Stokes' shift (~5952 cm^{-1} in methanol) leading to the broadening of the spectra. Thus the solvent dependent steady state fluorescence spectral shifts confirm that the ICT state produced immediately after photo-excitation of **curcumin** is influenced both by the intramolecular and intermolecular proton transfer reactions. In a very recent study, the excited state photophysics of **curcumin** was reported in methanol and ethylene glycol using ultrafast fluorescence conversion spectroscopy and the lifetimes due to solvation and excited state intermolecular proton transfer (ESIPT) process have been distinctly resolved [63]. The longer component in the time scale of 70–105 ps, which also exhibits isotope effects in deuterated solvents, has been attributed to the ESIPT process.

In recent years, a lot of work has been focused on the synthesis of 4,4-difluoro-4-bora-3a,4adiaza-*s*-indacene (borondipyrromethene, BDP, or BODIPY)-based fluorescent probes and their application [72-73] as selective and efficient sensors of ionic species. BDP dyes have many valuable qualities such as high photostability, high fluorescence quantum yields, and relatively high absorption coefficients. Furthermore, they are photoexcitable with visible light, have narrow emission bandwidths with high peak intensities, and are amenable to structural modification [74]. Absorption and emission energies of the BDP are affected by the nature of the substituents on the dipyrromethene and the boron atom. Recently, Rohand et al showed that molecule **1** (Figure 2.2) is an enable to substitution at the 3- and 5-positions by a variety of nucleophiles [75] and that the photochemical properties of the BDP are highly dependent on the nature of these substituents [76]. A series of aza-BDP dyes **1a-1g**, having a

range of different substituted-aryl groups were prepared by Burgess et al [77] (Figure 2.2). The absorption spectra of compounds **1** show strong $S_0 \rightarrow S_1$ transitions with absorbance maxima between 650 and 798 nm (Figure 2.2a). The absorption spectra of compounds **1** indicate that introduction of electron-donating groups onto the aryl substituents results in significant bathochromic shifts. The largest red-shift in the series was observed for compound **1g**, which has two strongly electron-donating groups attached to the 3-aryl substituents in ortho- and para-positions. This is consistent with the idea that the HOMO/LUMO energy levels of the aza-BDP core are influenced in such a way that fluorescence is enhanced by the electron rich aryl substituents. Comparison of molecules **1c-1e** with the rest of those in the series implies that the presence of an ortho-methoxy group on the 3-aryl substituent correlates with a blue-shift in the absorbance, but this may be overridden by a strongly electron-donating group in the para-position of the same aromatic ring (Figure 2.3).

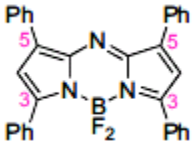

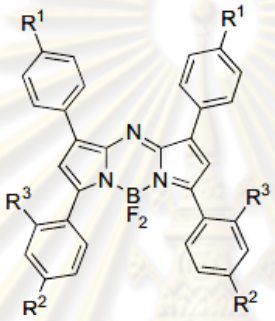

cpd	R^1	R^2	R^3
a	OMe	I	H
b	Br	OMe	H
c	H	H	OMe
d	Br	H	OMe
e	I	H	OMe
f	Br	OMe	OMe
g	Br	NMe_2	OMe

Figure 2.2 Structure of compound 1a-1g.

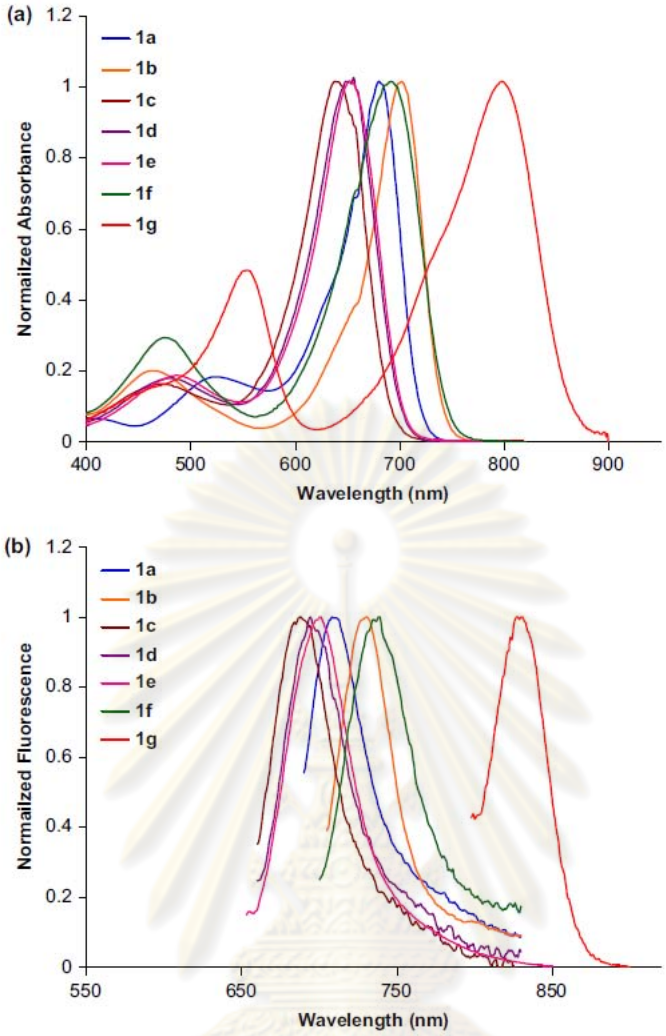

Figure 2.3 (a) Normalized absorption and (b) fluorescence spectra of compound **1a-1g** in toluene at 5 mM

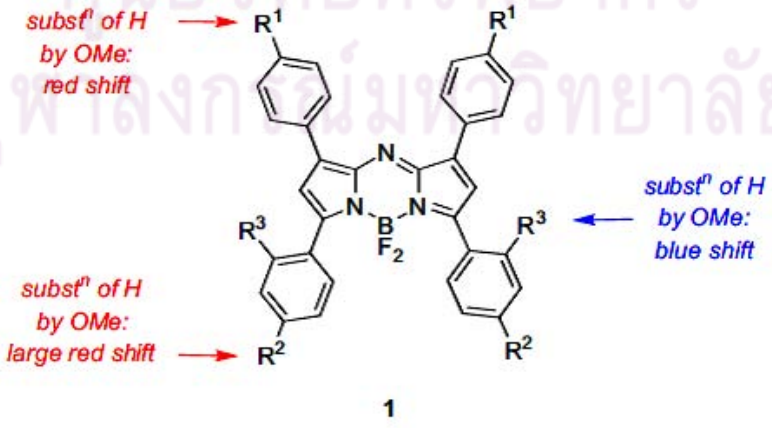

Figure 2.4 Key spectroscopic data for the aza-BDP derivatives **1a-g**

Fluorescence spectra the new dyes are also shown in Figure 2.3b. Their emission maxima range from 676 to 830 nm in toluene. These studies show that the fluorescence emissions observed from aza-BDP dyes can be manipulated by altering the electronic substituents on the aryl substituents. Red-shifts in the fluorescence tend to correspond to strongly electron-donating para-groups, at least for the 3-aryl substituent.

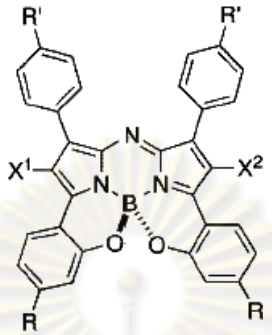

2a-h

	A	**b**	**C**	**d**	**e**	**F**	**G**	**h**
R	**H**	**H**	**OMe**	**NMe_2**	**H**	**H**	**OMe**	**H**
R′	**H**	**Br**	**Br**	**Br**	**Br**	**Br**	**H**	**OMe**
X^1	**H**	**H**	**H**	**H**	**Br**	**Br**	**H**	**H**
X^2	**H**	**H**	**H**	**H**	**H**	**Br**	**H**	**H**

Figure 2.5 Structure of compound **2a**-**2h**

Loudet and co works [78] investigated the photophysical properties of **2a-h** (Figure 2.5). The result showed that the longest absorbance/emission wavelength maxima (765/782 nm) were observed for derivative **2g** containing electron donating methoxy substituents on the benzo{1,3,2}oxazaborinine rings. In addition, the absorbance spectra showed only a small sensitivity to solvent polarity. For example, the $\lambda_{max,\ abs}$ of **2g** in DMF is only red-shifted by 5 nm when compared to 761 nm in cyclohexane. Inspection of fluorescence maxima for **2g** and **2h** revealed a small blue shift trend in polar solvents.

BDP is attracted considerable attention especially within the past few years in a variety of potential applications such as ion sensing and signaling [79], energy transfer cassettes [80], light-harvesting systems [81], fluorescent labeling of biomolecules [82], and as potential sensitizers in photodynamic therapy [83]. Ekmekci and co-workers [84] have successfully designed and synthesized of new BDP-based chemosensor (compound **3**) for selective and sensitive reporting of cyanide ions in solution at micromolar concentrations. The treatment of compound **3** with Bu_4NCN in acetonitrile displays a large decrease in emission intensity and a reversible color change from red to blue on contact with cyanide ions as shown in Figure 2.6. In the case of CN^-, the absorption band at 561 nm decreased, while a new band at 594 nm appeared. The emission band of compound **3** at 571 nm (ex. 560 nm.) showed the 14-fold fluorescent quenching upon the addition of 30 μM CN^-. The mechanism for ON-OFF switching in the presence of CN^- was suggested in Scheme 2.7.

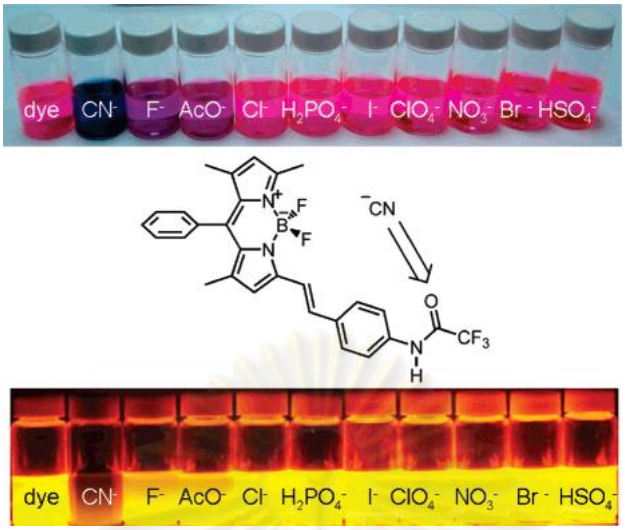

Figure 2.6 Colorimetric changes of compound **3** upon the addition of cyanide ions

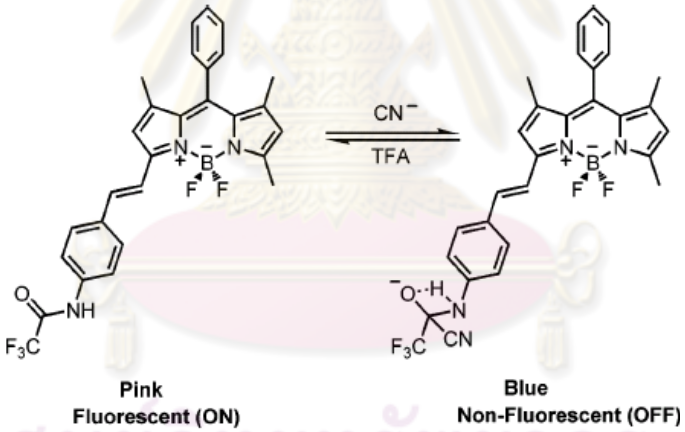

Figure 2.7 Suggested Mechanism for ON-OFF switching of compound **3** within the presence of CN^- Ions

Absorption and emission spectra of polymer film doped with compound **3** were obtained, and 10 nm bathochromic shifts were observed in absorption and emission maxima. A solution containing tetrabutylammonium cyanide in acetonitrile (1 mM) was sprayed onto the film, and the solvent was evaporated in air. A blue nonfluorescent image appeared on the regions exposed to cyanide ions (Figure 2.8).

Figure 2.8 Fluorescence image of poly(methyl methacrylate) polymer sheets doped with chemosensor **3**

New BODIPY derivative (compound **4**) [85] was synthesized for operating in 'turn-off-on' mode for selective and sensitive detection of cyanide ions in a water-organic solventmixture. Compound **4** is a fluorescent molecule having a relatively high quantum yield (Φ_F = 0.24) and absorption peak at 537 nm. To determine the cyanide sensing ability, compound **4** was converted to non-fluorescent 'off-mode' by complexation with Cu(II) ions. As expected from the very high stability constant of the tetracyanocuprate(II) complex ion, the addition of cyanide to the copper(II) complex of **4** released the free receptor, sensing in fluorescent 'on-mode' of the chemosensor and absorption wavelength-ratiometric behaviour in the reverse direction was observed including an isosbestic point at 549 nm (Figure 2.9). The emission spectra in the presence of increasing cyanide to the copper(II) complex was observed increment in the emission intensity with a small hypsochromic shift (Figure 2.10). The sensor can detect cyanide concentrations as low as 0.66 μM in water.

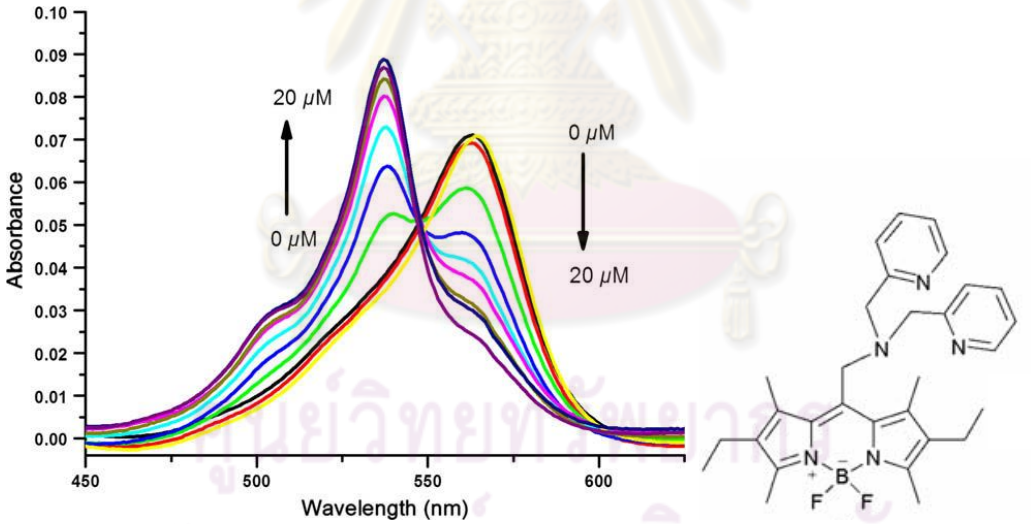

compound 4

Figure 2.9 Absorbance spectra of compound **4**+Cu(II) in the presence of increasing CN^- concentrations (0, 3.3, 6.7, 10.0, 11.7, 13.3, 15.0, 16.7, 18.3 and 20.0 μM)

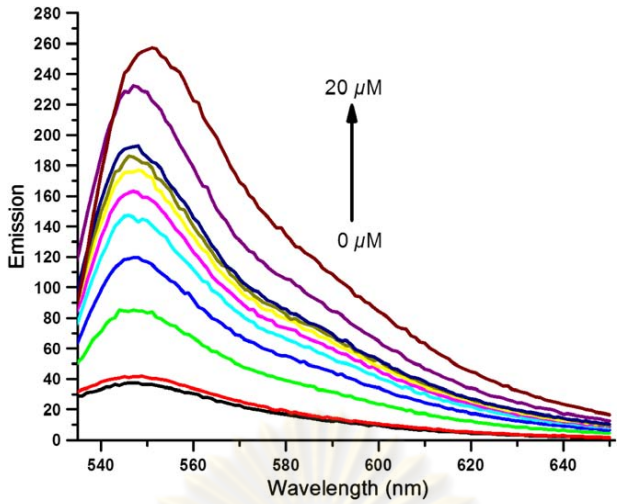

Figure 2.10 Emission spectra of compound **4**+Cu(II) in the presence of increasing CN^- concentrations (0, 3.3, 6.7, 10.0, 11.7, 13.3, 15.0, 16.7, 18.3 and 20.0 μM)

Huh and co-workers [86] combined three-coordinate borane as a donor and highly fluorescent BDP as an acceptor to construct a discrete and highly fluorescent borane-based receptor that utilizes intramolecular excitation energy-transfer transitions for the selective detection of cyanide ion (Figure 2.11). To examine the cyanide binding properties of compound **5**, UV–vis and fluorescence experiments were carried out. Compound **5** features two major absorption bands at 330 nm ($\log_\varepsilon$= 4.49) and 501 nm ($\log_\varepsilon$= 4.92) in THF assignable to the transition in the borane and the transition in the BDP moiety, respectively (Figure 2.12).

A comparison with the absorption spectra of the closely related mononuclear compounds **5** and Mes_2B(*p*-biphenyl), one can note that the wavelengths of the absorption maxima (λ_{max}) of the two fluorophores in **5** show almost no change, thus indicating the presence of little electronic communication between the two moieties. The orthogonal arrangement of the BDP and the adjacent phenylene ring fragments is probably responsible for this feature. The addition of cyanide to a THF solution of **5** leads to a decrease in the intensity of the absorption band of the borane moiety at 330 nm, while the band of the BDP fragment at 501 nm remains unchanged throughout the titrations (Figure 2.12).

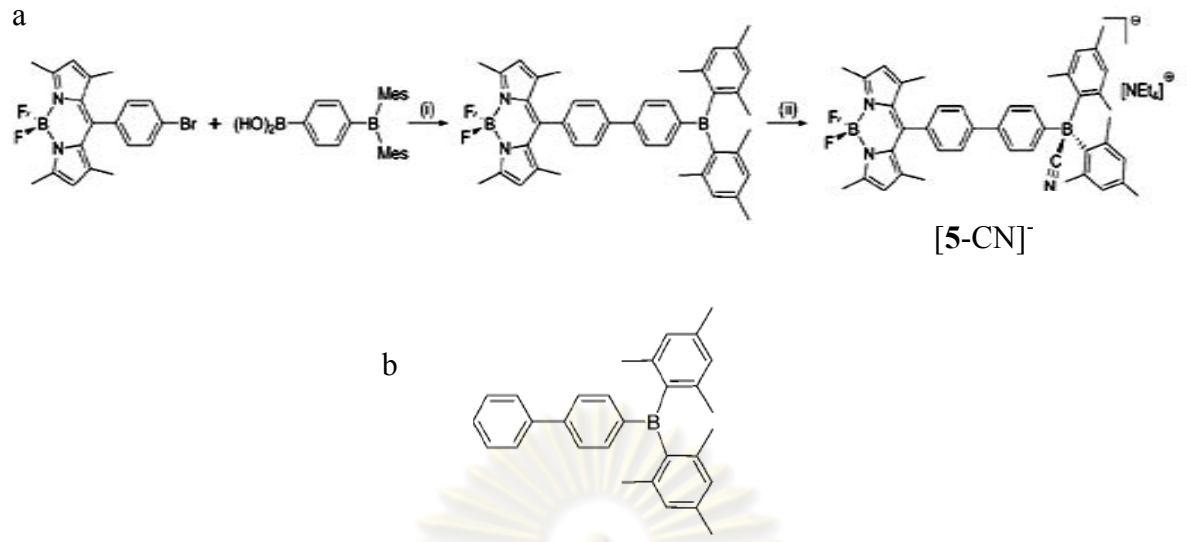

Figure 2.11 a) Schematical illustration of synthesis compound **5**. b) Structure of Mes_2(*p*-biphynyl)

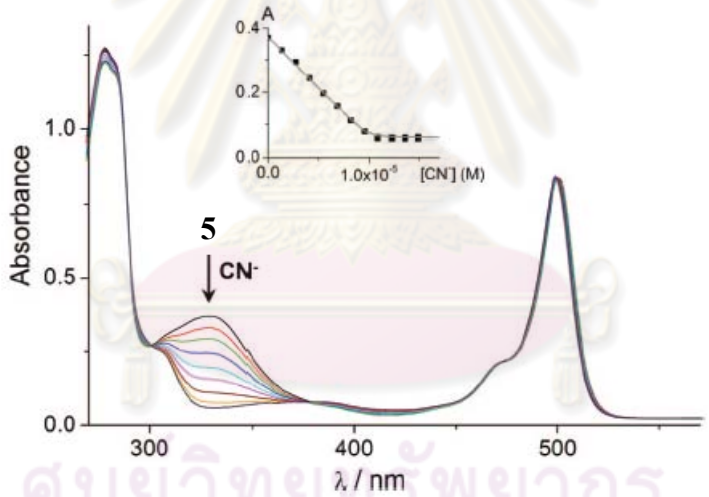

Figure 2.12 Spectral changes in the UV–vis absorption of a solution of **5** in THF (1.0 x 10^{-5} M) upon addition of Bu_4NCN (0–15 μM). The inset shows the absorbance at 330 nm as a function of [CN^-]

The independent absorption characteristics of the two fluorophores in **5** thus provide a basis for the utilization of **5** as a donor–acceptor pair for intramolecular energy-transfer transitions. The emission spectrum of **[5-CN]$^-$** irradiated at 330 nm exclusively exhibits a very intense green fluorescence (λ_{em} 510 nm; Figure 2.13, right) while the [Mes_2B(*p*-biphenyl)-CN^-] was irradiated at the same excitation giving a blue fluorescence at λ_{em} 394 nm (Figure 2.13, left). This result implies an energy transfer from the borane moiety induced by 330 nm irradiation to the BODIPY fragment, where subsequent emission occurs.

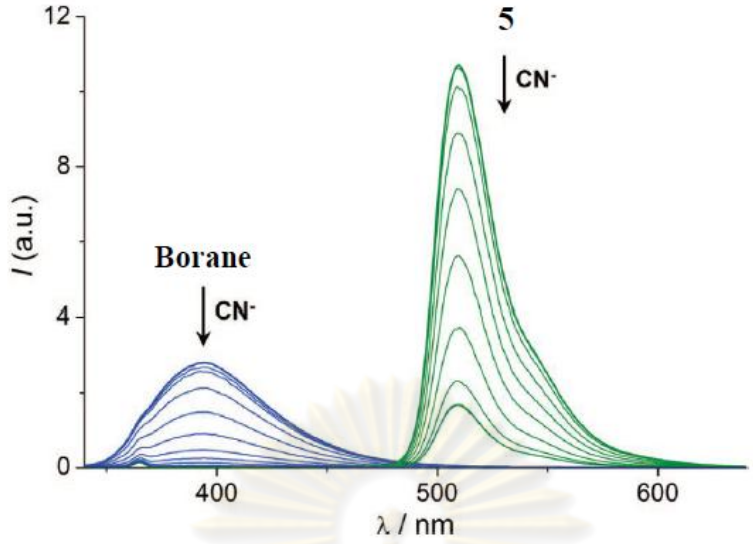

Figure 2.13 Comparison of the fluorescence response of solutions of **5** (right) and Mes_2B(*p*-biphenyl) (left) in THF (λ_{ex} 330 nm; 1.0 x 10^{-6} M) upon addition of Bu_4NCN (0-2 μM)

Hydroxyl-functionalized difluoroboron dibenzoylmethane, **BF_2-dbmOH**, was prepared for use as an initiator in the ring opening polymerization of lactide to produce **BF_2dbm** end-functionalized polylactide, **BF_2-dbmPLA** [87]. The optical properties of the boron initiator and polymer were investigated in CH_2Cl_2 solution and in the solid state (Figure 2.14). UV/vis spectroscopic data are similar for **BF_2dbmOH** (λ_{max} = 397 nm, ε = 53 000 M^{-1} cm^{-1}) and **BF_2-dbmPLA** (λ_{max} = 396 nm, ε = 50 100 M^{-1} cm^{-1}), showing high molar absorptivities characteristic of this family of compounds. Under black light illumination (λ_{max} = 365 nm) in air, intense blue fluorescence is observed for **BF_2-dbmOH** (Figure 2.14C) and **BF_2-dbmPLA** (λ_{max} = 436 nm), and the fluorescence quantum yields of both molecule, Φ_F, are very high (**1**: 0.95; **2**: 0.89) compared to those of **BF_2-dbm** and 1,3-di(4-methoxyphenyl)-propane-1,3-dione as 0.20 and 0.85, respectively. Due to the near UV excited fluorescence, solutions appear blue even in ambient light or upon flashlight illumination.

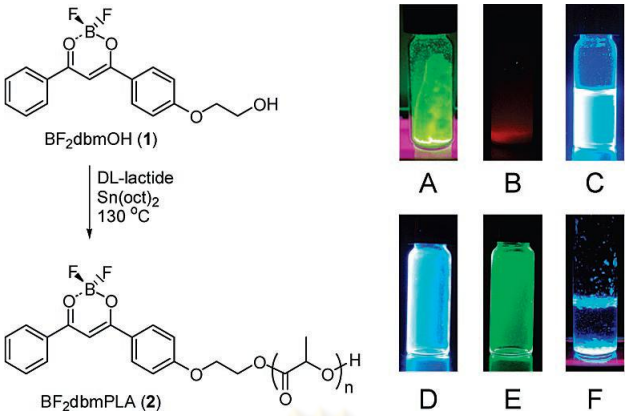

Figure 2.14 Polymer synthesis and boron initiator and polymer luminescence (λ_{max} = 365 nm; room temperature in air unless indicated). BF_2-dbmOH: (A) solid-state green-yellow fluorescence; (B) red phosphorescence (77 K); (C) blue fluorescent CH_2Cl_2 solution. BF_2-dbmPLA: (D) short-lived blue fluorescence and (E) long-lived green phosphorescence for a thin film (N_2); (F) blue fluorescent particle suspension in H_2O after 45 days.

By incorporating a classic boron dye into a common biopolymer, a readily processable, single-component, multi-emissive material exhibiting intense fluorescence, delayed fluorescence, and unusual room-temperature phosphorescence is achieved. The optical properties of **BF_2-dbmPLA** are responsive to temperature, oxygen, and the polarity and rigidity of the local medium.

2.2 Objective and scope of this research

The main goals of this research are to design and synthesize a naked-eye sensor for detection of cyanide and study on the optical properties of **BF_2-CurOH**. To study on photophysical properties, therefore, the substituted-OH **BF_2-curcumin** derivatives (**BF_2-CurOMe**, **BF_2-CurmonoTs** and **BF_2-CurdiTs**) were synthesized. Since **curcumin**, **BF_2-CurOH** and **BF_2-CurmonoTs** contain hydroxyl groups capable to interact with anions. The anion complexations were investigated by UV-visible and fluorescence spectroscopy.

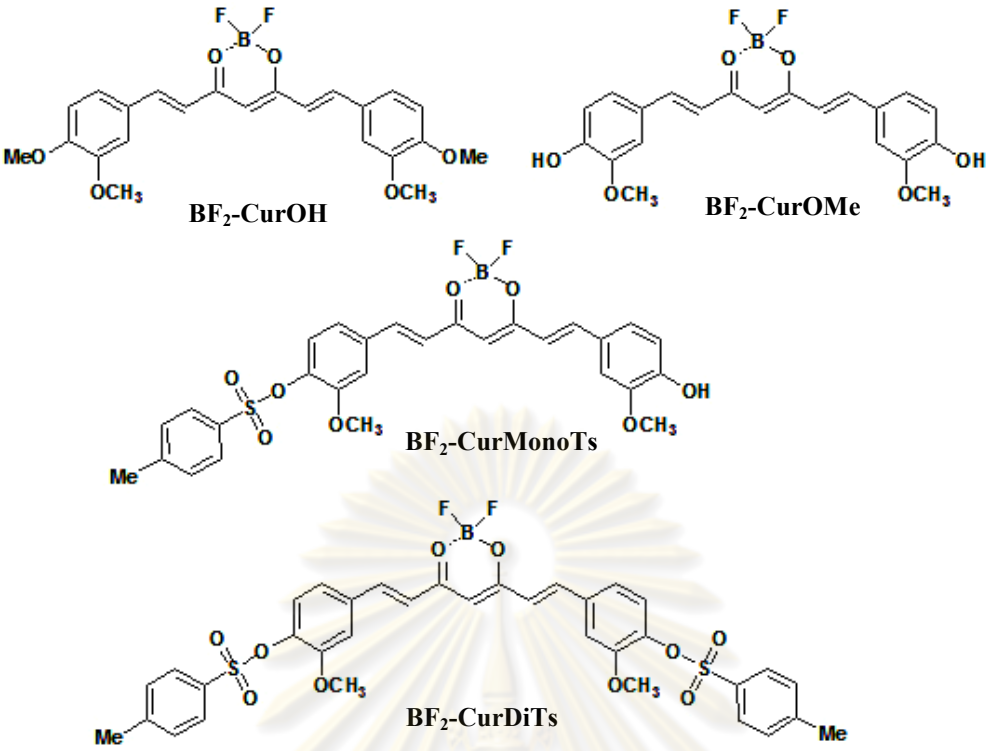

Figure 2.15 Molecular structures of **BF_2-curcumin** derivatives were studied in this work

CHAPTER III

EXPERIMENTAL SECTION

3.1 General procedures

3.1.1 Analytical instrument

Nuclear magnetic resonance (NMR) spectra were recorded on a Varian 200, 400 and Bruker DRX 400 MHz nuclear resonance spectrometers. In all cases, samples were dissolved in deuterated DMSO. The chemical shifts were recorded in part per million (ppm) using a residue proton solvents as internal reference. Elemental analysis was carried out on CHNS/O analyzer (Perkin Elmers PE 2400 series II). MALDI-TOF mass spectra were recorded on Bruker Daltonic using doubly recrystallized 2-cyano-4-hydroxy cinnamic acid (CCA) as matrix. Absorption spectra were measured by a Varian Cary 50 UV-Vis spectrophotometer. Fluorescence spectra were performed on Varian spectrofluorometer by personal computer data processing unit. The light source is Cary Eclipse a pulsed xenon lamp and a detector is a photomultiplier tube.

3.1.2 Materials

Unless otherwise specified, the solvents and all materials were reagent grades purchased from Fluka, BDH, Aldrich, Carlo erba, Merk or Lab scan and used without further purification. Commercial grade solvents such as acetone, dichloromethane, hexane, methanol and ethyl acetate were purified by distillation before used. Dimethylformamide for set up the reaction was dried over calcium hydride and freshly distilled under nitrogen atmosphere prior to use.

Column chromatography was carried out on silica gel (Kieselgel 60, 0.063-0.200 mm, Merck). Thin layer chromatography (TLC) was performed on silica gel plates (Kieselgel 60, F_{254}, 1 mm). Compounds on TLC plates were detected by the UV-light. Ethanol, chloroform, benzene, toluene, diethylether, methanol, dimethyl sulfoxide and dichloromethane used in UV-visible and fluorescence measurement (AR grade, Lab Scan) were dried over molecular sieve prior to use.

All synthesized compounds were characterized by ^{1}H-NMR spectroscopy, ^{1}H-NMR spectroscopy, mass spectrometry and elemental analysis.

3.2 Synthesis

3.2.1 Preparation of curcumin borondifluoride (BF_2-CurOH)

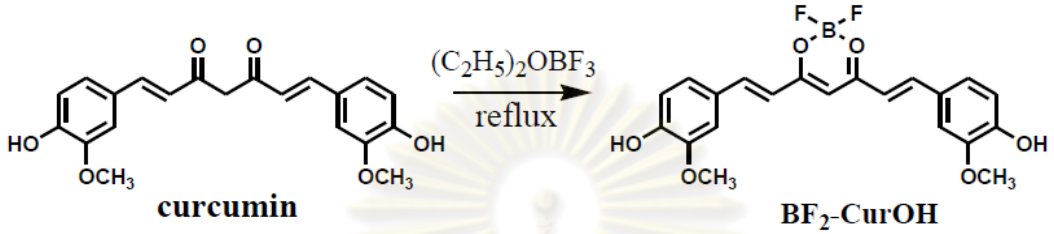

Into a 250 mL two-neck round bottom flask, **curcumin** (2.947g, 8 mmol) was dissolved in methanol (200 ml) to give a bright yellow solution. Borontrifluoride diethyl etherate (1.02 ml, 8 mmol) was added and the solution turned to red suddenly. The reaction was refluxed at 60 °C for 2 h under N_2 and then cooled down to room temperature. Solvent was removed under reduced pressure to obtain a red powder. The desired product, **BF_2-CurOH** 61% yield, was obtained as a red solid after recrystallization in MeOH:EtOAc (1:3).

Characterization data for BF_2-CurOH

^{1}H-NMR spectrum (400 MHz, DMSO-d_6) : δ (in ppm) = 10.09 (s, -O*H*, 2H), 7.90 (*J* = 15.6 Hz, d, -olifinic *H*, 2H), 7.45 (s, -Ar*H*, 2H), 7.32 (*J* = 8.0 Hz, d, -Ar*H*, 2H), 6.99, 6.85 (*J* = 8.0 Hz, d, -Ar*H*, 2H), 6.42 (s, -Ar*H*, 1H), 3.83 (s, - OCH_3, 6H,)

^{13}C-NMR spectrum (100 MHz, DMSO-d_6) : δ (in ppm) = 56.18, 101.60, 112.73, 116.39, 118.22, 125.78, 126.39, 147.37, 148.62, 151.86, 179.03

MS(ESI): m/z for $C_{21}H_{19}BF_2O_6$ = 443.26 [M^+]

Elemental analysis:

Anal. Caled for $C_{21}H_{19}BF_2O_6$	C, 60.60; H, 4.60
Found	C, 60.46; H, 4.71

3.2.2 Preparation of methylation curcumin borondifluoride (BF_2-CurOMe)

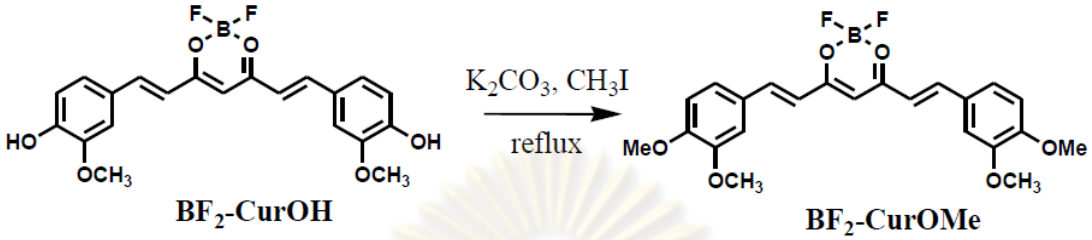

BF_2-CurOH **BF_2-CurOMe**

Into a 250 mL two-neck round bottom flask equipped with a magnetic bar and a reflux condensor, a solution of **BF_2-CurOH** (0.416 g, 1 mmol) and anhydrous potassium carbonate in methanol (100 ml) was mixed and stirred for 10 min. Methyl iodide (1.5 mL, 2 mmol) in methanol (4 mL) was added dropwise into the mixture. The reaction mixture was refluxed at 60 °C overnight. The solvent was removed by rotary evaporator to obtain crude product. The crude product was dissolved in ethyl acetate and washed with water. The organic layer was dried over anhydrous sodium sulfate and evaporated to dryness under reduced pressure. The desired product (**BF_2-CurOMe**) was obtained as a purple crystalline solid (73 %yield) after recrystallization in hexane/ethyl acetate.

Characterization data for BF_2-CurOMe

^{1}H-NMR spectrum (400 MHz, DMSO-d_6) : δ (in ppm) = 7.95 (*J* = 16.0 Hz, d, -olifinic *H*, 2H), 7.47 (s, -Ar*H*, 2H,), 7.45 (*J* = 8.4 Hz, d, - Ar*H*, 2H), 7.08 (*J* = 25.2 Hz, d, - Ar*H*, 2H,), 7.08 (s, -Ar*H*, 2H), 6.49 (s, -Ar*H*, 1H), 3.82 (s, - OC*H*$_3$, 12H,)

^{13}C-NMR spectrum (100 MHz, DMSO-d_6): δ (in ppm) = 56.11, 56.22, 102.20, 111.63, 112.23, 119.30, 125.64, 127.54, 147.28, 149.55, 153.01, 179.50

MS(ESI): m/z for $C_{23}H_{23}BF_2O_6$ = 445.63 $[M+H]^+$

Elemental analysis:

Anal. Caled for $C_{23}H_{23}BF_2O_6$	C, 62.18; H, 5.22
Found	C, 62.53; H, 5.32

3.2.3 Preparation of tosylation curcumin borondifluoride (BF_2-CurmonoTs and BF_2-CurdiTs)

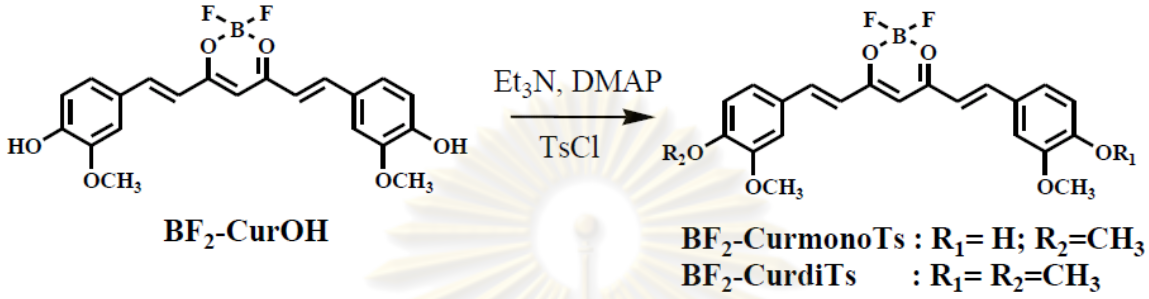

BF_2-CurOH

BF_2-CurmonoTs : R_1= H; R_2=CH_3
BF_2-CurdiTs : R_1= R_2=CH_3

Into a 100 mL two-neck round bottom flask, a solution of **BF_2-CurOH** (0.277 g, 0.67 mmol), DMAP (4-dimethylaminopyridine) and triethylamine (0.084 mL, 2.01 mmol) was mixed and stirred for 30 min in dichloromethane (30 mL) at 0 °C under nitrogen atmosphere. A solution of para-toluenesulfonyl chloride (0.284 g, 1.49 mmol) in dichloromethane (10 mL) was added dropwise through the additional funnel over 30 min into the mixture. Upon completion of the reaction, a solution of HCl (3 M) was added into the mixture to adjust pH to be 1 and stirred for 30 min. The reaction was extracted with water and the organic solvent was evaporated. The crude product was purified by column chromatography using 5% ethyl acetate in dichloromethane to afford **BF_2-CurmonoTs** and **BF_2-CurdiTs** (23 and 71% yield, respectively)

Characterization data for BF_2-CurmonoTs

^{1}H-NMR spectrum (400 MHz, CD_3Cl) : δ (in ppm) = 7.97 (*J* = 15.6 Hz, d, -olifinic *H*,-, 1H), 7.85 (*J*= 15.2 Hz, d, -olifinic *H*, 1H), 7.70 (*J*= 8.0 Hz, d, -Ar*H*, 2H), 7.26 (*J* = 8Hz, d, -Ar*H*, 2H), 7.07 (d, -Ar*H*, 2H), 7.03 (s, -Ar*H*, 1H), 6.93 (d, -Ar*H*, 1H), 6.90 (s, -ArO*H*, 1H), 6.54 (*J*= 15.6 Hz , d, -C*H*=C*H*-, 3H), 6.01 (*J*= 17.2 Hz , d, -C*H*=C*H*-, 2H), 3.90 (s, -OCH_3, 3H), 3.56 (s, -OCH_3, 3H), 1.98 (s, -CH_3, 3H)

MS(ESI): m/z for $C_{28}H_{25}BF_2O_6S$ = 570.87 $[M+H]^+$

Characterization data for BF_2-CurdiTs

^{1}H-NMR spectrum (400 MHz, CD_3Cl) : δ (in ppm) = 7.91 (*J* = 16 Hz, d, -olifinic *H*,-, 2H), 7.70 (*J*= 8.4 Hz, d, -Ar*H*, 4H), 7.26 (*J*= 8.0 Hz, d, -Ar*H*, 4H), 7.15 (d, -Ar*H*, 4H), 6.96 (s, -C*H*=C*H*-, 2H), 6.59 (*J*= 15.6 Hz , d, -C*H*=C*H*-, 2H), 6.04 (s, -C*H*=C*H*-, 1H), 3.57 (s, -OCH_3, 6H), 2.40 (s, -CH_3, 6H)

^{13}C-NMR spectrum (100 MHz, CD_3Cl) : δ (in ppm) = 21.76, 55.74, 102.56, 112.91, 121.34, 121.67, 124.74, 128.59, 129.55, 133.0, 133.73, 140.92, 145.48, 146.38, 152.35, 180.06

MS(ESI): m/z for $C_{35}H_{31}BF_2O_{10}S_2$ = 725.68 $[M+H]^+$

Elemental analysis:

Anal. Caled for $C_{35}H_{31}BF_2O_6S_2$	C, 58.02; H, 4.31
Found	C, 58.79; H, 4.52

3.3 UV-visible and fluorescence studies of BF_2-CurOH, BF_2-CurOMe, BF_2-CurmonoTs and BF_2-CurdiTs

3.3.1 UV-visible studies of BF_2-CurOH, BF_2-CurOMe, BF_2-CurmonoTs and BF_2-CurdiTs

Typically, a 0.01 M solution of **BF_2-CurOH, BF_2-CurOMe, BF_2-CurmonoTs** and **BF_2-CurdiTs** in dichloromethane was prepared in a 10 mL volumetric flask (shown in Table 3.1). The stock solution (1 mL) was pipetted into volumetric flask (10 mL) for preparing the 1 x 10^{-6} M solution.

The 2 mL of 1.0 x 10^{-6} M **BF_2-CurOH, BF_2-CurOMe, BF_2-CurmonoTs** and **BF_2-CurdiTs** in dichloromethane was placed in a 1-cm quartz cuvette and the absorption spectra were recorded from 200-800 nm at ambient temperature.

Table 3.1 Amounts of **BF_2-CurOH, BF_2-CurOMe, BF_2-CurmonoTs** and **BF_2-CurdiTs** used in in UV-visible spectrophotometry studies

Compound	molecular weight ($gmol^{-1}$)	weight (mg)
BF_2-CurOH	416.18	41.61
BF_2-CurOMe	444.23	44.42
BF_2-CurmonoTs	570.37	57.04
BF_2-CurdiTs	724.55	72.46

3.3.2 Fluorescence studies of BF_2-CurOH, BF_2-CurOMe, BF_2-CurmonoTs and BF_2-CurdiTs

Typically, a 0.01 M solution of **BF_2-CurOH, BF_2-CurOMe, BF_2-CurmonoTs** and **BF_2-CurdiTs** in dichloromethane was prepared in a 10 mL volumetric flask (shown in Table 3.1). The stock solution (1 mL) was pipetted into volumetric flask (10 mL) for preparing the 1 x 10^{-6} M solution.

The 2 mL of 1.0 x 10^{-6} M **BF_2-CurOH, BF_2-CurOMe, BF_2-CurmonoTs** and **BF_2-CurdiTs** in dichloromethane was putted in a 1-cm quartz cuvette and the fluorescent spectra were measured at ambient temperature. The excitation wavelength of each solution was shown in Table 3.2.

Table 3.2 The excitation wavelength that used in studies in fluorescence

Compound	excitation wavelength (nm)
BF_2-CurOH	497.1
BF_2-CurOMe	503.0
BF_2-CurmonoTs	482.1
BF_2-CurdiTs	460.1

3.4 Solvatochromism studies of BF_2-CurOH and BF_2-CurOMe

The solvatochromic effects were investigated by using Kamlet-Taft (Linear Solvation Energy Relationship). The values of the π^*, α, and β parameters are the representative of the polarity/polarizability, the acidity (hydrogen bond donor, HBD), and the basicity (hydrogen bond accepter, HBA) of solvent, representatively on the following in eq 1.

$$y = y_0 + a\alpha + b\beta + c\pi^* \qquad \text{(Kamlet-Taft)} \qquad (1)$$

The solvent polarity which induce a shift of absorption spectra was investigated by $E_T(30)$ parameter. The parameters π^*, α, β and $E_T(30)$ is shown in Table 3.3.

Table 3.3 The property parameters of organic solvents HBD ability (α), HBA ability (β), polarity/polarizability (π*) and polarity $E_T(30)$ [89]

Solvent	α	β	π*	$E_T(30)$
Methanol	0.98	0.66	0.60	55.4
Ethanol	0.86	0.75	0.54	51.9
Toluene	0.00	0.11	0.54	33.9
Benzene	0.00	0.10	0.59	34.3
Chloroform	0.20	0.10	0.58	39.1
dichloromethane	0.13	0.10	0.82	40.7
diethyl ether	0.00	0.47	0.27	34.5
ethyl acetate	0.00	0.45	0.55	38.1
DMSO	0.00	0.76	1.00	45.1

3.4.1 Solvatochromism studies of BF_2-CurOH and BF_2-CurOMe by UV-visible spectrophotometry

Typically, a 0.01 M solution of **BF_2-CurOH** and **BF_2-CurOMe** in dichloromethane was prepared in common organic solvents (methanol, ethanol, dichloromethane, toluene, benzene, chloroform, ethyl acetate, diethyl ether and DMSO). The stock solution (1 mL) was pipetted into volumetric flask (10 mL) for preparing the 1 x 10^{-6} M solution.

The 2 mL of 1.0 x 10^{-6} M **BF_2-CurOH** and **BF_2-CurOMe** in common organic solvents (methanol, ethanol, dichloromethane, toluene, benzene, chloroform, ethyl acetate, diethyl ether and DMSO) were putted in a 1-cm quartz cuvette and absorption spectra were recorded from 200-800 nm at ambient temperature.

3.4.2 Solvatochromism studies of BF_2-CurOH and BF_2-CurOMe by fluorescence spectrophotometry

Typically, 0.01 M solution of **BF_2-CurOH** and **BF_2-CurOMe** in common organic solvents (methanol, ethanol, toluene, benzene, chloroform, dichloromethane, diethyl ether, ethyl acetate and DMSO) was prepared in a 10 mL volumetric flask (shown in Table 3.1). The stock solution (1 mL) was pipetted into volumetric flask (10 mL) for preparing the 1×10^{-6} M solution.

The 2 mL of 1.0×10^{-6} M **BF_2-CurOH** and **BF_2-CurOMe** in common organic solvents (methanol, ethanol, toluene, benzene, chloroform, dichloromethane, diethyl ether, ethyl acetate and DMSO) were placed in 1-cm quartz cuvette and fluorescence spectra were recorded at ambient temperature.

3.5 Complexation studies of ligand BF_2-CurOH and curcumin by UV-visible spectrophotometry

3.5.1 Complexation studies of ligand BF_2-CurOH and curcumin with various anions: fluoride, chloride, bromide, iodide, acetate, benzoate and cyanide

Typically, 0.01 M solution of tetrabutyl ammonium hexafluorophophate ($[Bu_4N][PF_6]$) (0.3874 g) in 100 mL of CH_3CN:H_2O (4:1, v/v) was prepared. Stock solution of 0.0005 M solution of **BF_2-CurOH** and **curcumin** in the solvent was prepared in a 10 mL volumetric flask (shown in Table 3.4). The stock solutions (0.25 mL) were pipetted into volumetric flask (25 mL) for preparing the solution to 5×10^{-6} M. A solution of guest in 0.01 M tetrabutyl ammonium hexafluorophophate in CH_3CN:H_2O (4:1, v/v) was prepared in a 10 mL volumetric flask. Solution of 0.01 M of anion (CN^-, F^-, Cl^-, Br^-, I^-, BzO^- and AcO^- as tertbutylammonium salt) in CH_3CN:H_2O (4:1, v/v) was prepared in a 10 mL volumetric flask (shown in Table 3.4).

Table 3.4 Amounts of **BF_2-CurOH**, **curcumin**, CN^-, F^-, Cl^-, Br^-, I^-, BzO^- and AcO^- as tertbutylammonium salt used in studies in UV-visible spectrophotometry

Compound	molecular weight ($gmol^{-1}$)	weight (mg)
BF_2-CurOH	416.18	2.49
Curcumin	368.38	1.84
Bu_4NCN	268.48	2.68
Bu_4NF	261.46	2.61
Bu_4NCl	277.92	2.78
Bu_4NBr	322.38	3.22
Bu_4NI	369.38	3.69
$Bu_4NC_6H_5CO_2$	363.58	3.64
$Bu_4NC_2H_3O_2$	301.51	3.02

Absorption spectra of **BF_2-CurOH**, **curcumin** and both of anion complexes were recorded from 200-800 nm at ambient temperature. The solution of anion (1 mL) was added directly to 2.00 mL of 0.5 x 10^{-6} M of **BF_2-CurOH** (or **curcumin**) in a 1-cm quartz cuvette by pipette and stirred for 30 seconds. Absorption spectra were measured after each addition. Table 3.5 shows gust:host ratios used in the experiments.

Table 3.5 Amounts of anions solutions were used to prepare various anions:ligand ratios

Anion	[anion] M	guest : host ratio
Fluoride	1.01×10^{-3}	150:1
Chloride	0.98×10^{-3}	150:1
Bromide	1.01×10^{-3}	150:1
Iodide	1.03×10^{-3}	150:1
Acetate	0.99×10^{-3}	150:1
Benzoate	1.00×10^{-3}	150:1
Cyanide	1.00×10^{-3}	150:1

3.5.2 Complexation studies of ligand BF_2-CurOH with cyanide ion by UV-visible titration

Typically, 0.01 M solution of tetrabutyl ammonium hexafluorophophate ($[Bu_4N][PF_6]$) (0.3874 g) in 100 mL of CH_3CN:H_2O (4:1, v/v) was prepared. Stock solution of 0.00075 M solution of **BF_2-CurOH** (0.003728 g) in the solvent was prepared in a 10 mL volumetric flask. The stock solution (0.1 mL) was pipetted into volumetric flask (10 mL) for preparing the solution to 7.5×10^{-6} M. A solution of 0.001 M of cyanide tertbutylammonium salt in CH_3CN:H_2O (4:1, v/v) was prepared in a 10 mL volumetric flask. UV-vis spectra of ligand **BF_2-CurOH** and cyanide complexes were recorded from 200-800 nm at ambient temperature. The solution of cyanide anions was added directly to 2.00 mL of 7.5×10^{-6} M of ligand **BF_2-CurOH** in a 1-cm quartz cuvette by microsyringe and stirred for 30 seconds. UV-vis spectra were measured after each addition to have guest:host ratios from 0:1 to 100:1 as shown in Table 3.6.

Table 3.6 The concentration of CN^- ion was used in anion complexation studies with ligand **BF_2-CurOH** and the final ratios of guest:host

Point	CN^-/L	[L] mM	[CN^-] mM	V of CN^- (mL)	V total (mL)
1	0.00	7.50×10^{-3}	0	0	2.00
2	1.0	7.46×10^{-3}	7.46×10^{-3}	0.01	2.01
3	2.0	7.42×10^{-3}	1.48×10^{-2}	0.02	2.02
4	3.0	7.39×10^{-3}	2.22×10^{-2}	0.03	2.03
5	4.0	7.35×10^{-3}	2.94×10^{-2}	0.04	2.04
6	5.0	7.32×10^{-3}	3.66×10^{-2}	0.05	2.05
7	6.0	7.28×10^{-3}	4.37×10^{-2}	0.06	2.06
8	7.0	7.25×10^{-3}	5.07×10^{-2}	0.07	2.07
9	8.0	7.21×10^{-3}	5.77×10^{-2}	0.08	2.08
10	9.0	7.18×10^{-3}	6.46×10^{-2}	0.09	2.09
11	11.0	7.11×10^{-3}	7.82×10^{-2}	0.11	2.11
12	13.0	7.04×10^{-3}	9.15×10^{-2}	0.13	2.13
13	15.0	6.98×10^{-3}	1.05×10^{-1}	0.15	2.15
14	17.0	6.91×10^{-3}	1.18×10^{-1}	0.17	2.17
15	20.0	6.81×10^{-3}	1.36×10^{-1}	0.20	2.20
16	23.0	6.73×10^{-3}	1.55×10^{-1}	0.23	2.23
17	26.0	6.64×10^{-3}	1.73×10^{-1}	0.26	2.26
18	29.0	6.55×10^{-3}	1.90×10^{-1}	0.29	2.29
19	33.0	6.44×10^{-3}	2.12×10^{-1}	0.33	2.33
20	37.0	6.33×10^{-3}	2.34×10^{-1}	0.37	2.37
21	40.0	6.25×10^{-3}	2.50×10^{-1}	0.40	2.40

Point	CN^-/L	[L] mM	$[CN^-]$ mM	V of CN^- (mL)	V total (mL)
22	50.0	6.00×10^{-3}	3.00×10^{-1}	0.50	2.50
23	60.0	5.77×10^{-3}	3.46×10^{-1}	0.60	2.60
24	70.0	5.55×10^{-3}	3.89×10^{-1}	0.70	2.70
25	80.0	5.36×10^{-3}	4.29×10^{-1}	0.80	2.80
26	90.0	5.17×10^{-3}	4.66×10^{-1}	0.90	2.90
27	100.0	5.00×10^{-3}	5.00×10^{-1}	1.00	3.00

3.5.3 Complexation studies of ligand curcumin with cyanide ion by UV-visible titration

Typically, 0.01 M solution of tetrabutyl ammonium hexafluorophophate ($[Bu_4N][PF_6]$) (0.3874 g) in 100 mL of CH_3CN:H_2O (4:1, v/v) was prepared. Stock solution of 0.00075 M solution of **curcumin** (0.00276 g) in the solvent was prepared in a 10 mL volumetric flask. The stock solution (0.1 mL) was pipetted into volumetric flask (10 mL) for preparing the solution to 7.5×10^{-6} M. A solution of 0.001 M of cyanide tertbutylammonium salt in CH_3CN:H_2O (4:1, v/v) was prepared in a 10 mL volumetric flask. UV-vis spectra of ligand **curcumin** and cyanide complexes were recorded from 200-800 nm at ambient temperature. The solution of cyanide anions was added directly to 2.00 mL of 7.5×10^{-6} M of ligand **curcumin** in a 1-cm quartz cuvette by microsyringe and stirred for 30 seconds. UV-vis spectra were measured after each addition to have guest:host ratios from 0:1 to 100:1.

Table 3.7 The concentration of CN^- ion was used in anion complexation studies with ligand curcumin and the final ratios of guest:host

Point	CN^-/**curcumin**	[**curcumin**] mM	[CN^-] mM	V of CN^- (mL)	V total (mL)
0	0	7.50×10^{-3}	0	0	2
1	1	7.44×10^{-3}	7.44×10^{-5}	0.015	2.015
2	2	7.39×10^{-3}	1.48×10^{-4}	0.03	2.03
3	3	7.33×10^{-3}	2.20×10^{-4}	0.045	2.045
4	4	7.28×10^{-3}	2.91×10^{-4}	0.06	2.06
5	5	7.23×10^{-3}	3.61×10^{-4}	0.075	2.075
6	6	7.18×10^{-3}	4.31×10^{-4}	0.09	2.09
7	7	7.13×10^{-3}	4.99×10^{-4}	0.105	2.105
8	8	7.08×10^{-3}	5.66×10^{-4}	0.12	2.12
9	9	7.03×10^{-3}	6.32×10^{-4}	0.135	2.135
10	10	6.98×10^{-3}	6.98×10^{-4}	0.15	2.15
11	11	6.93×10^{-3}	7.62×10^{-4}	0.165	2.165
12	12	6.88×10^{-3}	8.26×10^{-4}	0.18	2.18
13	13	6.83×10^{-3}	8.88×10^{-4}	0.195	2.195
14	14	6.79×10^{-3}	9.50×10^{-4}	0.21	2.21
15	15	6.74×10^{-3}	1.01×10^{-3}	0.225	2.225
16	18	6.61×10^{-3}	1.19×10^{-3}	0.27	2.27
17	19	6.56×10^{-3}	1.25×10^{-3}	0.285	2.285
18	20	6.52×10^{-3}	1.30×10^{-3}	0.3	2.3
19	21	6.48×10^{-3}	1.36×10^{-3}	0.315	2.315

Point	CN^-/**curcumin**	[**curcumin**] mM	[CN^-] mM	V of CN^- (mL)	V total (mL)
20	22	6.44×10^{-3}	1.42×10^{-3}	0.33	2.33
21	23	6.40×10^{-3}	1.47×10^{-3}	0.345	2.345
22	24	6.36×10^{-3}	1.53×10^{-3}	0.36	2.36
23	25	6.32×10^{-3}	1.58×10^{-3}	0.375	2.375
24	26	6.28×10^{-3}	1.63×10^{-3}	0.39	2.39
25	27	6.24×10^{-3}	1.68×10^{-3}	0.405	2.405
26	28	6.20×10^{-3}	1.74×10^{-3}	0.42	2.42
27	29	6.16×10^{-3}	1.79×10^{-3}	0.435	2.435
28	30	6.12×10^{-3}	1.84×10^{-3}	0.45	2.45
29	32	6.05×10^{-3}	1.94×10^{-3}	0.48	2.48
30	34	5.98×10^{-3}	2.03×10^{-3}	0.51	2.51
31	36	5.91×10^{-3}	2.13×10^{-3}	0.54	2.54
32	38	5.84×10^{-3}	2.22×10^{-3}	0.57	2.57
33	40	5.77×10^{-3}	2.31×10^{-3}	0.6	2.6
34	42	5.70×10^{-3}	2.40×10^{-3}	0.63	2.63
35	44	5.64×10^{-3}	2.48×10^{-3}	0.66	2.66
36	46	5.58×10^{-3}	2.57×10^{-3}	0.69	2.69
37	48	5.51×10^{-3}	2.65×10^{-3}	0.72	2.72
38	50	5.45×10^{-3}	2.73×10^{-3}	0.75	2.75
39	53	5.37×10^{-3}	2.84×10^{-3}	0.795	2.795
40	56	5.28×10^{-3}	2.96×10^{-3}	0.84	2.84
41	59	5.20×10^{-3}	3.07×10^{-3}	0.885	2.885
42	62	5.12×10^{-3}	3.17×10^{-3}	0.93	2.93

Point	CN^-/**curcumin**	[**curcumin**] mM	[CN^-] mM	V of CN^- (mL)	V total (mL)
43	65	5.04×10^{-3}	3.28×10^{-3}	0.975	2.975
44	69	4.94×10^{-3}	3.41×10^{-3}	1.035	3.035
45	73	4.85×10^{-3}	3.54×10^{-3}	1.095	3.095
46	77	4.75×10^{-3}	3.66×10^{-3}	1.155	3.155
47	81	4.67×10^{-3}	3.78×10^{-3}	1.215	3.215
48	85	4.58×10^{-3}	3.89×10^{-3}	1.275	3.275
49	90	4.48×10^{-3}	4.03×10^{-3}	1.35	3.35
50	95	4.38×10^{-3}	4.16×10^{-3}	1.425	3.425
51	100	4.29×10^{-3}	4.29×10^{-3}	1.5	3.5

3.6 Complexation studies of ligand BF_2-CurOH and curcumin by fluorescence spectrophotometry

3.6.1 Complexation studies of ligand BF_2-CurOH and curcumin with various anions: fluoride, chloride, bromide, iodide, acetate, benzoate and cyanide

Typically, 0.01 M solution of tetrabutyl ammonium hexafluorophophate ($[Bu_4N][PF_6]$) (0.3874 g) in 100 mL of CH_3CN:H_2O (4:1, v/v) was prepared. Stock solution of 0.005 M solution of **BF_2-CurOH** and **curcumin** in the solvent were prepared in a 10 mL volumetric flask (shown in Table 3.4). The stock solution (0.25 mL) was pipetted into volumetric flask (25 mL) for preparing the solution to 5×10^{-6} M. A solution of guest in 0.01 M tetrabutyl ammonium hexafluorophophate in CH_3CN:H_2O (4:1, v/v) was prepared in a 10 mL volumetric flask. Solution of 0.001 M of anion (CN^-, F^-, Cl^-, Br^-, I^-, BzO^- and AcO^- as tertbutylammonium salt) in CH_3CN:H_2O (4:1, v/v) was prepared in a 10 mL volumetric flask (shown in Table 3.4).

Fluorescence spectra of **BF_2-CurOH**, **curcumin** and both of anion complexes were recorded from 200-800 nm at ambient temperature. The solution of anion was added directly to 2.00 mL of 5.0×10^{-6} M **BF_2-CurOH** (or **curcumin**) in a 1-cm quartz cuvette by microsyringe and stirred for 30 seconds. Absorption spectra were measured after each addition. Table 3.5 shows gust:host ratios used in titration the experiments.

3.6.2 Complexation studies of ligand BF_2-CurOH with cyanide ion by fluorescence titration

Typically, 0.01 M solution of tetrabutyl ammonium hexafluorophophate ($[Bu_4N][PF_6]$) (0.3874 g) in 100 mL of $CH_3CN:H_2O$ (4:1, v/v) was prepared . Stock solution of 0.0075 M solution of **BF_2-CurOH** (0.03728 g) in the solvent was prepared in a 10 mL volumetric flask. The stock solution (10 μL) was pipetted into volumetric flask (10 mL) for preparing the solution to 7.5 x 10^{-6} M. A solution of 0.001 M of cyanide tertbutylammonium salt in $CH_3CN:H_2O$ (4:1, v/v) was prepared in a 10 mL volumetric flask.

Fluorescence spectra of ligand **BF_2-CurOH** and cyanide complexes were recorded from 200-800 nm at ambient temperature. The solution of cyanide anions was added directly to 2.00 mL of 7.5 x 10^{-6} M of ligand **BF_2-CurOH** in a 1-cm quartz cuvette by microsyringe and stirred for 30 seconds. Fluorescence spectra were measured after each addition to have guest:host ratios from 0:1 to 100:1. Fluorescence spectra of ligand **BF_2-CurOH** and cyanide complexes were recorded from 520-800 nm at ambient temperature. The solution of cyanide anions was added directly to 2.00 mL of 7.5 x 10^{-6} M of ligand **BF_2-CurOH** in a 1-cm quartz cuvette by microsyringe and stirred for 30 seconds. Fluorescence spectra were measured after each addition to have guest:host ratios from 0:1 to 100:1.

3.6.3 Complexation studies of ligand curcumin with cyanide ion by fluorescence titration

Typically, 0.01 M solution of tetrabutyl ammonium hexafluorophophate ($[Bu_4N][PF_6]$) (0.3874 g) in 100 mL of $CH_3CN:H_2O$ (4:1, v/v) was prepared. Stock solution of 0.0075 M solution of **curcumin** (0.00276 g) in the solvent was prepared in a 10 mL volumetric flask. The stock solution (10 μL) was pipetted into volumetric flask (10 mL) for preparing the solution to 7.5 x 10^{-6} M. A solution of 0.001 M of cyanide tertbutylammonium salt in CH3CN:H_2O (4:1, v/v) was prepared in a 10 mL volumetric flask. Fluorescence spectra of ligand **curcumin** and cyanide complexes were recorded from 200-800 nm at ambient temperature. The solution of cyanide anions was added directly to 2.00 mL of 7.5 x 10^{-6} M of ligand curcumin in a 1-cm quartz cuvette by microsyringe and stirred for 30 seconds. Fluorescence spectra were measured after each addition to have guest:host ratios from 0:1 to 100:1. Fluorescence spectra of ligand **curcumin** and cyanide complexes were recorded from 520-800 nm at ambient temperature. The solution of cyanide anions was added directly to 2.00 mL of 7.5 x 10^{-6} M of ligand **curcumin** in a 1-cm quartz cuvette by microsyringe and stirred for 30 seconds. Fluorescence spectra were measured after each addition to have guest:host ratios from 0:1 to 100:1.

3.7 Determination of detection limit of BF_2-CurOH with cyanide ion by UV-visible spectroscopy

Typically, 0.01 M solution of tetrabutyl ammonium hexafluorophophate ($[Bu_4N][PF_6]$) (0.3874 g) in 100 mL of $CH_3CN:H_2O$ (4:1, v/v) was prepared. Stock solution of 0.005 M solution of **BF_2-CurOH** (24.85 mg) in the solvent was prepared in a 10 mL volumetric flask. The stock solution (10 μL) was pipetted into volumetric flask (10 mL) for preparing the solution to 5 x 10^{-6} M. Determination of standard deviation (SD) was calculated from absorbance at λ = 507 nm.

3.8 Interference studies by fluorescence spectroscopy

Typically, 0.01 M solution of tetrabutyl ammonium hexafluorophosphate of $CH_3CN:H_2O$ (4:1, v/v) was prepared in all interference studies. Solution of 3.75 x 10^{-5} M of host **BF_2-CurOH** and **curcumin** in 25 mL of the solvent were prepared in a volumetric flask. The solution of guest was prepared in volume metric flask (shown in Table 3.8). The ligand solution (2 mL), CN^- solution (2 mL) and guest (2 mL) were pipetted into same 10 mL volumetric flask and adjusted the total volume to 10 mL. The emission spectra were recorded toward all experiment.

Procedure for determination of relative error: (i) Record the emission intensity of free ligand **BF_2-CurOH** and **curcumin**, (ii) Record the emission intensity of complexation between ligand and CN^-, (iii) Record the emission of complexation ligand + CN^- after adding the foreign guest. The value of relative error was calculated by $(\Delta F_1 - \Delta F_2)/\Delta F_1 \times 100$, where ΔF_1 is the fluorescence decrement of emission intensity of complexation of ligand and CN^- compared to free ligand, ΔF_2 is the fluorescence decrement of emission intensity of complexation ligand + CN^- + foreign guest compared to free ligand.

Table 3.8 Amount of CN^- and anions that used in interference studies with ligand BF2-CurOH and curcumin for fluorescence studie

compound	MW	volume (mL)	conc. ($x10^{-6}$)	weight(g)
BF_2-CurOH	416.18	25	37.5	0.00039
Curcumin	368.38	25	37.5	0.00034
F^-	261.46	10	1500000	3.9219
Cl^-	277.92	10	1500000	4.1688
Br^-	322.38	10	1500000	4.8357
I^-	369.38	10	1500000	5.5407
OAc^-	301.51	10	1500000	4.52265
Bnz^-	363.58	10	1500000	5.4537
$H_2PO_4^-$	339.46	10	1500000	5.0919
CN^-	268.48	50	1500	0.020136

3.9 Determination of quantum yields of curcumin, BF_2-CurOH, BF_2-CurOMe, BF_2-CurmonoTs and BF_2-CurdiTs

The standard compound should be chosen to ensure the absorption at the excitation wavelength for the test sample, and, if possible, emission band is in a similar region. In addition, the chosen concentration range of standard solution and sample solution in 10 mm fluorescence cuvette prepared according to the absorbance of spectrum within 0.1 at the excitation wavelength.

The standard compound used in this experiment was quinine bisulphate which was prepared in a concentration range of 1.8 – 9.0 micromolar. The concentration range of **curcumin, BF_2-CurOH, BF_2-CurOMe, BF_2-CurmonoTs** and **BF_2-CurdiTs** are shown in Table 3.9. All of them were dissolved in dichloromethane.

Procedure for determination of quantum yield: (i) Record the UV-vis absorbance of each solution, (ii) Record the fluorescence spectra of the environment of solution as UV-vis technique. Calculate and note down the integrated fluorescence intensity *vs* absorbance. The result should be a straight line with gradient (Grad.) and intercept = 0.

Table 3.9 The concentration of **curcumin, BF_2-CurOH, BF_2-OMe, BF_2-monoTs** and **BF_2-CurdiTs** were used to determine quantum yield

Compound	Concentration (μM)
Quinine bisulphate	18.00
	36.00
	54.00
	72.00
	90.00
Curcumin	0.40
	0.46
	0.50
	0.53
	0.61
BF_2-CurOH	0.23
	0.34
	0.77
	0.85
	1.06

Compound	Concentration (μM)
BF_2-CurOMe	0.22
	0.33
	0.39
	0.48
	0.51
BF_2-CurmonoTs	0.61
	0.70
	0.97
	1.64
	1.91
BF_2-CurdiTs	0.97
	1.38
	1.82
	2.21
	2.68

CHAPTER IV

RESULTS AND DISCUSSION

4.1 Design concept

Curcumin contains a β-diketone moiety which behaves a keto-enol tautomerism (Figure 4.1). Most of **curcumin** prefers to exist in form of an intramolecular hydrogen bond in solution. The structure of the enol form is perfectly planar and allows resonance within the two benzene parts resulting in the light absorption in visible spectral region. The fixation of **curcumin** to enol form can be improvement the optical property of **curcumin** because more rigid molecule induced a higher π-conjugated system and electron delocalization occurs easily between two aromatic rings.

In several years ago, **curcumin** has been used for detection of boron in various types of matrixes [1]. The β-diketone position of **curcumin** can be fixed to enol form by boron. On the basic of this strategy, we place $\mathbf{BF_2}$ moiety at β-diketone position to improve the optical property of **curcumin**. The coordination of $\mathbf{BF_2}$ was expected to enhance the planarity structure of **curcumin** which influence on improvement optical property of **curcumin**. Concerning the $\mathbf{BF_2}$ part, it might lead to the marked difference of acceptability and donatability of molecule. Consequently, its photophysical properties were attractive to be applied in a field of molecular device.

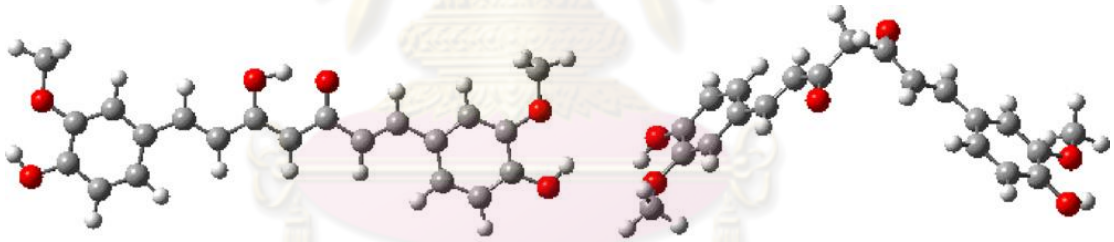

Figure 4.1 Optimized structures of the **curcumin** in enol form and diketone form

From these advantages mentioned above, we have focused on studying the photophysical behavior of molecule modified on hydroxyl group of $\mathbf{BF_2}$**-CurOH**. Therefore, $\mathbf{BF_2}$**-CurOH** and its substituted-OH derivatives (**BF_2-CurOMe**, **BF_2-CurmonoTs** and **BF_2-CurdiTs**) were synthesized by coordinating $\mathbf{BF_2}$ group at β-diketone of **curcumin** and modifying on hydroxyl group of $\mathbf{BF_2}$**-CurOH**. The synthesis pathway is shown in Scheme 4.1. Since $\mathbf{BF_2}$**-CurOH** and $\mathbf{BF_2}$**-CurmonoTs** contain hydroxyl groups capable to interact with anions, the anion complexations were investigated by ^{1}H-NMR, UV-visible and fluorescence spectroscopy.

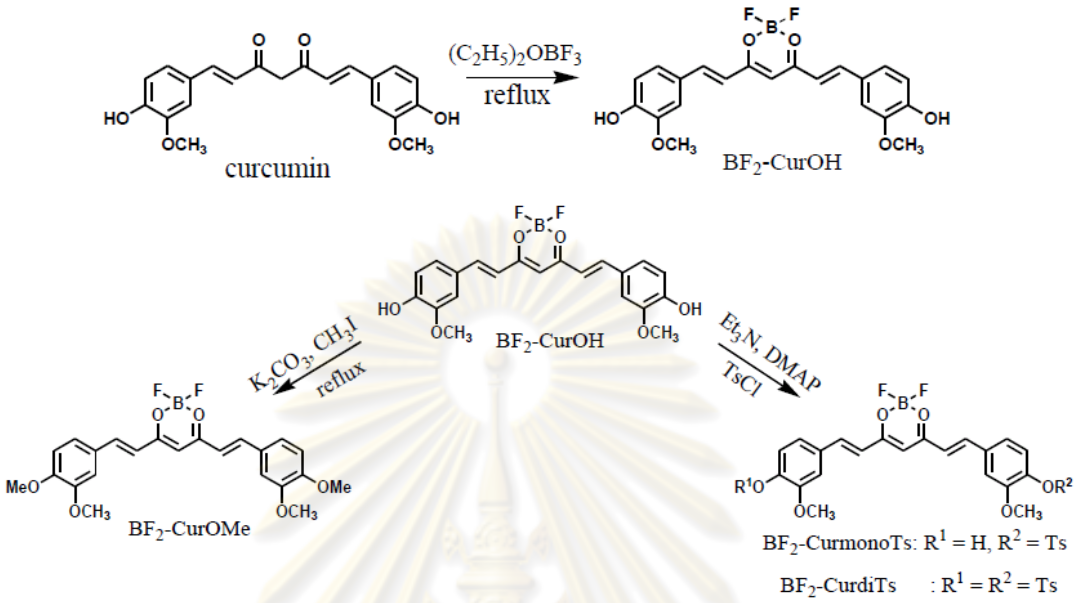

Scheme 4.1. Synsthesis pathway of **BF_2-CurOH**, **BF_2-CurOMe**, **BF_2-CurmonoTs** and **BF_2-CurdiTs**

4.2 Synthesis and characterization of curcumin borondifluoride (BF_2-CurOH)

The desired **BF_2-CurOH** was prepared from **curcumin** illustrated in Scheme 4.1. After adding the borontrifluoride diethyl etherate into the solution of **curcumin**, bright yellow solution turned to be red suddenly. The residual was purified by precipitation using methanol and ethyl acetate to obtain the red solid in 61 %yield. Most of proton signals in ^{1}H-NMR spectrum of **BF_2-CurOH** show the downfield shift compared to **curcumin** because the borondifluoride moiety is electron withdrawing group. The β-diketone moiety coordinates with borondifluoride which was observed by ^{1}H-NMR spectroscopy (Figure 4.2).

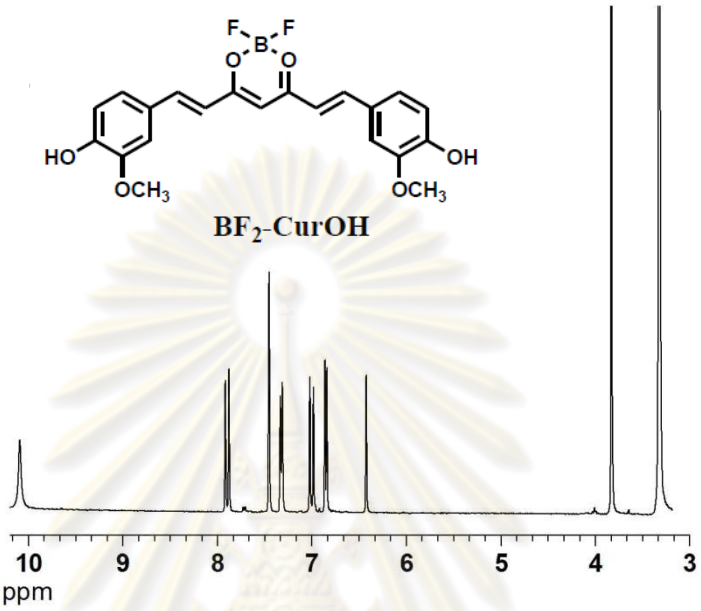

Figure 4.2 The ^{1}H-NMR spectrum of **BF_2-CurOH** in DMSO-d_6

4.3 Synthesis and characterization of curcumin borondifluoride methylation (BF_2-CurOMe)

The **BF_2-CurOH** was reacted with 5 equiv. of anhydrous sodium carbonate as base in methanol under nitrogen atmosphere for 10 min resulting in the color change from red to dark blue solution. It is indicative of the deprotonation on hydroxyl group. The blue reaction was added with iodomethane and refluxed for overnight until completed. After recrystallization in hexane/ethyl acetate, the **BF_2-CurOMe** was obtained as purple crystalline solid in 73 %yield. The ^{1}H-NMR spectrum of **BF_2-CurOMe** displayed the characteristic peaks of methoxy proton (O*C*H_3) at 3.822 ppm and a concomitant with the disappearance of hydroxyl protons. Additionally, the aromatic protons shifted to downfield at 7.954-6.424 ppm (Figure 4.3).

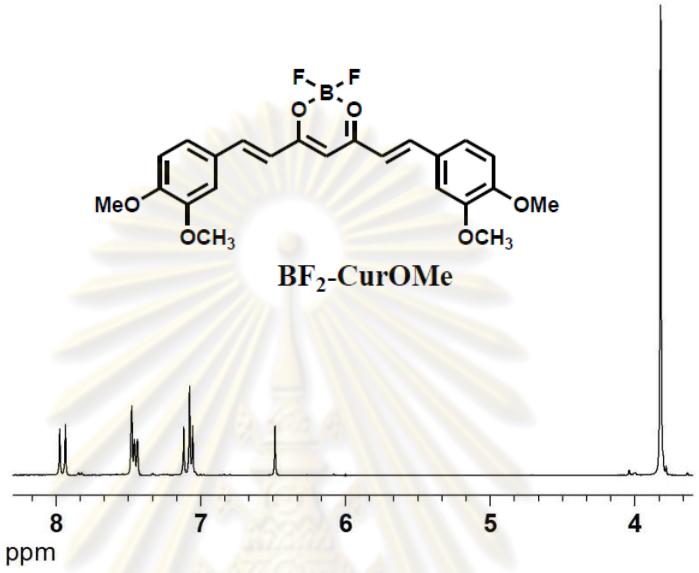

Figure 4.3 The ^{1}H-NMR spectrum of **BF_2-CurOMe** in DMSO-d_6

4.4 Synthesis and characterization of curcumin borondifluoride mono-tosylation (BF_2-CurmonoTs) and di-tosylation borondifluoride (BF_2-CurdiTs).

Compound **BF_2-CurmonoTs** and **BF_2-CurdiTs** were accomplished by nucleophilic substitution between **BF_2-CurOH** and *p*-toluenesulfonyl chloride using triethylamine as base in dichloromethane at 0 °C under nitrogen atmosphere. The products were purified by column chromatography using 5% ethyl acetate in dichloromethane to afford **BF_2-CurmonoTs** 23 %yield and **BF_2-CurdiTs** 71 %yield. The ^{1}H-NMR spectrum of **BF_2-CurmonoTs** (Figure 4.4) displayed the characteristic peaks of tosylate protons at 3.56 corresponding to 3 protons of Ar-C*H*$_3$, 7.25 and 7.7 ppm assigned to 4 aromatic protons. The ^{1}H-NMR spectrum of **BF_2-CurdiTs** (Figure 4.5) displayed the different patterns from **BF_2-CurmonoTs**. The methoxy protons of monoTs appeared 2 peaks at 3.90 and 3.56 ppm indicating the diffent environment of OCH_3 on the end of benzene rings.

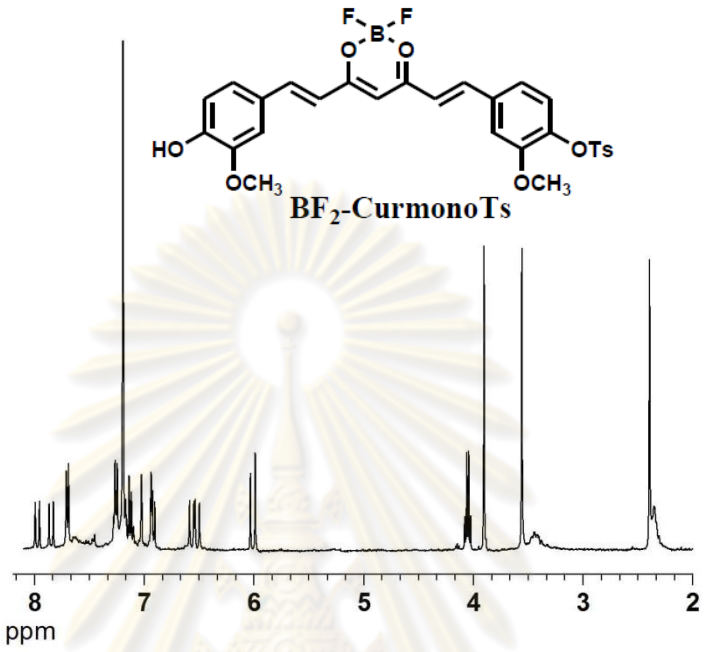

Figure 4.4 ^{1}H -NMR spectrum of **BF_2-CurmonoTs** in CD_3Cl

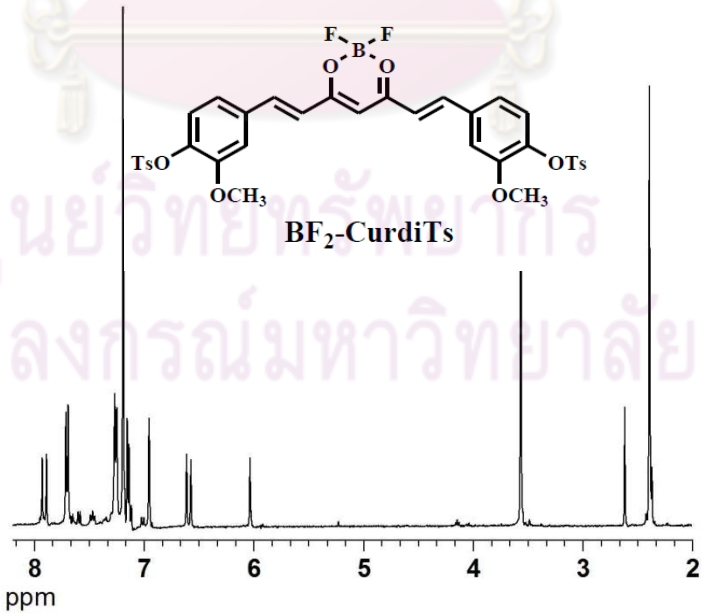

Figure 4.5 ^{1}H -NMR spectrum of **BF_2-CurdiTs** in CD_3Cl

4.5 UV-visible and fluorescence spectra of BF_2-CurOH, BF_2-CurOMe, BF_2-CurmonoTs and BF_2-CurdiTs

We have focused on studying the optical properties behavior of molecules modified on hydroxyl group of **BF_2-CurOH**. **BF_2-CurOH** and its substituted-OH derivatives (**BF_2-CurOMe**, **BF_2-CurMonoTs** and **BF_2-CurDiTs**) exhibit a strong absorption band in CH_2Cl_2 (shown in Table 4.1). It was found that when hydroxyl group was functionalized with electron-donation group such as **BF_2-CurOMe**, the maximum absorption spectrum showed a slightly red shift at 502.1 nm. Contrustly, the occurrence of the blue shift of absorption band was observed when the hydroxyl group of molecule was modified by electron-withdrawing group such as tosyl group (Figure 4.6). From these results, the substituted group may influence on the acceptability of the **BF_2** part. Their relative transition energies should depend on the relative electron affinities of the donor fragment (**curcumin** part). The electron-withdrawing group attached on donor fragment will decrease the electron acceptability of **BF_2** part inducing the blue shift of absorption band, while the electron-donor group will enhance the acceptability of **BF_2** part resulting in the red-shifted absorption band.

Table 4.1 Maximum absorption and emission of **BF_2-CurOH**, **BF_2-CurOMe**, **BF_2-CurMonoTs** and **BF_2-CurDiTs** at concentration 1.0 x 10^{-6} M in CH_2Cl_2

compound	absorption (nm)	emission (nm)	quantum yield	ε (10^5 cm^{-1} mol^{-1} L)
BF_2-CurOH	497	557.01	0.62	0.82
BF_2-CurOMe	502.1	570.00	0.61	1.29
BF_2-CurMonoTs	492.0	562.00	0.22	0.33
BF_2-CurDiTs	436.0, 460.1	505.07	0.48	0.34

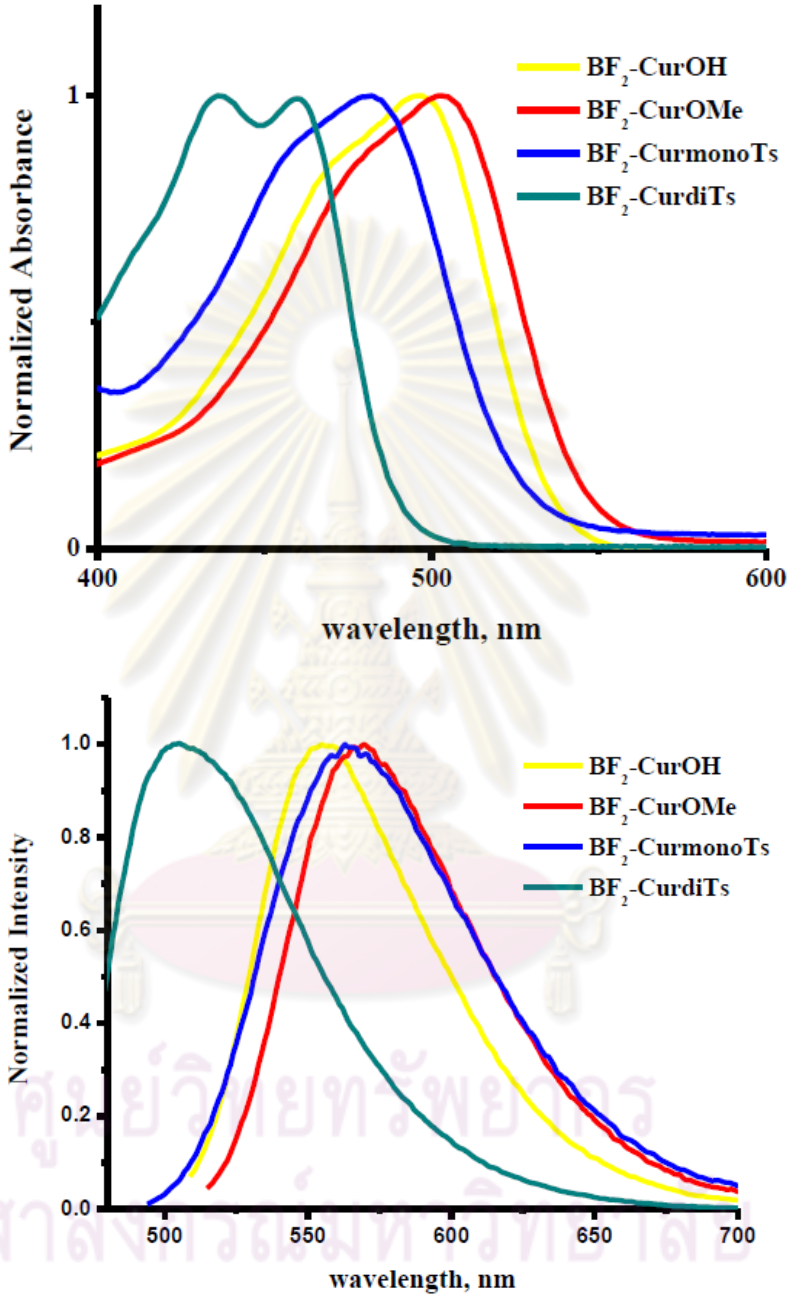

Figure 4.6 The normalized UV-visible spectra (a) and fluorescence spectra (b) of **BF_2-CurOH**, **BF_2-CurOMe**, **BF_2-CurmonoTs** and **BF_2-CurdiTs** at concentration 1.0 x 10^{-6} M in CH_2Cl_2

The emission spectra of **BF_2-CurOH**, **BF_2-CurOMe**, and **BF_2-CurDiTs** demonstrated red shift corresponding electron donatability the substituted group. However, the maximum emission wavelength of **BF_2-CurMonoTs** was observed at 562 nm which is higher than **BF_2-CurOH** (557.01), shown in Table 4.1. It is notable that unsymmetrical structure of **BF_2-CurMonoTs** on benzene ring induces the higher relaxation of electron resulting in the red-shifted emission band compared to **BF_2-CurOH**.

4.6 Solvatochromic studies of BF_2-CurOH and BF_2-CurOMe

Absorption and emission spectra of **BF_2-CurOH** and **BF_2-CurOMe** were derived from an inversion of singlet state excited states; π-π* transition. Interestingly photophysical characteristics of **BF_2-CurOH** and **BF_2-CurOMe** act as a solvent dependent molecule according to the results shown in Figure 4.7 and Table 4.2.

Table 4.2 The maximum absorption and emission wavelength of **BF_2-CurOH** in difference solvents

Solvent	absorption	Emission	Φ_{flu}
Diethyl ether	492.9	527.01	0.436
Toluene	495.9 and 467.0	582.84 and 521.04	0.404
Benzene	498.1	534.85	0.424
Chloroform	497.0	554.77	0.395
Dichloromethane	497.0	557.01	0.497
Ethanol	503.1	586.91	0.025
Methanol	500.0	592.05	0.009
DMSO	527.0	612.94	-

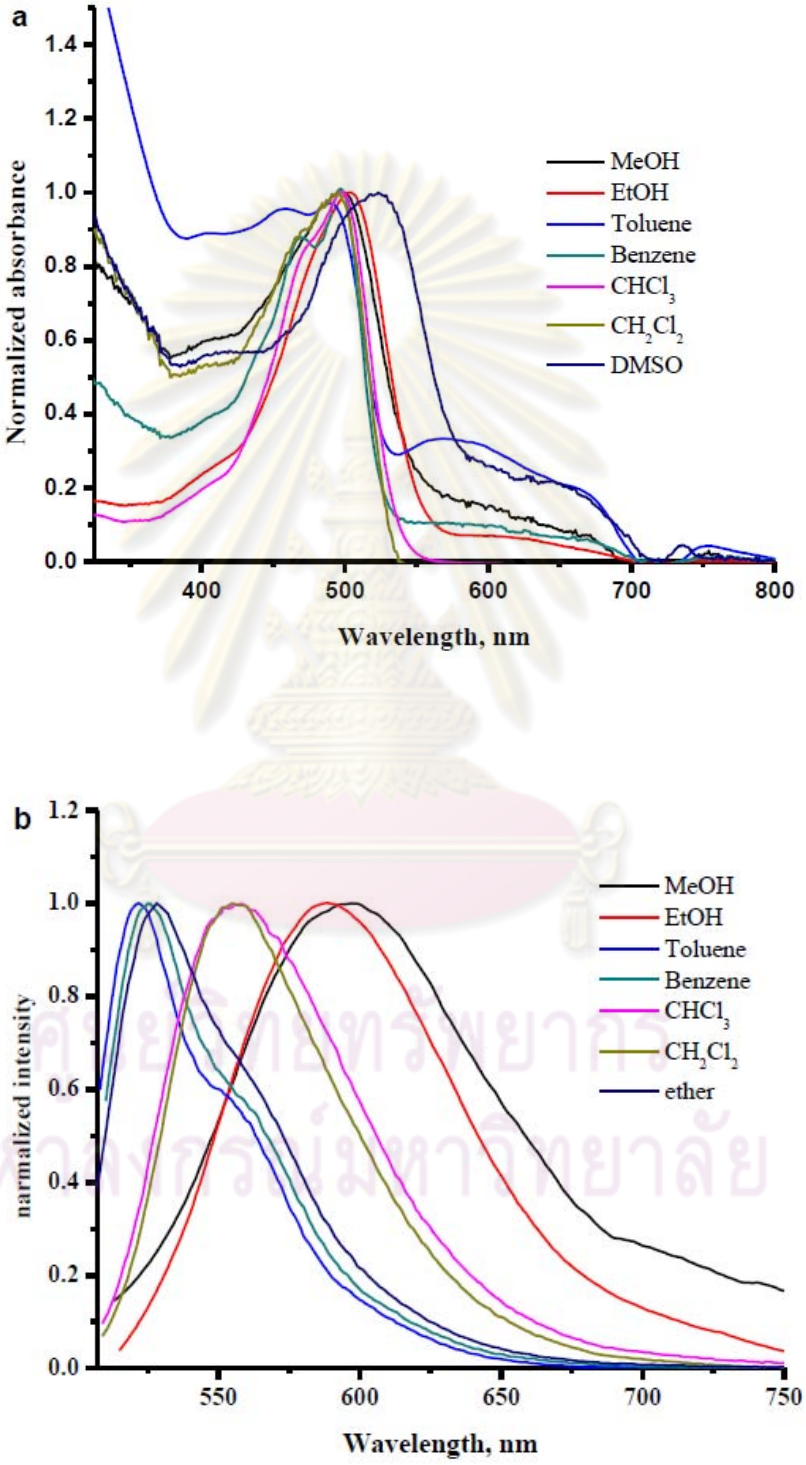

Figure 4.7 Absorption (a) and emission (b) spectra of **BF_2-CurOH** in difference solvents

According to, the absorption and emission bands have shown a bathochromic shift from diethyl ether to DMSO. Our first assumption is that the spectral shift of emission and absorption may depend on only the solvent polarity. To confirm this hypothesis, the correlation between λ_{max} of absorption band and $E_T^N(30)$ parameter corresponding to each solvent was displayed in Figure 4.8. The $E_T^N(30)$ values of various solvents which used in this research were obtained from the literature [89]. The linear plot of this relationship gave a poor R^2 value ($R^2 = 0.6304$) indicating that they have other solvent parameters affecting on the photophysical properties of **BF_2-CurOH**.

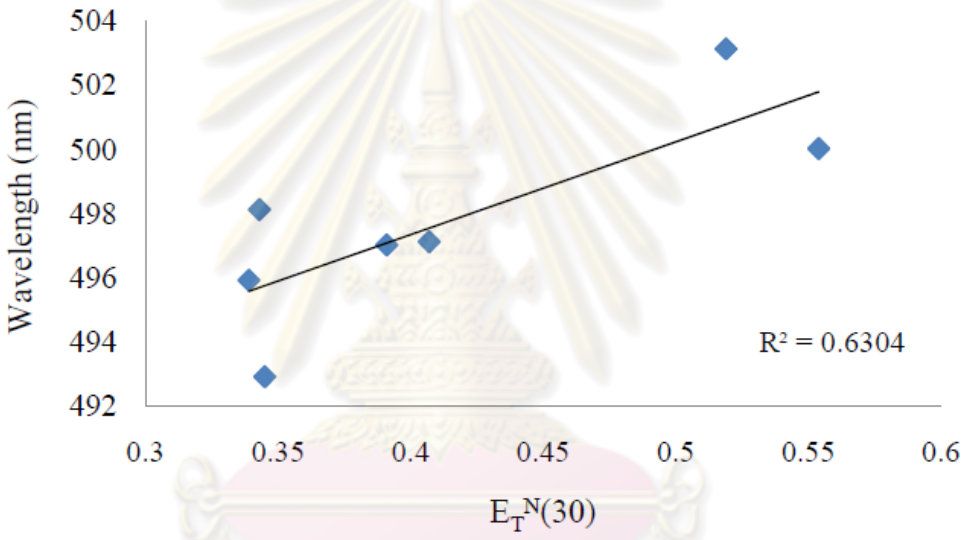

Figure 4.8 The liner plots on plotting λ_{max} (the maximum absorption) versus the solvent parameter $\boldsymbol{E_T^N(30)}$ of **BF_2-CurOH**

To study the solvatochromic effect, we use Kamlet-Taft (Linear Salvation Energy Relationship, LSER) which put the π^*, α, and β parameters in the representatives of the polarity/polarizability, the acidity (hydrogen bond donor, HBD), and the basicity (hydrogen bond accepter, HBA) of solvent, respectively, on the following in eq 4.1.

$$y = y_0 + a\alpha + b\beta + c\pi^* \qquad \text{(Kamlet-Taft)} \qquad (4.1)$$

The coefficients y_0, a, b, c, and correlation coefficients (r) were evaluated by the multiple linear regression fit of calculated and measured ν_{max} corresponding to the Kamlet-Taft relationship relied on the absorption spectra of **BF_2-CurOH** were summarized in Table 4.3.

Table 4.3 The correlation coefficients of *a*, *b*, and *c* of the Kamlet-Taft parameters; α, β, and π^*, respectively, and Correlation Coefficient (R^2) for **BF_2-CurOH**

Entry	y_0	a	b	c	R^2
1	19.92722	-0.00174	-	-	$3x10^{-6}$
2	20.27436	-	-0.82492	-	0.391
3	20.95487	-	-	-1.74686	0.825
4	20.29019	0.46577	-1.18457	-	0.560
5	20.97330	-0.05114	-	-1.75285	0.828
6	21.02790	-	-0.49303	-1.51792	0.951
7	20.97397	0.23645	-0.70298	-1.39275	0.991

According to Table 4.3, entry 7 gave an acceptable correlation coefficient (R^2=0.991, shown in Figure 4.9) when *a*, *b* and *c* have the numerical values revealing that the photophysical properties of **BF_2-CurOH** in various solvents depend on polarity, HBD and HBA of solvent (Figure 4.9).

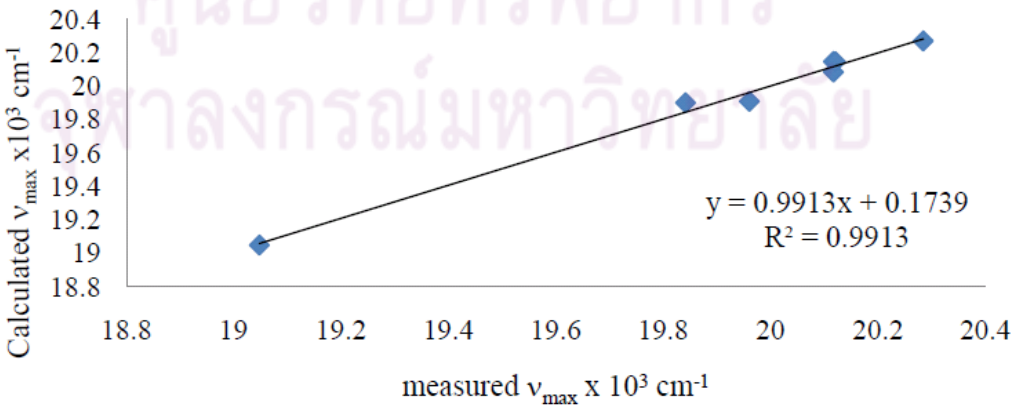

Figure 4.9 Relationship between calculated and measured $\tilde{\nu}_{max}$ values for **BF_2-CurOH** dissolved in the difference solvent

Figure 4.9 displays a plot of the measured absorption wavelength versus the calculated absorption wavelength for the selected solvents such as methanol, ethanol, toluene, benzene, chloroform, diethyl ether, and DMSO. The data fits the Kamlet-Taft model well with a correlation coefficient value of 0.9913. The best qualitative regression fit obtained for the compound **BF_2-CurOH** is represented by eq 4.2.

$$\tilde{\nu}_{max} \text{x} 10^3[\textbf{BF}_2\textbf{-CurOH}] = 20.97397 + 0.23645\alpha - 0.70298\beta - 1.39275\pi^* \qquad (4.2)$$

In the case of **BF_2-CurOMe** characteristic spectra of **BF_2-CurOMe** in various solvents were illustrated in Table 4.4 and Figure 4.10.

Table 4.4 The maximum absorption and emission wavelength of **BF_2-CurOMe** in difference solvents

Solvent	absorption	emission	Φ_{flu}
Diethyl ether	490.1 and 465.1	521.94	0.464
Toluene	502.1 and 476.1	531.02	0.458
Benzene	504.0	532.79	0.501
Chloroform	500.0	555.07	0.544
Dichloromethane	502.1	570.0	0.485
Ethanol	492.1	574.85	0.083
Methanol	491.0	582.94	0.021
DMSO	513.0	587.05	0.035

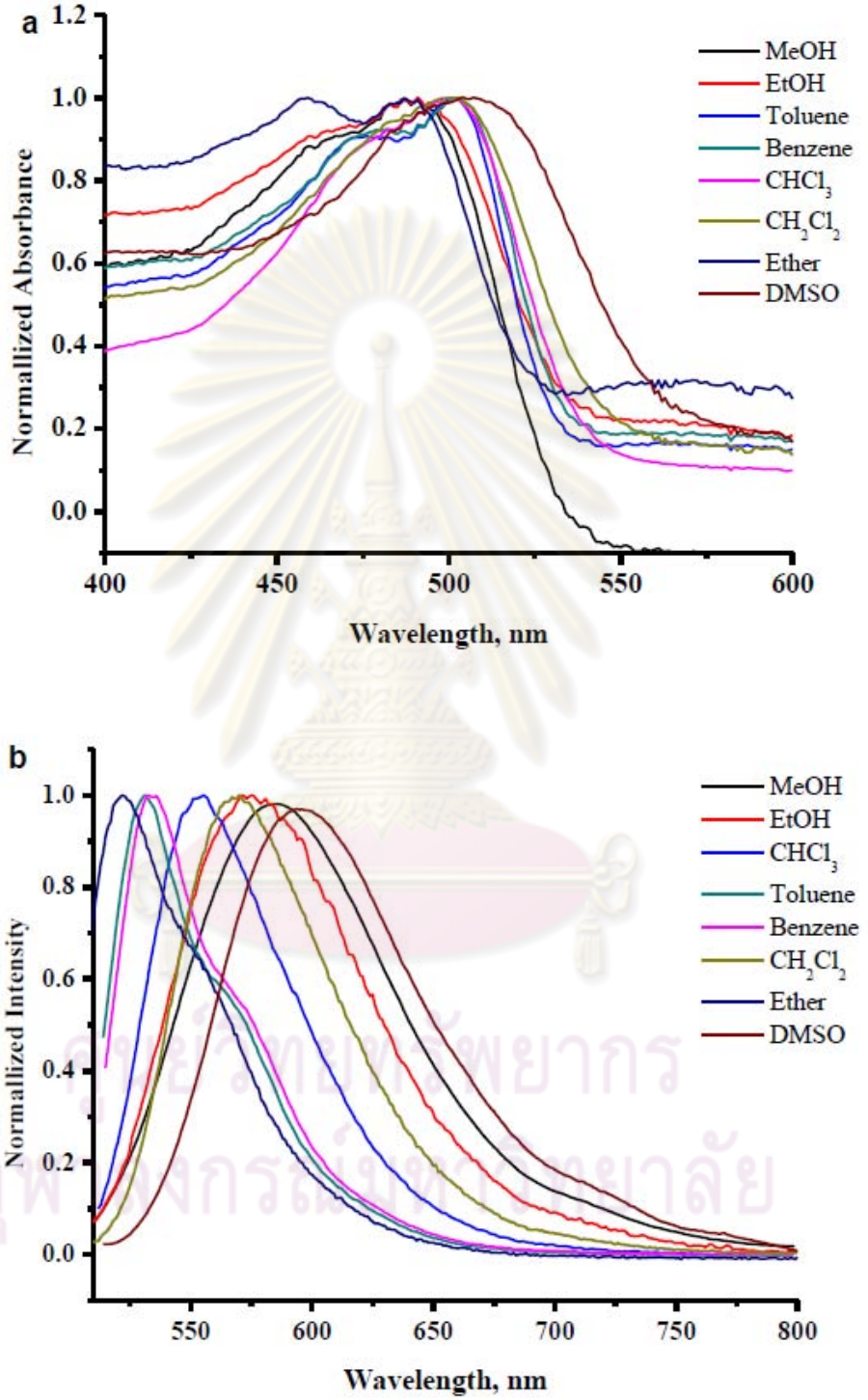

Figure 4.10 Absorption (a) and emission (b) spectra of **BF_2-CurOMe** in various solvents

The absorption properties of **BF_2-CurOMe** behave a fluctuation upon increasing solvent polarity. From $E_T^N(30)$ parameter, the values are proportional to the wavelength of **BF_2-CurOMe** (except methanol and ethanol). The positive solvatochromic behavior of **BF_2-CurOMe** was observed in aprotic solvent. However, the R^2 of the graph is not significant (R^2=0.4398, Figure 4.11). Therefore, it was concluded that the solvent effect of **BF_2-CurOMe** behaves similarly to that of **BF_2-CurOH**. This is the most reasonable to use the Kamelt-Taft equation to evaluate the solvent effect for **BF_2-CurOMe**.

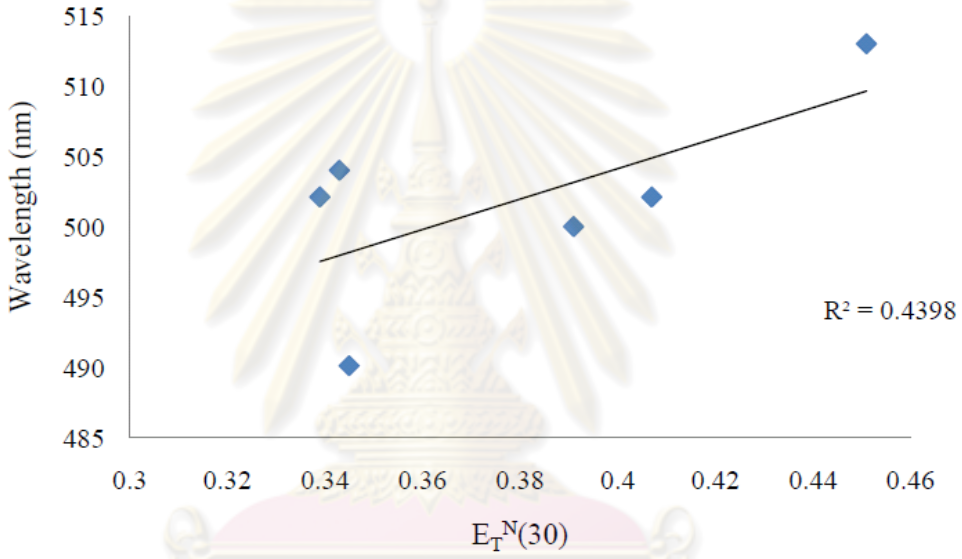

Figure 4.11 The liner plots of λ_{max} (the maximum absorption) of **BF_2-CurOMe** versus the solvent parameter $\boldsymbol{E_T^N(30)}$

The solvatochromic effect by Kamlet-Taft equation shows the high quality effects as indicated by correlation coefficients (0.9975) for special mathematical functions of $\tilde{\nu}_{max}$ with α, β, and π^* obtained from the selected solvents such as methanol, ethanol, toluene, benzene, chloroform, diethyl ether, and DMSO (Figure 4.12). The qualitative best regression fits obtained for the compounds **BF_2-CurOMe** is represented by eq 4.3.

$$\tilde{\nu}_{max} \text{x} 10^3 \text{ [}\mathbf{BF_2\text{-}CurOMe}\text{]} = 20.61684 + 0.38775\alpha + 0.20517\beta - 1.32081\pi^* \quad (4.3)$$

Table 4.5 Solvent-Independent Correlation Coefficients *a*, *b*, and *c* of the Kamlet-Taft parameters α, β, and π^*, respectively, and Correlation Coefficient (R^2) for **BF_2-CurOMe**

Entry	y_0	a	b	c	R^2
1	19.89146	0.50595	-	-	0.410
2	19.94797	-	0.21578	-	0.038
3	20.78696	-	-	-1.27095	0.622
4	19.96854	0.60522	-0.25155	-	0.446
5	20.61698	0.47168	-	-1.21571	0.437
6	20.70557	-	0.54945	-1.52609	0.844
7	20.61684	0.38775	0.20517	-1.32081	0.997

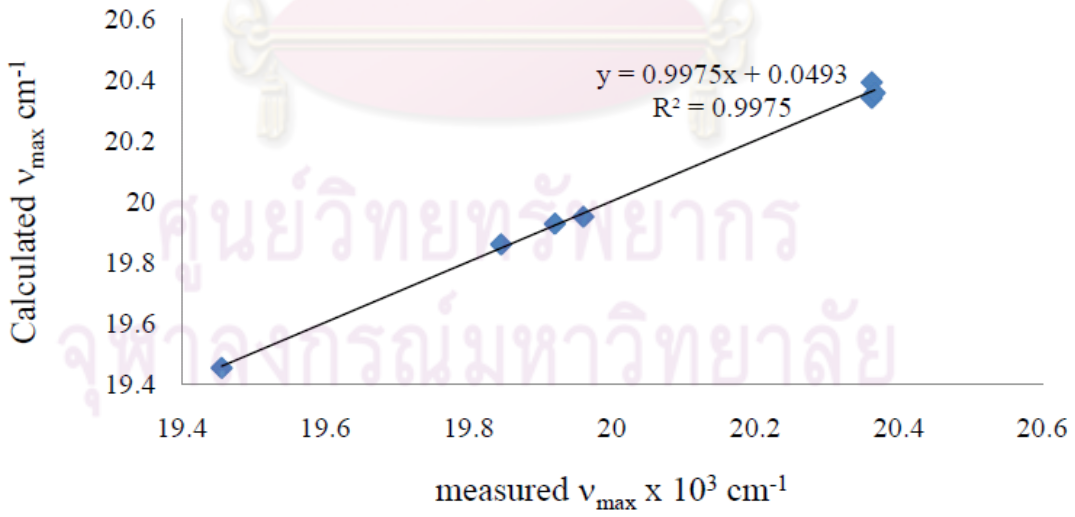

Figure 4.12 Relationship between calculated and measured $\tilde{\nu}_{max}$ values for **BF_2-CurOMe** dissolved in the difference solvents

Comparing the coefficient in equations 2 and 3, the values of coefficient *a* (HBA) and *c* (π*) between **BF_2-CurOH** and **BF_2-CurOMe** gave a small difference but a large difference for the coefficient *b* (HBD). It is also noticed that the absorption properties of **BF_2-CurOMe** displayed the fluctuation upon increasing solvent polarity unlike the absorption manner of **BF_2-CurOH** possibly caused by the hydrogen bond accepting abilities. The solvent effects on multiparametric correlation of spectral data (π,β, and α) for **BF_2-CurOH** is in order of solvent polarizability factor, hydrogen bond accepting abilities and hydrogen bond donating abilities while **BF_2-CurOMe** obtained the most significant effect of solvent polarizability factor. Focusing on each solvatochromic parameters, the sign of the correlation coefficient *b* belonging to **BF_2-CurOH** is negative which is indicative of the favorable hydrogen bonding with a protophilic solvent leading to appearance of red-shifted absorption band.[90] Unlike in the case of **BF_2-CurOMe**, the correlation coefficient displayed a positive sign. Undoubtedly, the absorption maximum of **BF_2-CurOMe** in methanol and ethanol showed a blue shift of ~13 nm compared to that in benzene (results listed in table 4.4). Surprisingly, the coefficient *b* value from Kamlet-Taft equation can explain the fluctuated absorption manner of **BF_2-CurOMe** with increasing solvent polarity from benzene to DMSO. The negative sign of the *c* coefficients indicates the electronically excited state of these molecules with a stronger solvation stabilized upon increasing the solvent dipolarity/polarizability resulting in a good agreement with bathochromic shift of absorption maxima on going from benzene to DMSO. Moreover, the absolute *c* value is markedly larger than the *a* and *b* coefficients for **BF_2-CurOH** and **BF_2-CurOMe** assuming that the donatability or acceptability hydrogen bonds of the used solvents is much weaker than solute-solvent dipole-dipole interaction. However, the investigated **BF_2-CurOH** and **BF_2-CurOMe** behaved a positive solvatochromism with increasing dipolarity/polarizability, acidity and basicity of solvents.

4.7 The complexation studies by UV-vis technique

The characteristic spectra of **BF_2-CurOH** and **curcumin** in CH_3CN:H_2O (4:1, v/v) display the absorption bands at 507.0 and 417.1 nm, respectively (show in Figure 4.13).

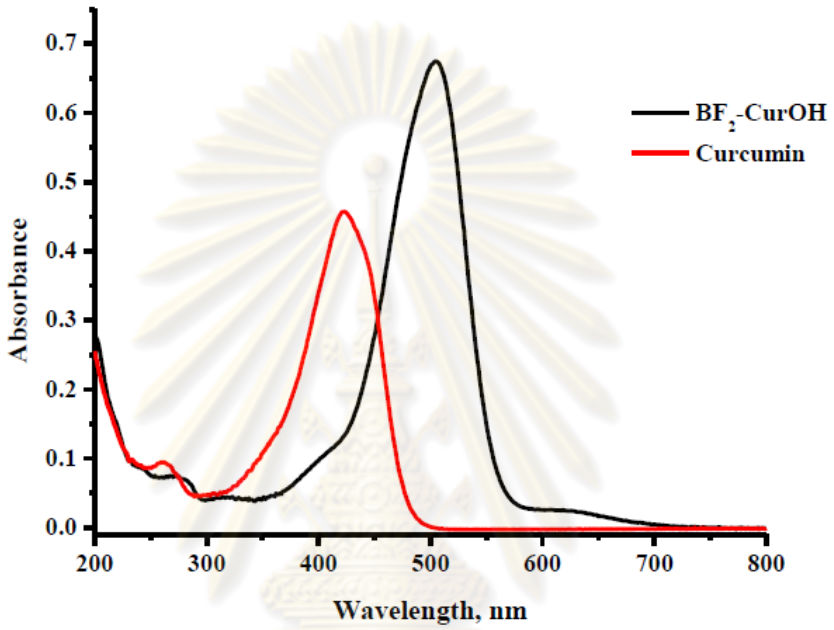

Figure 4.13 The UV-visible absorption spectra of ligand BF_2-CurOH and **curcumin** at concentration $5.0x10^{-6}$ M in CH_3CN:H_2O (4:1 v/v)

The complexation properties of **BF_2-CurOH** as well as **curcumin** with various anions were measured in CH_3CN:H_2O (tetrabutylammonium hexafluorophosphate as supporting electrolyte).

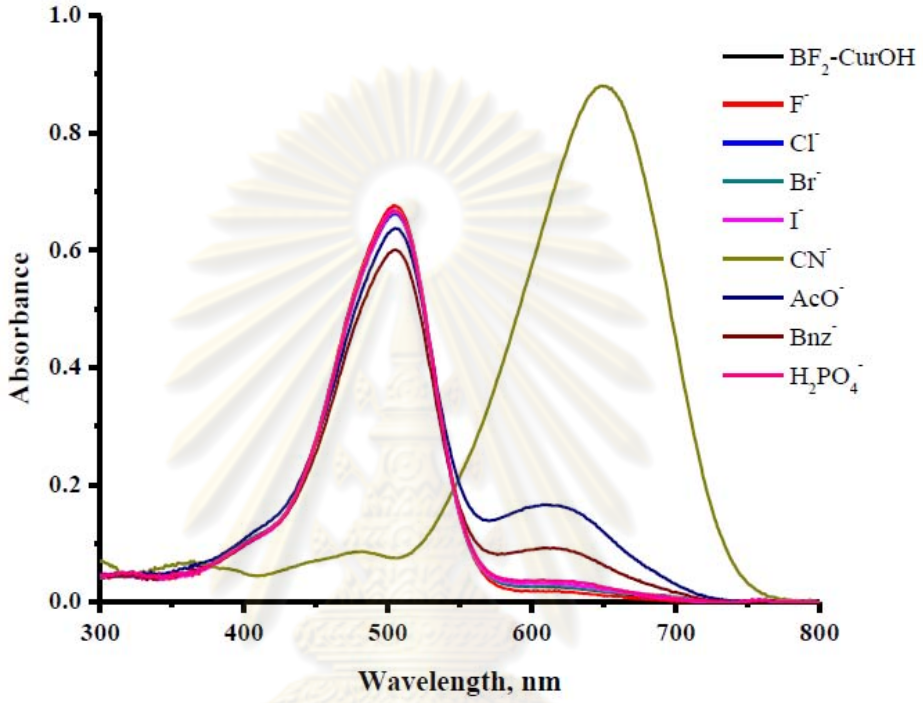

Figure 4.14 The UV-visible spectra of **BF_2-CurOH** (5 μM) in CH_3CN:H_2O (4:1, v/v) in the presence of 100 equivalent of varies anions

Upon the addition of CN^-, the absorption band at 507.0 nm decreased obviously with the appearance of a new strong absorption band at 649.0 nm. In the presence of AcO^- and Bnz^-, the absorption band at 507 nm decrease slightly and a weak absorption band at 625 nm were intensified. The no changes of the absorption spectra of **BF_2-CurOH** were observed in the case of F^-, Cl^-, Br^-, I^- and $H_2PO_4^-$ (shown in Figure 4.14).

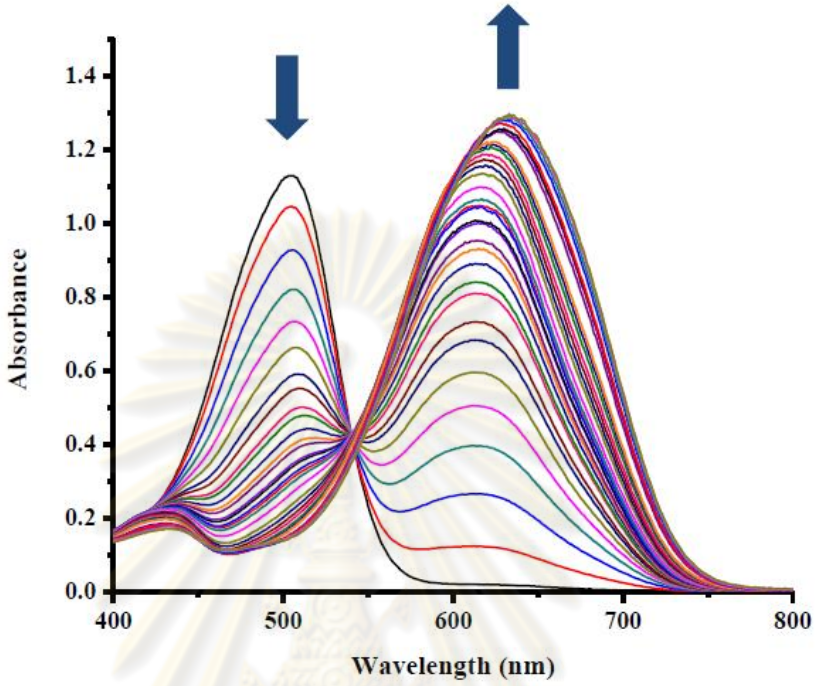

Figure 4.15 UV-visible titration spectra of **BF_2-CurOH** ($7.5x10^{-6}$ M) upon gradual addition of CN^- in CH_3CN:H_2O (4:1, v/v) from 0-100 equivalent

In order to determine the complexation of **BF_2-CurOH** and CN^-, the UV-titration was performed in Figure 4.15. The absorption band of **BF_2-CurOH** at 507.0 nm is progressively decreased while a new band at 649.0 nm develops upon adding CN^-. The UV-visible titration was measured at least twice. The log β values were calculated from equation 4.4 by fitting the data of the absorption band at 507 and 649 nm. The results showed the best fit between the calculated and measure curves (showed in Figure 4.16a and 4.16b) with the R^2 value of 0.9896 for the absorbance at 507 nm giving the log β value of 8.8 ± 0.00 as shown in Figure 4.16.

$$\boldsymbol{A} = \frac{(\boldsymbol{A_0}+\boldsymbol{A_{lim}}\boldsymbol{\beta}[guest\,]^2)}{(\mathbf{1}+\boldsymbol{\beta}[guest\,]^2)} \qquad (4.4)$$

A = absorbance of a particular concentration of guest
A_0 = initial absorbance
A_{lim} = limiting (final) absorbance
β = stability constant of the receptor with the guest
[guest] = concentration of guest

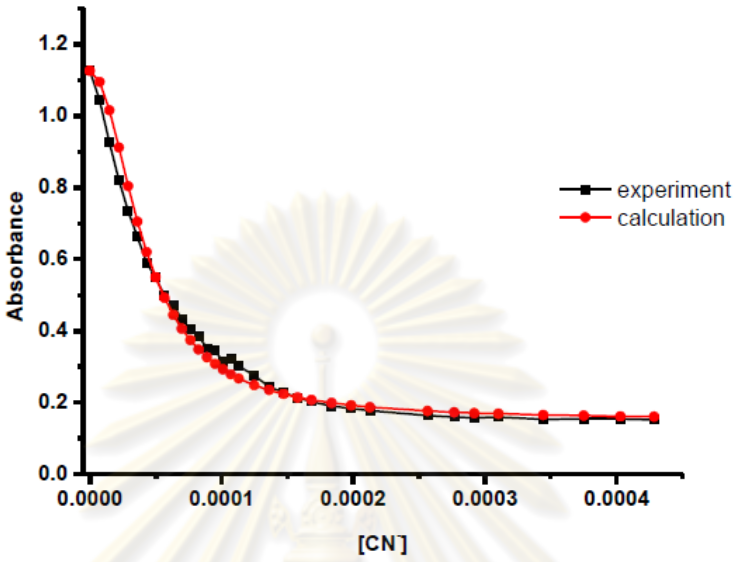

Figure 4.16 Comparing experiment data and calculated data form UV-visible titration of **BF_2-CurOH** and CN^- for stability constant. (a) at 507 nm

Similarly, the absorption spectra of **curcumin** in the presence of CN^- exhibited the red shift of 92.9 nm (from 417.1 to 510 nm).

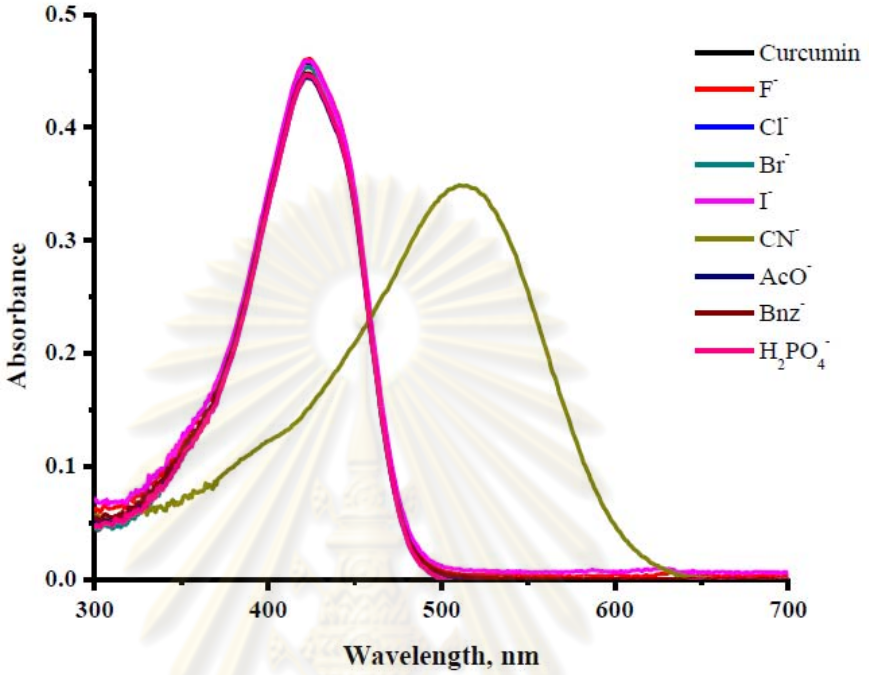

Figure 4.17 The UV-visible spectra of **curcumin** (5 μM) in CH_3CN:H_2O (4:1, v/v) in the presence of TBA salts of various anions (F^-, Cl^-, Br^-, I^-, CN^-, AcO^-, $PhCOO^-$ and $H_2PO_4^-$, 100 equiv, respectively)

Upon addition of CN^- into the solution of **curcumin**, a new absorption band was observed at 510.0 nm. In the case of other anions, no changes of the spectra and the appearance of a new band not observed.

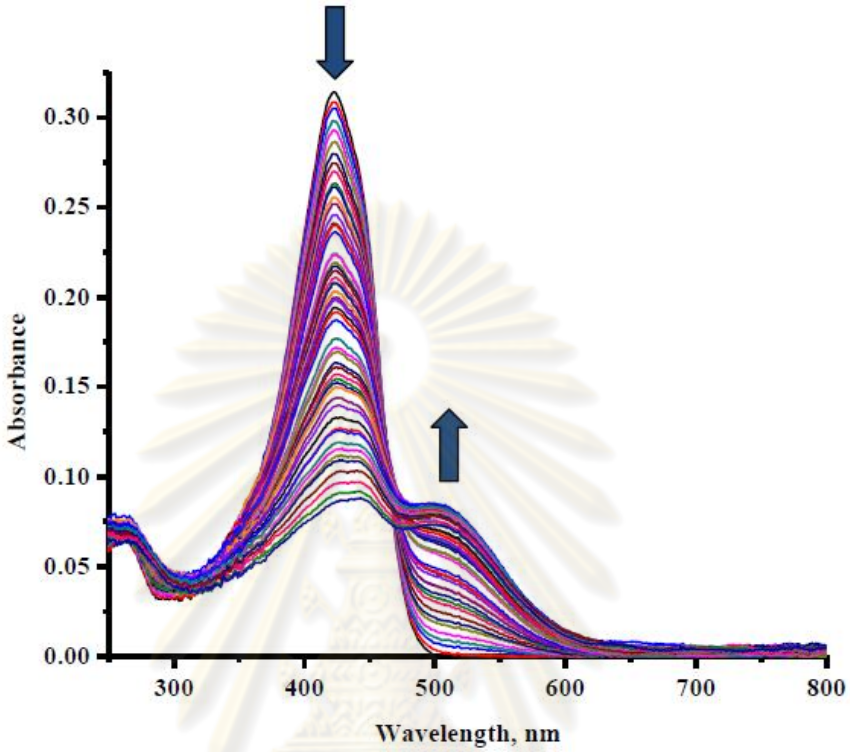

Figure 4.18 UV-visible titration spectra of **curcumin** ($7.5x10^{-6}$ M) upon gradual addition of CN^- in $CH_3CN:H_2O$ (4:1, v/v) from 0-100 equivalent

To verify the binding constant, UV-visible titration of **curcumin** and CN^- in $CH_3CN:H_2O$ was performed. From the UV-visible titration spectra (Figure 4.18), the absorbance at 417.1 nm dramatically decreased with a concomitant of the appearance of a weak absorption band at 510 nm. The log β value obtained by the best fit regression between the calculation and the measured experiments with the R^2 value of 0.9796 is 7.7 ± 0.00 corresponding to the absorption band at 510.0 nm.

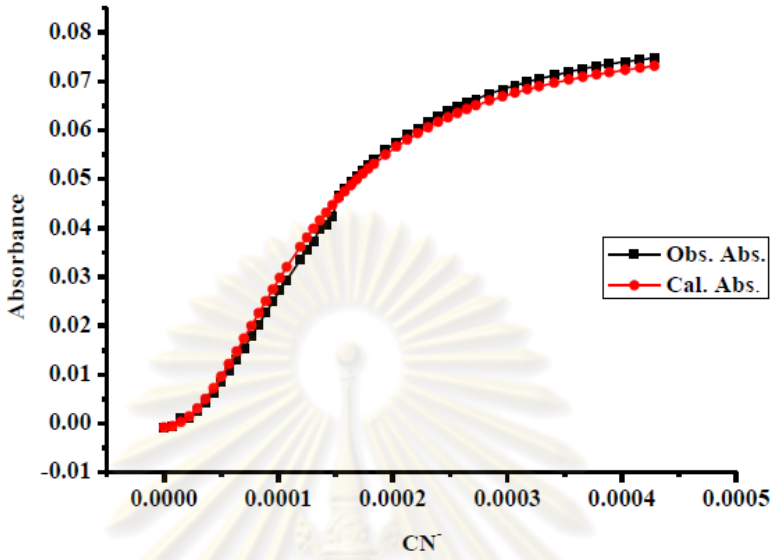

Figure 4.19 Comparing experiment data and calculated data form UV-visible titration of **curcumin** and CN^- for calculation of stability constant at 510 nm

Comparing the red shift in **BF_2-CurOH** and **curcumin** in the present of CN^- from UV-visible technique, the absorption spectra showed a red shift in $\Delta\lambda$ = 142 nm and 92.9 nm, respectively. The red shift of **BF_2-CurOH** is larger than that of **curcumin** possibly caused by a large charge separation between **BF_2** part and the end of aromatic rings and consequently to give a strong intermolecular charge transfer (ICT). Schematically illustrated in Scheme 4.2, the negative charges which occur in depotonation, could delocalize through π-conjugated bond to acceptor unit. Molecule **BF_2-CurOH** contains a **BF_2** unit as a stronger acceptor than a diketone unit of **curcumin**. A high charge separation between acceptor and donor unit in **BF_2-CurOH** was supported by deprotonation on hydroxyl group after adding CN^- resulting in excellent delocalization to **BF_2** unit. The excited state in a complex can be more stabilized by CN^- binding, resulting in a bathochromic shift in the absorption maxima.[91, 92] The selective binding with CN^- of both molecules can be descriped by the basicity of anion. This process cannot occur in fluoride ion, even as a high basicity since fluoride has a high hydration enthalpy and low basicity (ΔH^0_{hyd} = -504 kJ/mol, pKa = 3.18) in aqueous system.

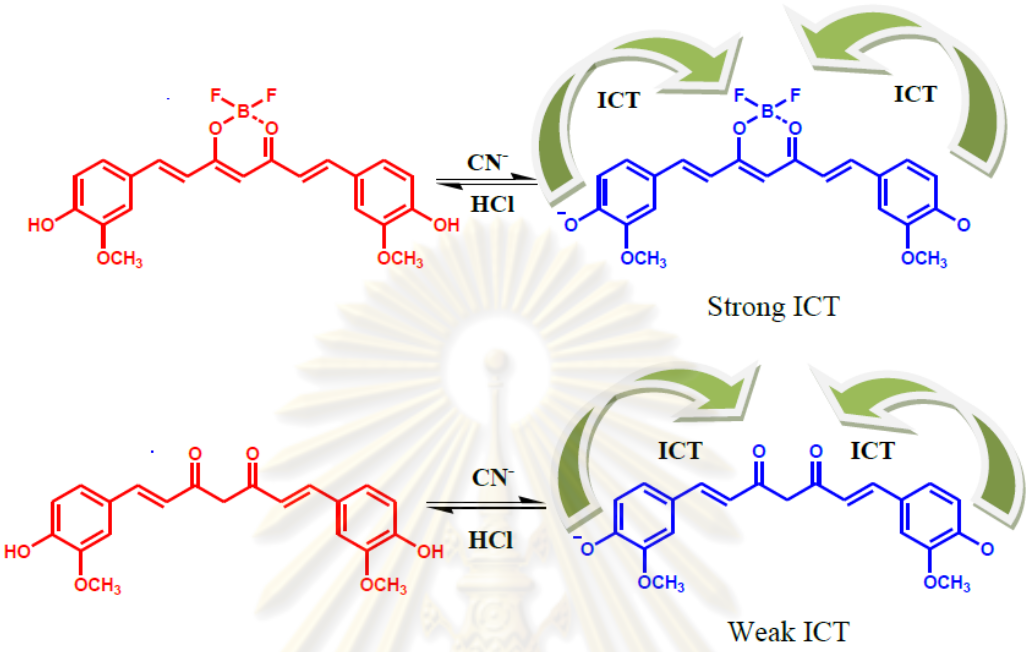

Scheme 4.2. The ICT process of **BF_2-CurOH** + **CN^-**

4.8 The complexation studies by fluorescence technique

Emission maximum of **BF_2-CurOH** and **curcumin** in CH_3CN:H_2O (4:1, v/v) were observed at 600 nm (ex. at 507 nm) and 534 nm (ex. 417.1 nm), respectively (Figure 4.20).

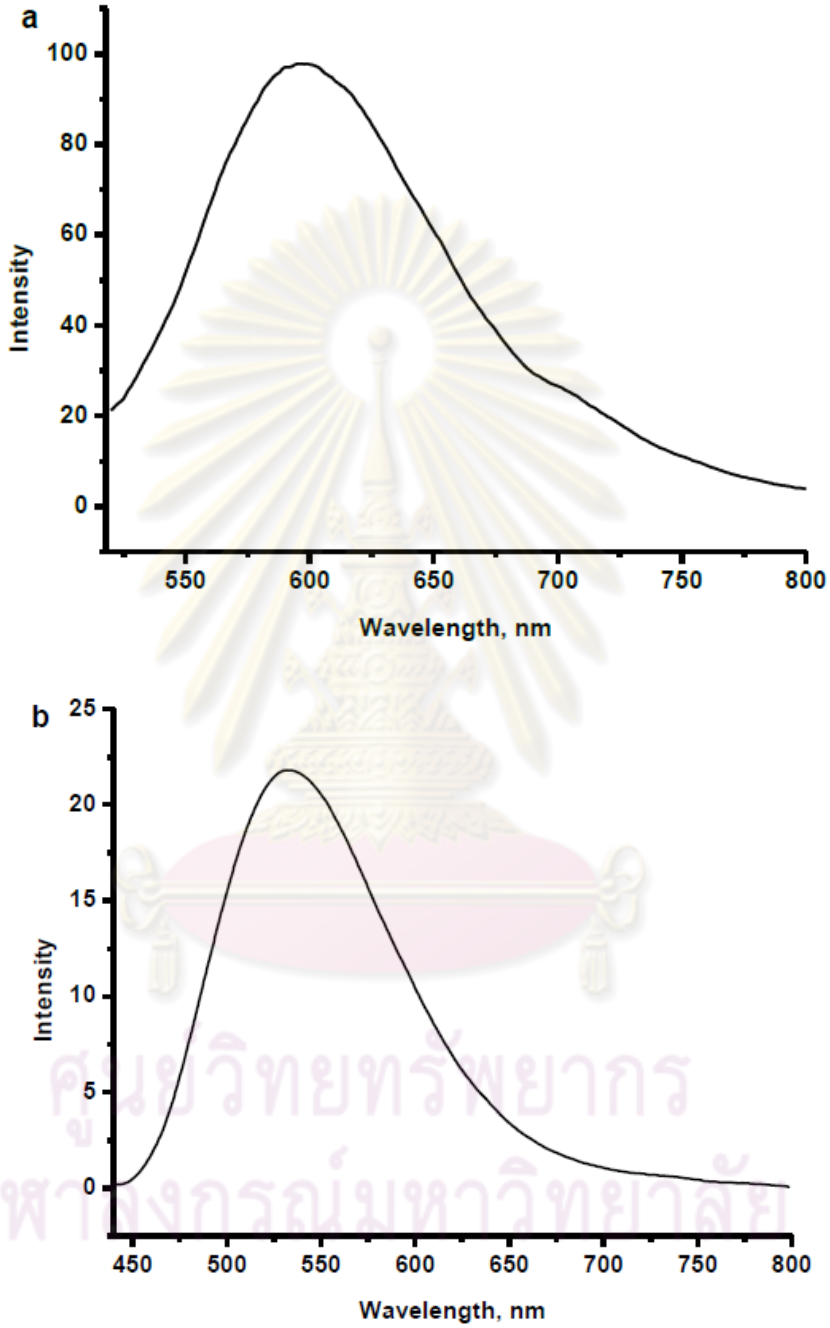

Figure 4.20 The emission spectra of ligand **BF_2-CurOH** (a) and **curcumin** (b) at concentration of $5.0x10^{-6}$ M in CH_3CN:H_2O (4:1, v/v)

From the Figure 4.20, **BF_2-CurOH** gives a stronger emission band than **curcumin**. Because more rigid molecule induced a higher π-conjugated system, electron delocalization occur easily between two aromatic rings. To investigate the anionic deprotonation on hydroxyl group of **BF_2-CurOH** and **curcumin**, fluorescent responses of **BF_2-CurOH** and various anions were examined in Figure 4.21.

Upon the addition of CN^-, the emission band at 600 nm of **BF_2-CurOH** was quenched completely. Interestingly, if the solution of **BF_2-CurOH** and CN^- was excited at 649 nm, the new emission band appeared at 750 nm (shown in Figure 4.21b). In contrast for other anions, the emission band at 649 nm slightly changes without an appearance of new emission band at 750 nm (shown in Figure 4.21a and 4.21b). The results revealed that **BF_2-CurOH** can interact to CN^- ion selectively over the other anions.

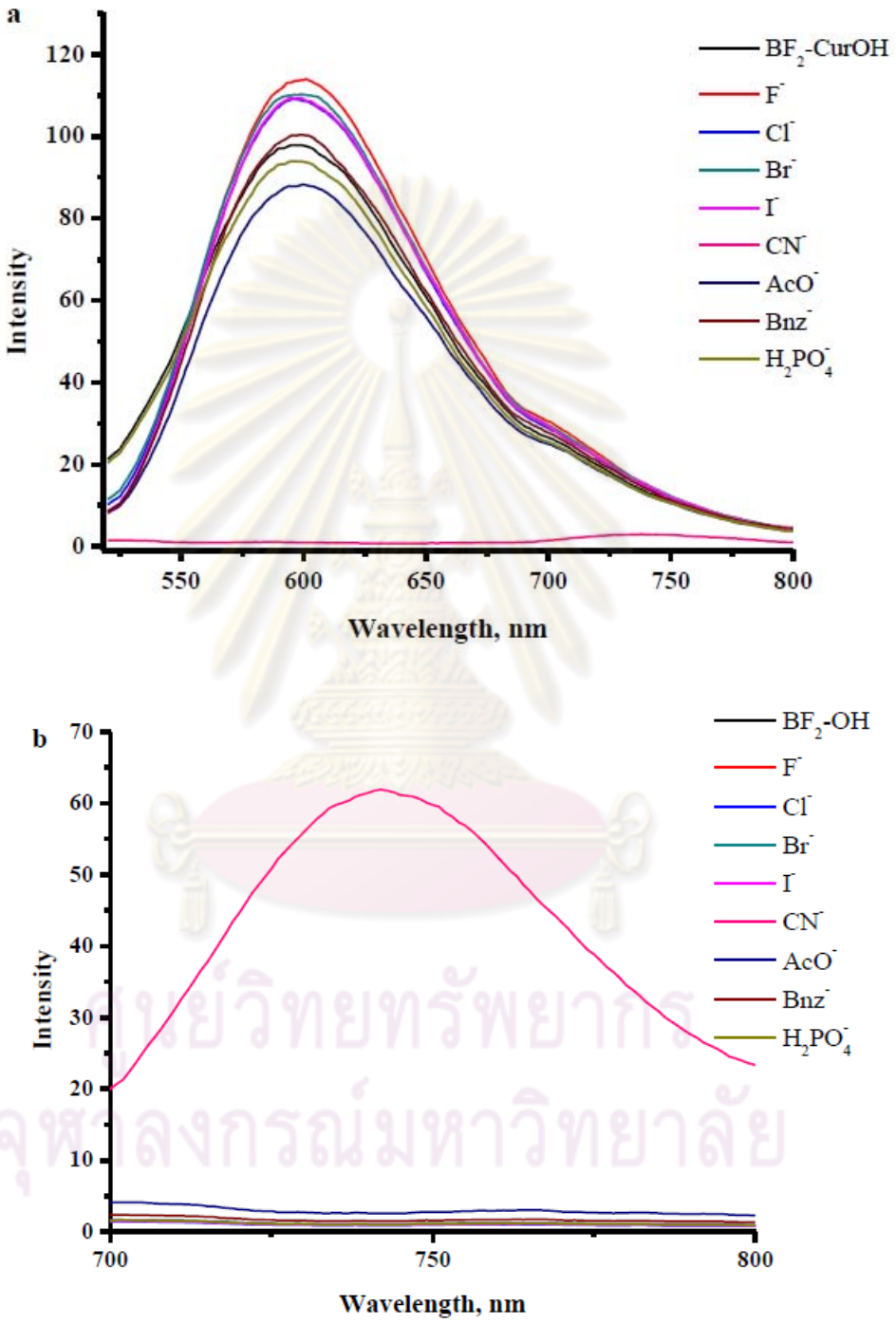

Figure 4.21 The fluorescence spectra of **BF_2-CurOH** at concentration of 5 μM in CH_3CN:H_2O (4:1, v/v) in the presence of 100 equivalent TBA salts of various anions (F^-, Cl^-, Br^-, I^-, CN^-, AcO^-, $PhCOO^-$ and $H_2PO_4^-$) (a) Excitation at 507 nm. (b) Excitation at 649 nm

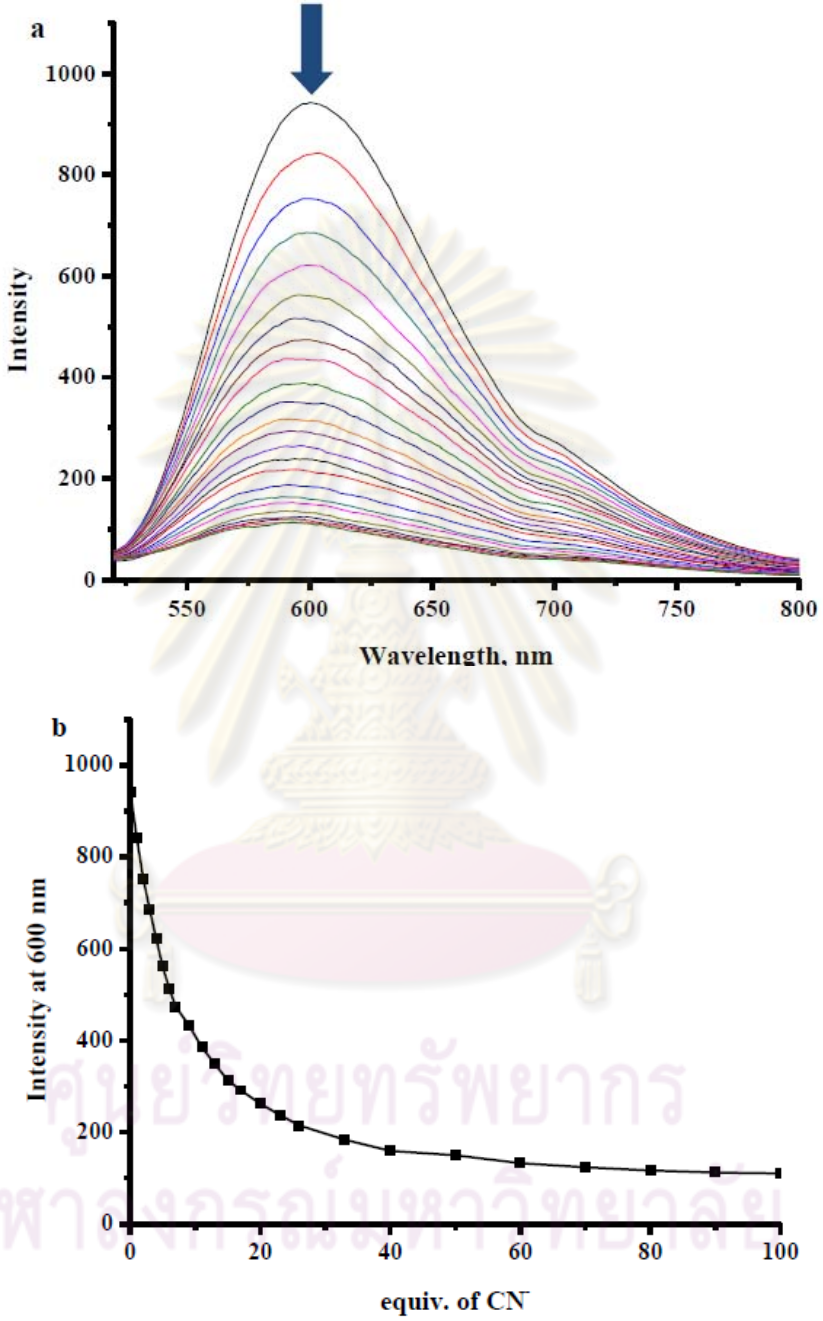

Figure 4.22 (a) Fluorescence spectra of BF_2-CurOH (7.5 x 10^{-6} M) under excitation at 507 nm in CH_3CN:H_2O (4:1, v/v) upon addition of increasing amount of CN^- (1.0x10^{-3} M). (b) Graph of quenching intensity at 600 nm

Considering fluorometric titration to determine the log β value, the fluorescence respond at 600 nm were dramatically quenched (Figure 4.22a) with the increment of CN^- into the solution of **BF_2-CurOH**. The emission band was quenched completely after adding 40 equiv of CN^- (Figure 4.22b). According to the obtained data, we have calculated the log β value of **BF_2-CurOH** in equation 4.5 (shown in Figure 4.24). The log β value of the CN^- complexation of **BF_2-CurOH** is 8.7 ± 0.00.

$$I = \frac{(I_0 + I_{lim}\beta[guest]^2)}{(1+\beta[guest]^2)} \qquad (4.5)$$

I = intensity of a particular concentration of guest
I_0 = initial intensity
I_{lim} = limiting (final) intensity
β = stability constant of the receptor with the guest
[guest] = concentration of guest

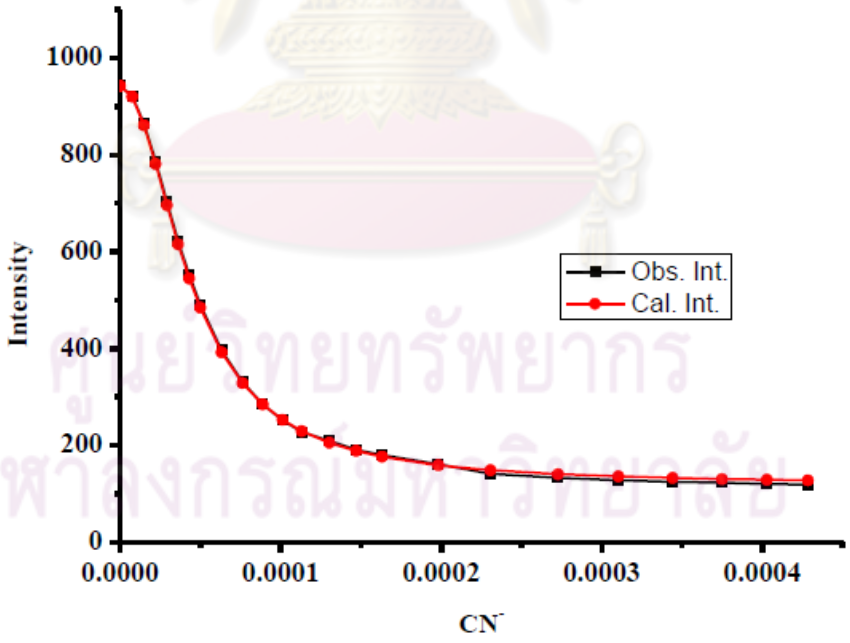

Figure 4.23 Comparing experiment data and calculated data form fluorescence titration of **BF_2-CurOH** and CN^- for calculation of stability constant at emission 600 nm

Concerning the λ_{em} at 750 nm (ex. 649 nm), the fluorescent titration exhibited the enhancement of fluorescence respons upon the addition of CN^-. This can be described that CN^- may interact with hydroxyl group to form hydroxy anion. Both negative charges prefered to delocalize via π-conjugated bond to **BF_2**-moiety resulting in increase of a high charge separation between **BF_2** group and benzene ring and subsequent to a large red shift of λ_{em} (150 nm).

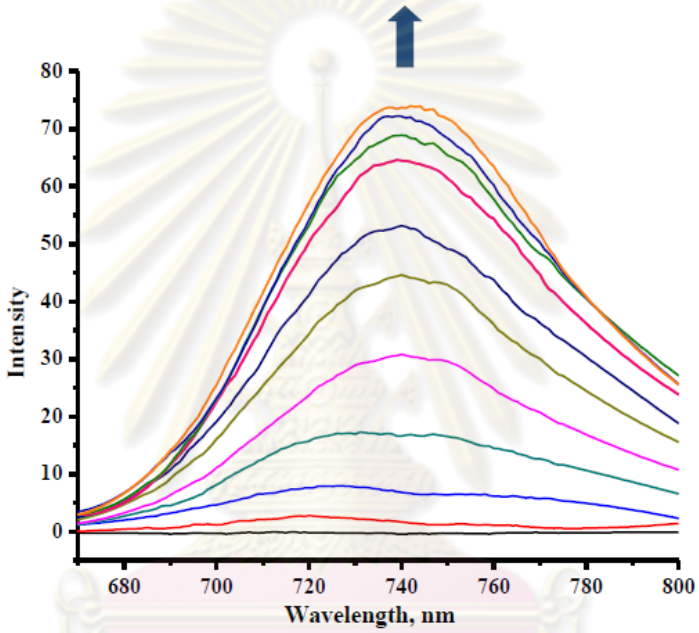

Figure 4.24 Fluorescence spectra of **BF_2-CurOH** ($7.5x10^{-6}$ M) under excitation at 649 nm in CH_3CN:H_2O (4:1, v/v) upon addition of increasing amount of CN^- ($1.0x10^{-3}$ M)

In the case of **curcumin**, upon the addition of 100 equivalent of CN^- to the solution of **curcumin**, a decrease in the emission band at 534 nm was monitored as shown in Figure 4.25. In the same conditions, no significant spectra changes were observed after adding 100 equivalents of other anions. The results suggested that **curcumin** was potentially available for selective CN^- detection over other anions.

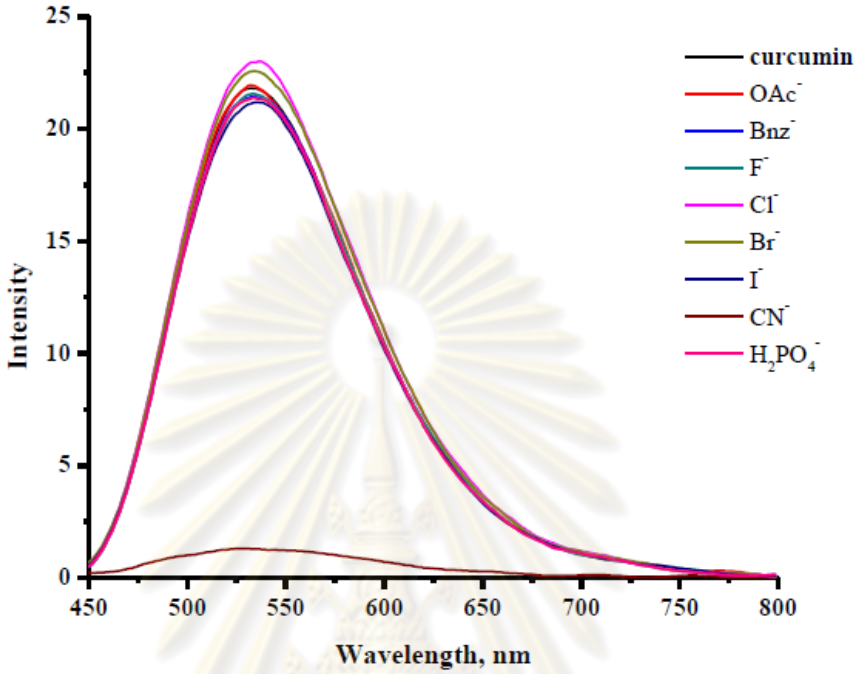

Figure 4.25 The fluorescence spectra of **curcumin** (5 μM) in CH_3CN:H_2O (4:1, v/v) in the presence of TBA salts of various 100 equivalents anions (F^-, Cl^-, Br^-, I^-, CN^-, AcO^-, $PhCOO^-$ and $H_2PO_4^-$, 100 equiv, respectively) under excitation at 417.1 nm.

The interaction of **curcumin** with CN^- was investigated by fluorescence spectrophotometric titration. The fluorescence spectra of **curcumin** was dramatically decreased upon the addition of CN^- as shown in Figure 4.26. Fitting of the experimental data gave a log β value of 7.7 ± 0.02 (Figure 4.27). From the fluorometric titration spectra, this clearly shows that PET was dominated upon the interaction with CN^-.

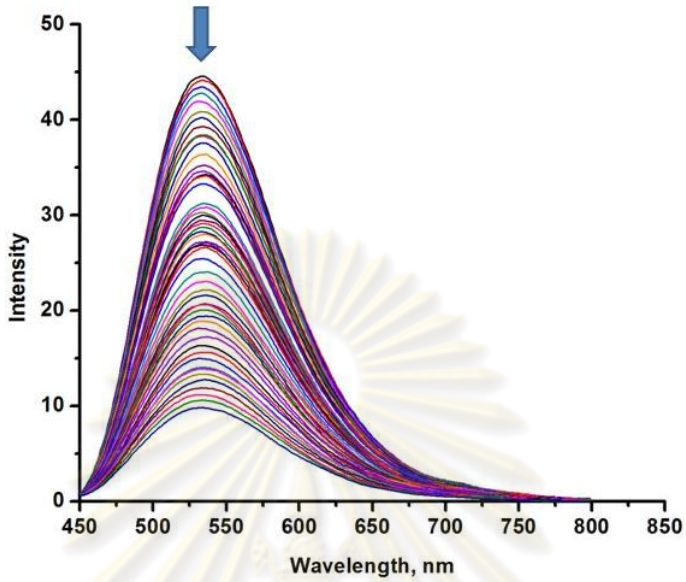

Figure 4.26 Fluorescence spectra of **curcumin** ($7.5x10^{-6}$ M) under excitation at 417 nm in $CH_3CN:H_2O$ (4:1, v/v) upon addition of increasing amount of CN^- ($1.0x10^{-3}$ M)

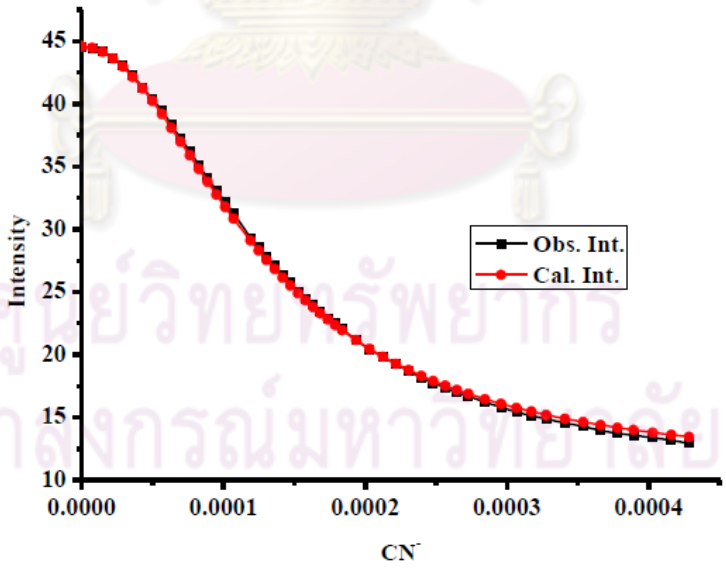

Figure 4.27 Comparing experiment data and calculated data form fluorescence titration of **curcumin** and CN^- for calculation of stability constant

4.9 Interference studies

The effect of foreign substances was evaluated by analyzing a standard solution of CN^- to the interference species added. The tolerance amount and the value (%) of relative error of **BF_2-CurOH** and **curcumin** are shown in Table 4.6 and 4.7. The criterion for interference is fixed at a ±10% relative error. From Table 4.6 and Figure 4.28, it can be seen that most coexisting substances show effects on the determination of CN^- for **curcumin**. For **BF_2-CurOH**, F^-, AcO^- and $H_2PO_4^-$ interfered the cyanide detection. Compared to **curcumin**, **BF_2-CurOH** is greater selective and sensitive for cyanide sensing in aqueous.

Table 4.6 Interference of foreign substances with the determination of **BF_2-CurOH** ($7.5x10^{-6}$ M).

Foreign substances	Amount added (molar ratio)	Relative error (%)
F^-	100	9.5
Cl^-	1000	9.7
Br^-	1000	2.8
I^-	1000	0.2
AcO^-	470	9.8
BnZ^-	1000	6.2
$H_2PO_4^-$	6	8.7

Table 4.7 Interference of foreign substances with the determination of **curcumin** ($7.5x10^{-6}$M)

Foreign substances	Amount added (molar ratio)	Relative error (%)
F^-	1000	131.2
Cl^-	1000	119.2
Br^-	1000	120.4
I^-	1000	116.0
AcO^-	1000	117.3
BnZ^-	1000	111.9
$H_2PO_4^-$	1000	124.8

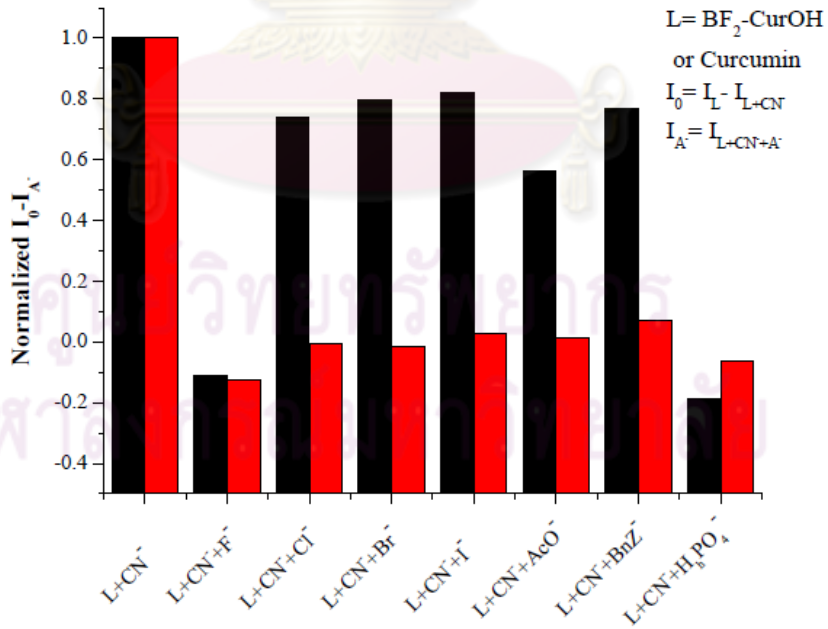

Figure 4.28 For effect of foreign substances with determination of CN^- red bar and black bar represent to **BF_2-CurOH** and **curcumin**, respectively

4.10 Detection limit

Detection limit in visual detection of CN^- for **BF_2-CurOH** was investigated from color change of solution. The red solution of **BF_2-CurOH** was changed to be blue solution by adding 22 μM of CN^- (shown in Figure 4.29).

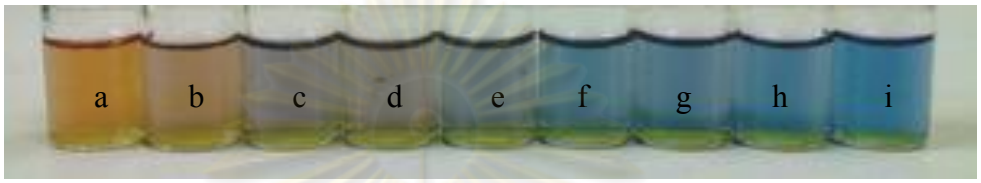

Figure 4.29 Colorimetric changes of BF_2-CurOH (1 x 10^{-5} M) upon the addition of cyanide in CH_3CN:H_2O (4:1, v/v) solution. (a. 0, b. 15, c. 22, d. 24, e. 29, f. 36, g. 43, h. 50 and i. 57 μM of CN^-)

Moreover, the detection limit of **BF_2-CurOH** was examined by UV-visible spectrophotometry. The 10 samples of **BF_2-CurOH** ($7.5x10^{-6}$ M) was prepared and measured in absorbance (Table 4.8). The standard deviation of absorbance is 0.3318 and linear plot was carried out between [CN^-] and absorbance (λ=505.0 nm). The concentration of **BF_2-CurOH** is $7.5x10^{-6}$ M and the concentration of guest in linear range is 0.76-7.4 μM giving a good linear correlation R^2 of 0.992 as shown in Figure 4.30. The detection limit of cyanide obtained by UV-visible technique is 0.14 μM for **BF_2-CurOH**.

Table 4.8 The absorbance of **BF_2-CurOH** $7.5x10^{-6}$ M

Point	Absorbance
1	1.35
2	1.33
3	1.28
4	1.37
5	1.38
6	1.37
7	1.32
8	1.38
9	1.32
10	1.37

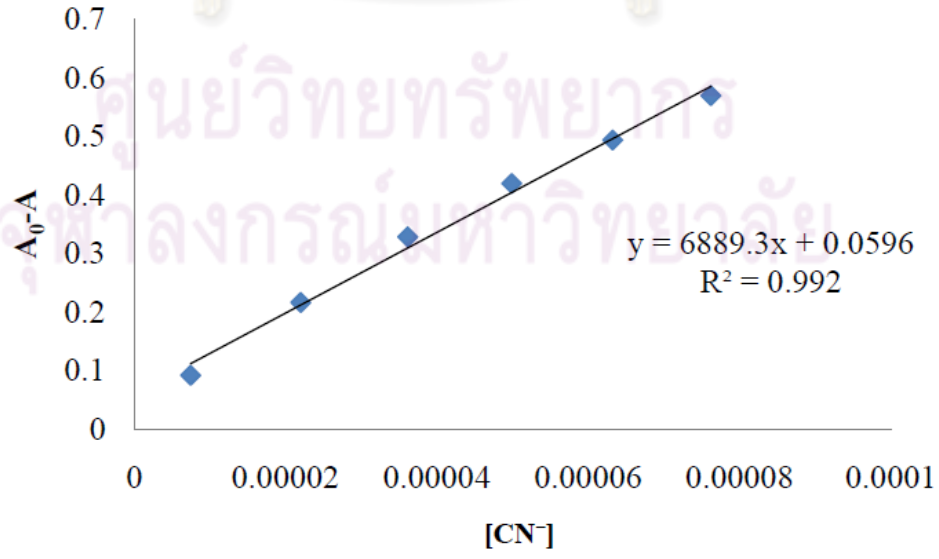

Figure 4.30 Linear plot between absorbance and concentration of with CN^-

Similarly, the detection limit of **curcumin** is also investigated by UV-visible spectrophotometry. The standard deviation of absorbance is 0.0169. The linear plot was carried out between [CN^-] and absorbance (λ=423 nm). The concentration of **curcumin** is $7.5x10^{-6}$ M and the concentration of guest in linear range is 9.5 – $19.5x10^{-5}$ M with a good linear correlation (R^2) value of 0.9984 (shown in Figure 4.30). The detection limit of CN^- detection is 9.33 μM for **curcumin**.

Table 4.9 The absorbance of **curcumin** $7.5x10^{-6}$ M

Point	Absorbance
1	0.38
2	0.35
3	0.34
4	0.34
5	0.34
6	0.33
7	0.35
8	0.33
9	0.33
10	0.34

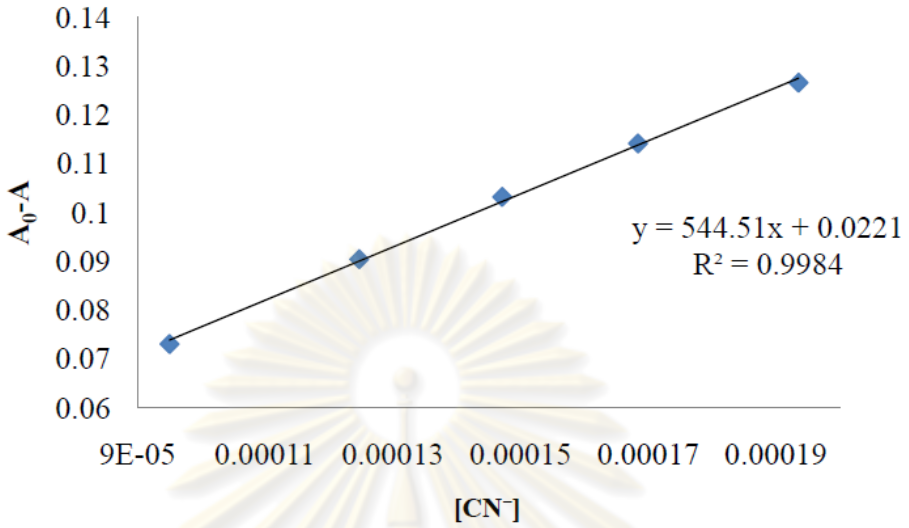

Figure 4.31 Linear plot between absorbance and concentration of **curcumin** with CN^-

Furthermore, the detection limit of CN^- sensing for **curcumin** obtained from the visual detection was investigated. The yellow solution of **curcumin** turned dramatically to the orange solution and to red solution. The visual capacity of CN^- detection can be observed with addition 99 μM of CN^- ion (shown in Figure 4.32).

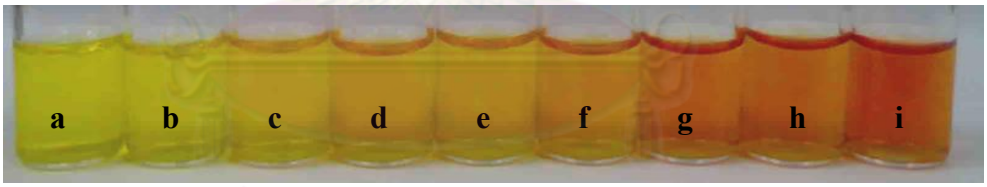

Figure 4.32 Colorimetric changes of **curcumin** (1 x 10^{-4} M) upon the addition of cyanide in CH_3CN:H_2O (4:1, v/v) solution. (a. 0, b. 50, c. 75, d. 99, e. 109, f. 124, g. 149, h. = 164 and i. 172 μM of CN^-)

From all data obtained from spectrophotometry, the results were collected in Table 4.10. The log β value from UV-visible and fluorescence of **BF_2-CurOH** is higher than those of **curcumin**. Additionally, the detection limits with naked-eye and UV-visible technique of **BF_2-CurOH** show lower than those of **curcumin**. From the comparing log β value and detection limit in **BF_2-CurOH** and **curcumin**, the results revealed that **BF_2-CurOH** is exhalent CN^- sensing.

Table 4.10 Summarize of log β values and detection limit of **curcumin** and **BF_2-CurOH** in spectrophotometry

Compound	Log β		Detection limit (μM)	
	UV-visible	Fluorescence	Naked-eye	UV-visible
Curcumin	7.7 ± 0.00	7.7 ± 0.02	99	9.33
BF_2-CurOH	8.8 ± 0.00	8.7 ± 0.00	22	0.14

CHAPTER V

CONCLUSION

Novel **curcumin** derivatives containing **BF_2**-incorporated **curcumin**, **BF_2-CurOMe**, **BF_2-CurmonoTs** and **BF_2-CurdiTs** were successfully synthesized. **BF_2-CurOMe** was obtained by the metylating **BF_2-CurOH** with methyl iodide using potassium carbonate as base. Mono and di-tosylated (**BF_2-curOTs** and **BF_2-curdiOTs**) compounds prepared by the reaction between tosyl chloride and **BF_2-curOH**, contained the electron-withdrawing group. The photophysical properties of the D-A-D sensors based on **BF_2**-incoorperated **curcumin** revealed that electron-withdrawing group attached on the donor parts of the molecule **(BF_2-CurmonoTs** and **BF_2-CurdiTs**) induced the hypsochromic shift in both absorptions and emissions. Conversely, the electron donating modified on the donor parts (**BF_2-CurOMe**) supported a higher stabilized energy level of the molecule and resulted in the bathochromic shift of absorption and emission spectra. The quantum yields of compounds, **BF_2-CurOH**, **BF_2-CurOMe**, **BF_2-CurmonoTs** and **BF_2-CurdiTs** in dichloromethane were 0.62, 0.61, 0.22 and 0.48, respectively. Particularly, the photophysical properties of **BF_2-curOH** and **BF_2-curOMe** exhibited the positive solvatochromic effect undergone the influence of the polarity and polarizability between solvent and solutes. These solvent effects were evaluated by Kamlet-Taft equation. The sign of correlation coefficient *c* belonging to both compounds were negative. It is indicative of the strong solvation stabilized upon increasing solvent polarity resulting in the bathochromic shift of absorption.

Concerning on the anion sensing, **BF_2-curOH** is excellent cyanide sensing with very high selectivity and sensitivity over **curcumin**. This approach was subjected to the deprotonation of hydroxyl group on the ends of the long π- conjugated aromatic rings as a result of a negative charge on oxygen atom which preferred to delocalize through π-conjugated bond giving ICT process. In comparison of **curcumin**, **BF_2-CurOH** containing **BF_2** moiety as a stronger acceptor than diketone showed larger red shifts of emission and absorption.**BF_2-CurOH** can be a naked-eye sensor for CN^- with a better detection limit than **curcumin**. The deprotonation abilities by CN^- to both compounds measured by UV-visible titration and fluorometric titration exhibited the log β values of 8.8 and 7.7 for **BF_2-CurOH** and **curcumin**, respectively. Interestingly, the foreign anions such as AcO^-, HPO_4^- and F^- can interfere the cyanide sensing for **BF_2-curOH** while all foreign anions, AcO^-, HPO_4^- and F^- , Cl^-, Br^- and I^- can affect the detection of cyanide for **curcumin** in aqueous solution.

REFFERENCES

[1] Lehn, J.-M. *Supramolecular Chemistry: Concepts and Perspectives*. Weinheim: VCH publisher, 1995.

[2] Lehn, J.-M. in Proceeding of the Centenary of the Geneva Conference Organic Chemistry: Its Language and Its State of the Art (Kisakurek, M. V. (Ed.) Weinheim: VCH publisher, 1993.

[3] Vogtle, F. *Supramolecular Chemistry: An introduction.* Chichesters: John Wiley & Sons, **1991**.

[4] Martinez-Manez, R. and Scancenon, F. *Chem. Rev.*103 (2003): 4419-4476.

[5] de Silva, A. P.; Gunaratne, H. Q. N.; Gunnlaugsson, T.; Huxley, A. J. M.; McCoy, C. P.; Rademacher, J. T.; Rice, T. E. *Chem. Rev.* 97 (1997): 1515-1566.

[6] Hou, X. and Kobir, K. *Chem. Lett.* 35 (2006): 116-118.

[7] Kovalchuk, A.; Bricks, J. L.; Reck, G.; Rurack, K.; Schulz, B.; Szumna, A. and WeiBhoff, H. *Chem. Commun.* (2004): 1946-1947.

[8] Hartley, J. H.; James, T. D.; Ward, C. J. *J. Chem. Soc., Perkin Trans. 1* (2000): 3155-3184.

[9] Beer, P. D.; Gale, P. A. *Angew. Chem., Int. Ed.* 40 (2001): 486-516.

[10] Echevarren, A.; Gala´n, A.; Lehn, J.-M.; de Mendoza, J. *J. Am.Chem. Soc.* 111 (1989): 4994-4995.

[11] Berger, M.; Schmidtchen, F. P. *J. Am. Chem. Soc.* 121 (1999): 9986-9993.

[12] Camiolo, S.; Gale, P. A.; Ogden, M. I.; Skelton, B. W.; White, A. H. *J. Chem. Soc., Perkin Trans. 2* (2001): 1294-1298.

[13] Shinoda, S.; Tadokoro, M.; Tsukube, H.; Arakawa, R. *Chem.Commun.* (1999): 181-182.

[14] Lehn, J.-M.; Me´ric, R.; Vigneron, J.-P.; Bkouche-Waksman, I.; Pascard C. *J. Chem. Soc., Chem. Commun.* (1991): 62-64.

[15] Kimura, E.; Koike, T. *Chem. Commun.* (1998): 1495-1500.

[16] Bazzicalupi, C.; Bencini, A.; Bianchi, A.; Cecchi, M.; Escuder, B.; Fusi, V.; García-Espanã, E.; Giorgi, C.; Luis, S. V.; Maccagni,G.; Marcelino, V.; Paoletti, P.; Valtancoli, B. *J. Am. Chem. Soc.* 121 (1999): 6807-6815.

[17] Alfonso, I.; Dietrich, B.; Rebolledo, F.; Gotor, V.; Lehn, J.-M. *Helv.Chim. Acta* 84 (2001): 280-295.

[18] Amendola, V.; Fabbrizzi, L.; Mangano, C.; Pallavicini, P.; Poggi, A.; Taglietti, A. *Coord. Chem. Rev.* 219-221 (2001): 821-837.

[19] Fabbrizzi, L.; Licchelli, M.; Rabaioli, G.; Taglietti, A. *Coord. Chem. Rev.* 205 (2000): 85-108.

[20] Miyaji, H. and Sessler, J. L. *Angew. Chem. Int. Ed,* 40 (2001): 154-157.

[21] Fabbrizzi, L. and Poggi, A.*Chem. Soc. Rev.* 24 (1995): 197-202.

[22] Gale, P. A.; Twyman, L.J.; Handlin, C. I. and J. L. Sesser. *Chem. Common.* (1999): 1851-1852.

[23] Smith, J. O.; Olson, D. A. and Armitage, B. A. *J. Chem. Soc.* 121 (1999): 2686-2695.

[24] Hennirich, G.; Sonnenschein, H. and U. Resch-Genger. *Tetrahedron Lett.* 42 (2001): 795-798.

[25] Kubo, Y.; Tsukahara, M.; Ishihara, S. and Tokita, S. *Chem. Commun.* (2000): 653-654.

[26] Raker, J.; Glass, T. E. *J. Org. Chem.* 67 (2002): 6113-6116.

[27] Ross Kelly, T.; and Kim, M. H. *J. Am. Chem. Soc.* 116 (1994): 7072-7080.

[28] Bourson, J.; Valeur, B. *J. Phys. Chem.* 93 (1989): 3871-3876.

[29] Fery-Forgues, S., Le Bris, M. T., Guette, J. P. Valeur, B., *J. Chem. Soc. Chem*. *Commun.* (1988): 384.

[30] Scheibe, G.; Felger, E.; Rossler, G. *Ber. Dtsch. Chem. Ges.* 60 (1927): 1406-1419.

[31] Sheppard, S. E. *Reu. Mod. Phys.* 14 (1942): 303-340.

[32] Hantzsch, A. *Ber. Dtsch. Chem. Ges.* 55 (1922): 953-979.

[33] Frlnik, J. *bans. karaday Soc*. 21 (1926): 536-542.

[34] Condon, C. U. *Phys. Rev.* 32 (1928): 858-872.

[35] Reichardt, C. *Solvents and Solvent Effects in Organic Chemistry,* 2nd ed.; VCH Publishers: Weinheim, 1988.

[36] Ishchenko, A. A. *Russ. Chem. Rev.* 60 (1991): 865-884.

[37] Kosower, E. M. *J. Am. Chem. Soc.* 80 (1958): 3253-3260.

[38] Dimroth, K.; Reichardt, C.; Siepmann, T.; Bohlmann, F. *Liebigs Ann. Chem.* 661 (1963): 1-37**.**

[39] Reichardt, C.; Harbusch-Gornert, E. *Liebigs Ann. Chem.* (1983): 721-743.

[40] Reichardt, C. *Chem. Rev.* 94 (1594): 2319-2358.

[41] Abboud, J.-L. M.; Kamlet, M. J.; Taft, R. W. *Prog. Phys. Org. Chem.* 13 (1981): 485-630.

[42] Pytela, O. *Collect. Czech. Chem. Commun.* 53 (1988): 1333-1423.

[43] Buncel, E.; Rajagopal, S. *Ace. Chem. Res.* 23 (1990): 226-231.

[44] Fawcett, W. R. *J. Phys. Chem.* 97 (1993): 9540-9546.

[45] Nishimura, N.; Kosako, S.; Sueishi, Y. *Bull. Chem. Soc. Jpn.* 57 (1984): 1617-1625**.**

[46] Nakatsuji, S.**;** Yahiro, T.; Nakashima, K.; Akiyama, S.; Nakazumi, H. *Bull. Chem. Soc. Jpn.* 64 (1991): 1641-1647.

[47] Reichardt, C. *Angew. Chem.* 91 (1979): 119-131.

[48] Exner, O. *Prog. Phys. Org. Chem.* 18 (1990): 129-161.

[49] Palm, V.; Palm, N. *Org. React. (Tartu)* 28 (1993): 125-150.

[50] Kamlet, M. J.; Abboud, J.-L. M.; Taft, R. W. *J. Am. Chem. Soc*. 99 (1977): 6027-6038.

[51] Mao, F.; Tyler, D. R.; Bruce, M. R. M.; Bruce, A. E.; Rieger, A. L.; Rieger, P. H. *J. Am. Chem. Soc.* 114 (1992): 6418-6424.

[52] Kamlet, M. J.; Abboud, J.-L. M.; Taft, R. W. *J. Am. Chem. Soc.* 99 (1977): 6027-6038.

[53] Kamlet, M. J., Hall, T. N.; Boykin, J.; Taft, R. W. *J. Org. Chem.* 44 (1979): 2599-2605.

[54] Taft, R. W.; Abboud, J.-L. M.; Kamlet, M. J. *J. Am. Chem. Soc.* 103 (1981): 1080-1086.

[55] Essfar, M.; Guiheneuf, G.; Abboud, J.-L. M. *J. Am. Chem. Soc.* 104 (1982): 6786-6787.

[56] Kamlet, M. J.; Taft, R. W. *J. Am. Chem. Soc.* 98 (1976): 377-383.

[57] Miller, J. N.; Miller. J. C. *Statistics and chemometric for analytical chemistry.* Harow: Prentice Hall, 2000.

[58] Aggarwal, B.B.; Sung, B. *Trends. Pharmacol. Sci.* 30 (2008): 85-94.

[59] Payton, F.; Sandusky, P.; Alworth, W. L. *J. Nat. Prod.* 70 (2007): 143-146.

[60] Shen L.; Ji, H.F. *Spectrochim. Acta-Part A* 67 (2007): 619-623.

[61] Khopde, S. M.; Priyadarsini, K. I.; Palit, D. K.; Mukherjee, T. *Photochem. Photobiol.* 72 (2000): 625-631.

[62] Chignell, C. F.; Bilski, P.; Reszka, K. J.; Motten, A. G.; Sik, R. H.; Dahl, T. A. *Photochem. Photobiol.* 59 (1994): 295-302.

[63] Adhikary, R.; Mukherjee, P.; Kee; T.W., Petrich; J. W. *J. Phys. Chem. B* 113 (2009): 5255-5261.

[64] Began, G.; Sudharshan, E.; Udaya Sankar, K; Appu Rao, A. G. *J. Agric Food Chem.* 47 (1999): 4992-4997.

[65] Inoue, K.; Yoshimura, Y.; Nakazawa, H. *Anal. Lett.* 34 (2001): 1711-1718.

[66] Zsila, F; Bikadi, Z; Simonyi, M. *Biochem Biophys Res Commun.* 301 (1999): 776-782.

[67] Bernabé-Pineda, M. T.; Ramírez-Silva, M.; Romero-Romo, E.; González-Vergara, Rojas-Hernández, A. *Spectrochimica Acta Part A* 60 (2004): 1091-1097.

[68] Shen, L.; Ji, H.-F. *Spectrochim. Acta Part A* 67 (2007): 619-623.

[69] Zsila, F.; Bikádi, Z.; Simonyi, M. *Tetrahedron Asymmetry* 14 (2003): 2433-2444.

[70] Balasubramanian, K. *Ind. J. Chem.* 30 (1991): 61-65.

[71] Nardo, L.; Paderno, R.; Andreoni, A.; Mason, M.; Haukvik, T.; Tonnesen, H. H.; *Spectroscopy* 22 (2008): 187-198,.

[72] Rurack, K.; Kollmannsberger, M.; Resch-Genger, U.; Daub, J. *J. Am. Chem. Soc.* 122 (2000): 968-969.

[73] Rurack, K.; Kollmannsberger, M.; Daub, J. *Angew. Chem. Int. Ed.* 40 (2001): 385-387.

[74] Loudet, A.; Burgess, K. *Chem. Rev*. 107 (2007): 4891-4932.

[75] Rohand, T.; Baruah, M.; Qin, W. W.; Boens, N.; Dehaen, W. *Chem. Commun*. (2006): 266-268.

[76] Qin, W. W.; Rohand, T.; Baruah, M.; Stefan, A.; Van der Auweraer, M.; Dehaen, W.; Boens, N. *Chem. Phys. Lett*. 420 (2006): 562-568.

[77] Loudet A., Bandichhor R., Wu L., Burgess K. *Tetrahedron*, 64 (2008): 3642-3654.

[78] Loudet, A.; Bandichhor, R.; Burgess, K.; Palma, A.; McDonnell, S. O.; Hall, M. J.; O'Shea, D. F. *Org. Lett.* 10 (2008): 4771-4774.

[79] Turfan, B.; Akkaya, E. U. *Org. Lett*. 4 (2002): 2857-2859.

[80] Burghart, A.; Thoresen, L. H.; Chen, J.; Burgess, K.; Bergström, F.; Johansson, L. B.-Å. *Chem. Commun.* (2000): 2203-2204.

[81] Yilmaz, M. D.; Bozdemir, O. A.; Akkaya, E. U. *Org. Lett*. 8 (2006): 2871-2873.

[82] Yee, M.; Fas, S. C.; Stohlmeyer, M. M.; Wandless, T. J.; Cimprich, K. A. *J. Biol. Chem.* 280 (2005): 29053-29059.

[83] Atilgan, S.; Ekmekci, S.; Dogan, A. L.; Guc, D.; Akkaya, E. U. *Chem. Commun.* (2006): 4398-4400.

[84] Ekmekci, Z.; Yilmaz, M. D.; Akkaya, E. U. *Org. Lett.* 10 (2008): 461-464.

[85] Guliyev, R.; Büyükcakir, O.; Sozmen, F.; Bozdemir, O.A. *Tetrahedron Letters* 50 (2009): 5139-5141.

[86] Huh, J. O.; Do, Y.; Lee, M. H. *Organometallics* 27 (2008): 1022-1025.

[87] Demas, J. N.; Keller, R. A. *J. Am. Chem. Soc.* 129 (2007): 8942-8943.

[88] Sah, R. N. and Brown, P.H. *Microchim. J.* 56 (1997): 285-304.

[89] Marcus,Y. *Chem. Soc. Rev.* 22 (1993): 409-416.

[90] Schreiter, K. and Spange, S. *J. Phys. Org. Chem.* 21 (2008): 242-250.

[91] Lee, D. H.; Lee, K. H.; Hong, J.-I. *Org. Lett.* 3 (2001): 5-8.

[92] Lee, D. H.; Lee, H. Y.; Lee, K. H.; Hong, J.-I. *Chem. Commun* (2001): 1188-1189.

APPENDIX

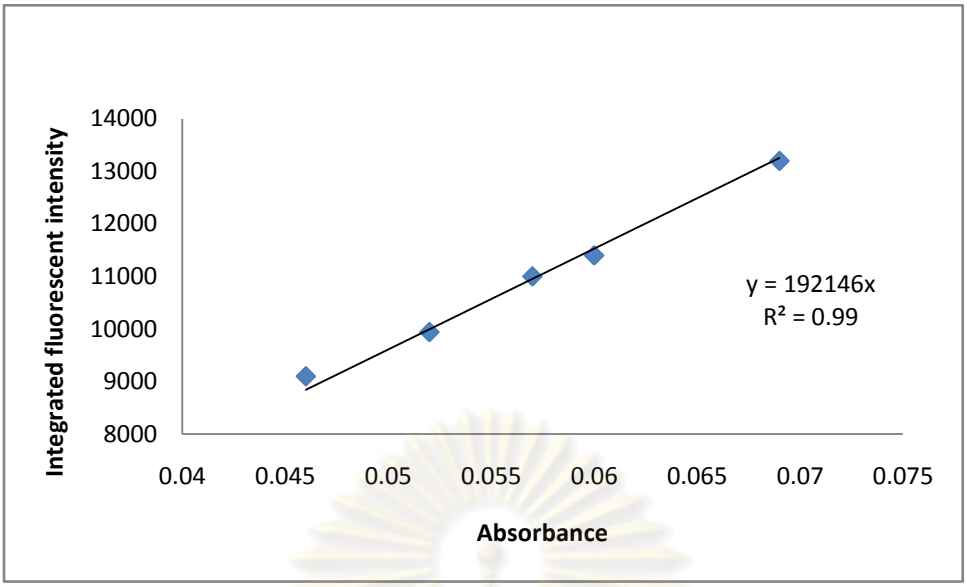

Figure A1 The linear plot between integrated fluorescence intensity (arbitrary units) and absorbance for **curcumin**

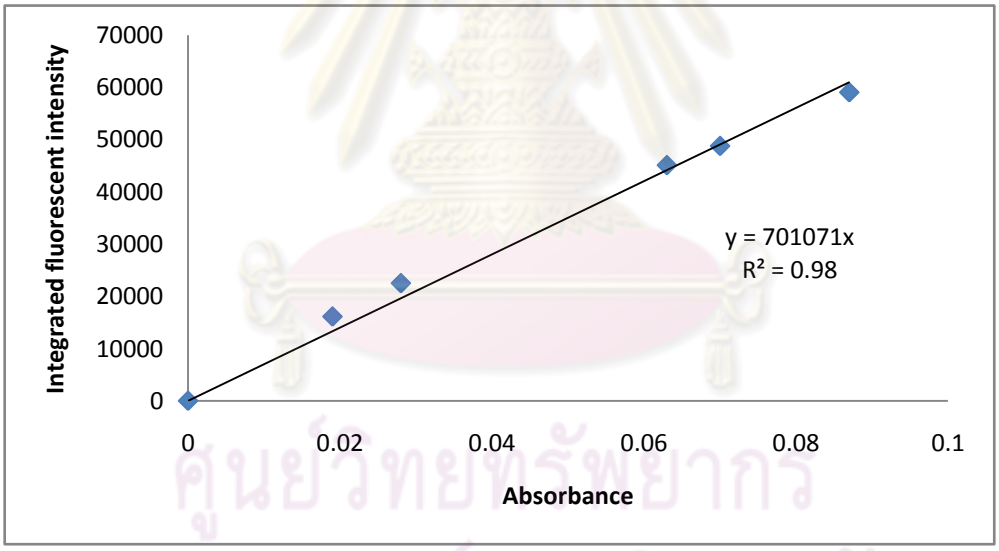

Figure A2 The linear plot between integrated fluorescence intensity (arbitrary units) and absorbance for **BF_2-OH**

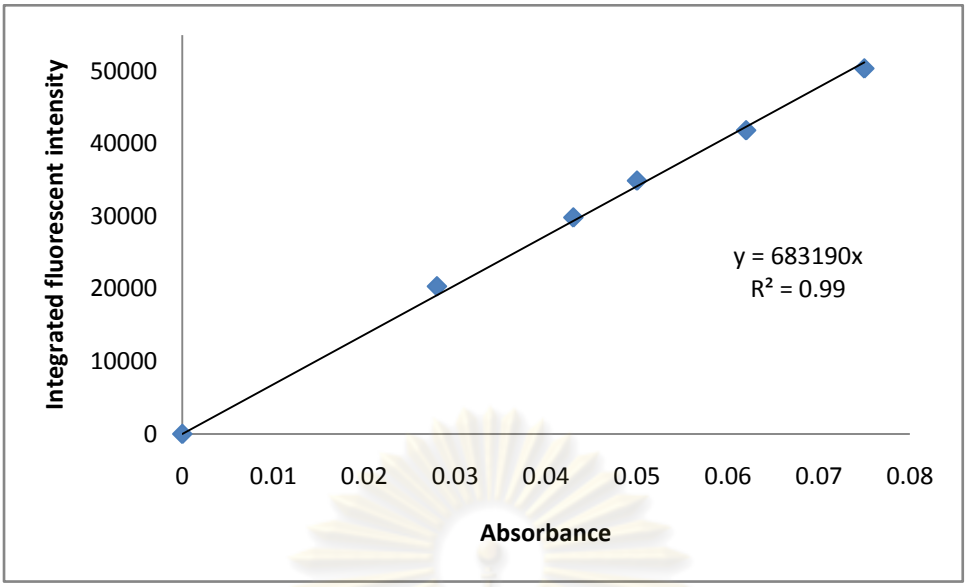

Figure A3 The linear plot between integrated fluorescence intensity (arbitrary units) and absorbance for **BF_2-OMe**

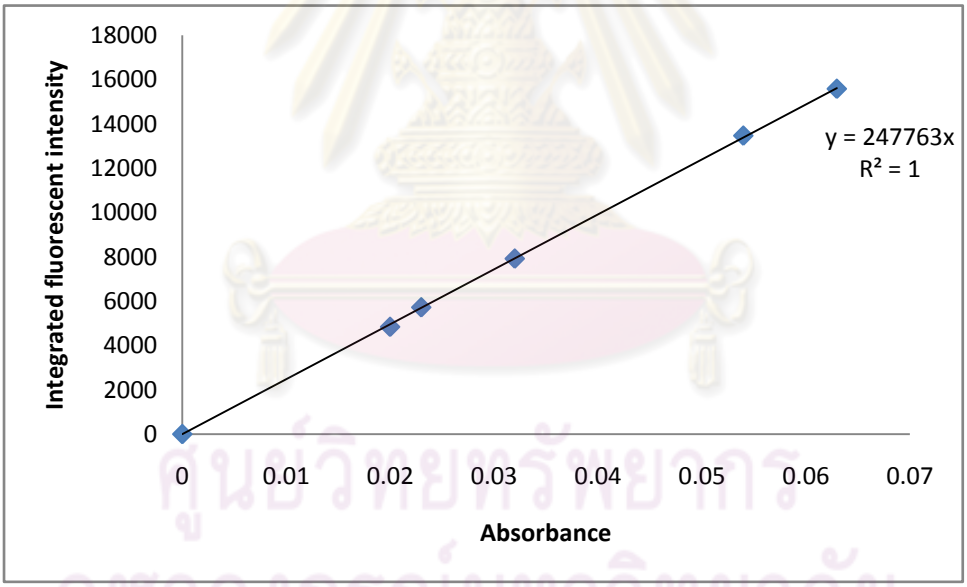

Figure A4 The linear plot between integrated fluorescence intensity (arbitrary units) and absorbance for **BF_2-monoTs**

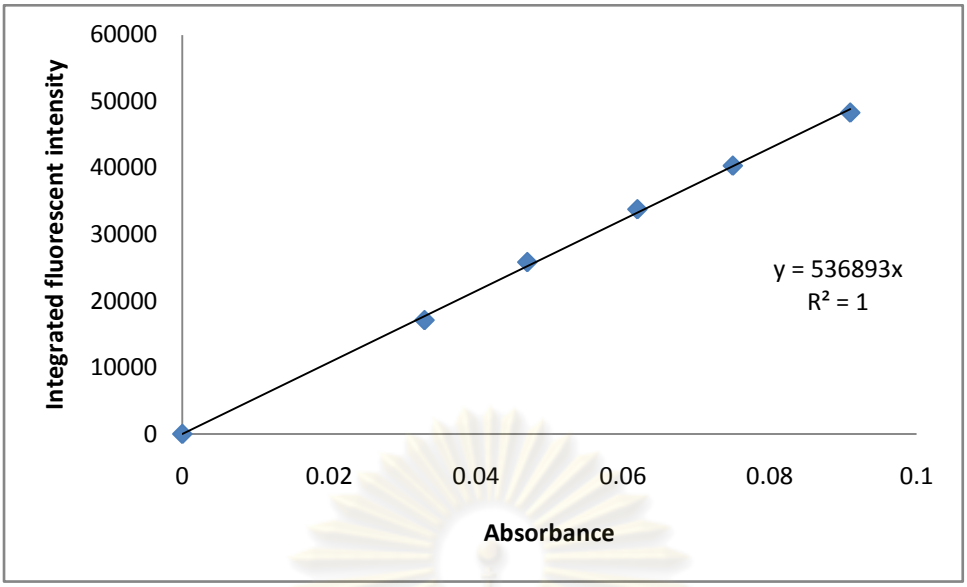

Figure A5 The linear plot between integrated fluorescence intensity (arbitrary units) and absorbance for **BF_2-diTs**

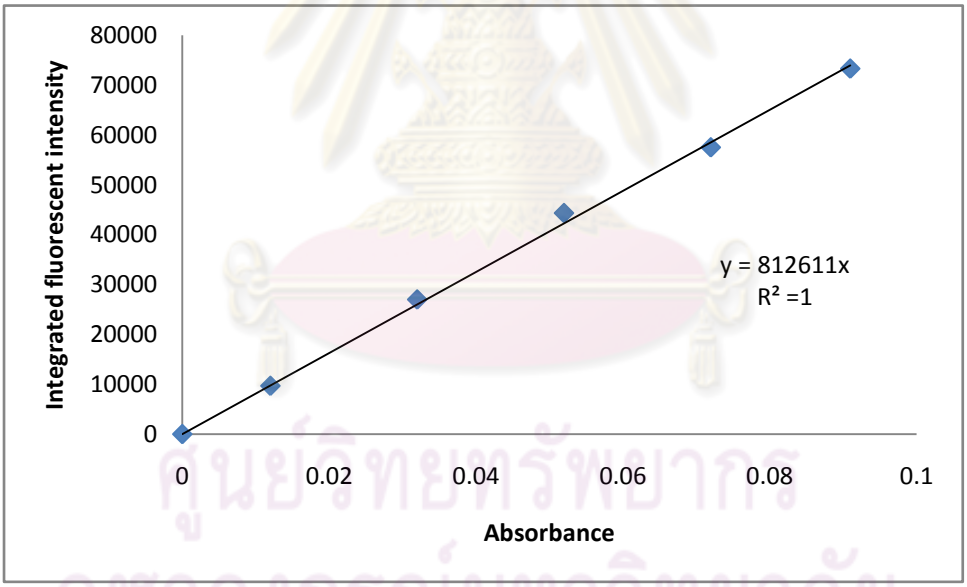

Figure A6 Linear plot between integrated fluorescence intensity (arbitrary units) and absorbance for Quinine bisulphate.

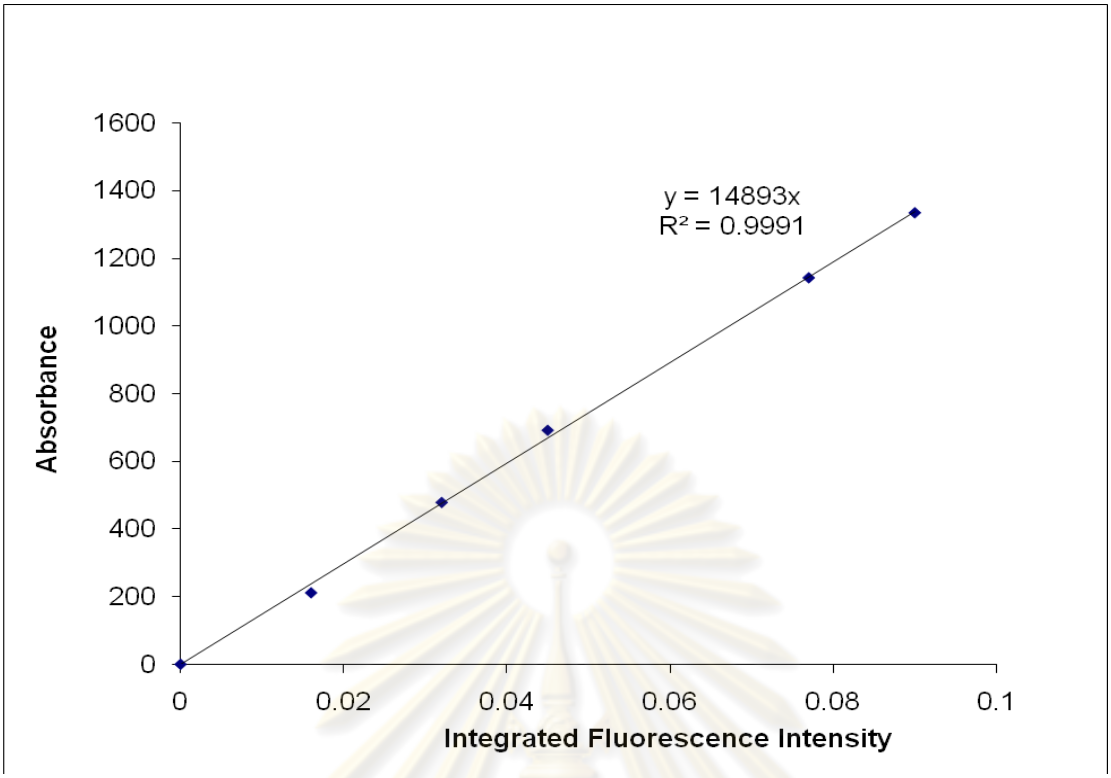

Figure A7 The linear plot between integrated fluorescence intensity (arbitrary units) and absorbance for **BF_2-OH** in MeOH

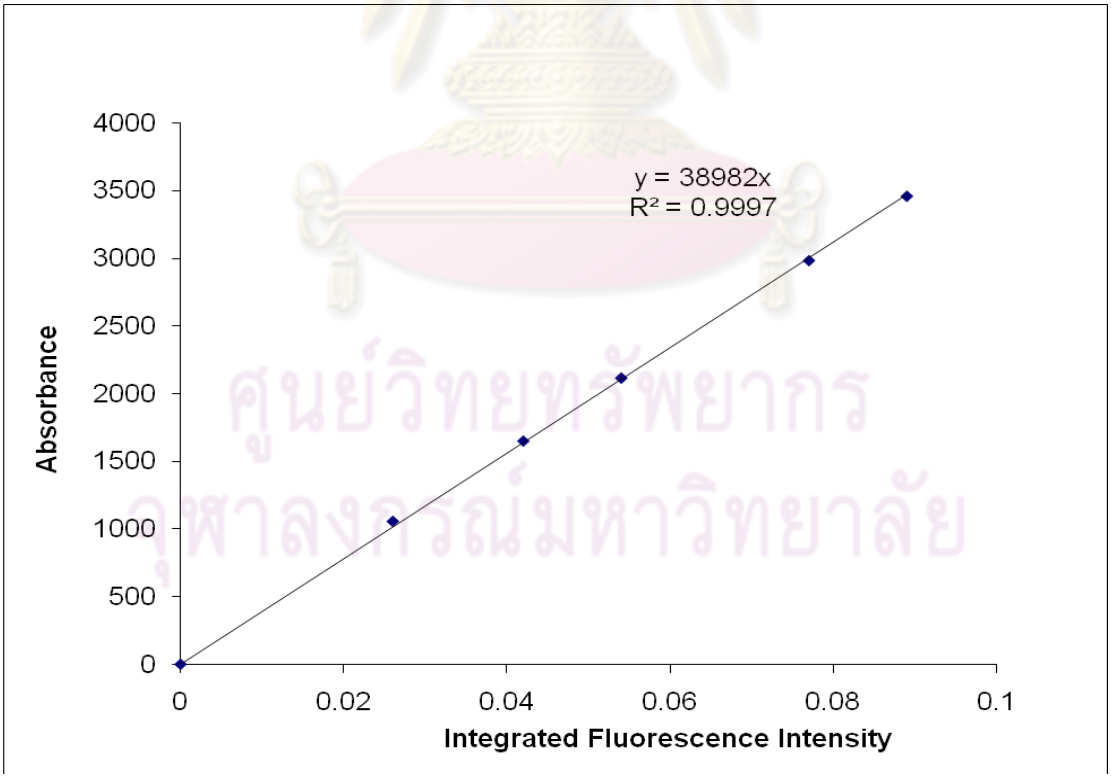

Figure A8 The linear plot between integrated fluorescence intensity (arbitrary units) and absorbance for **BF_2-OH** in EtOH

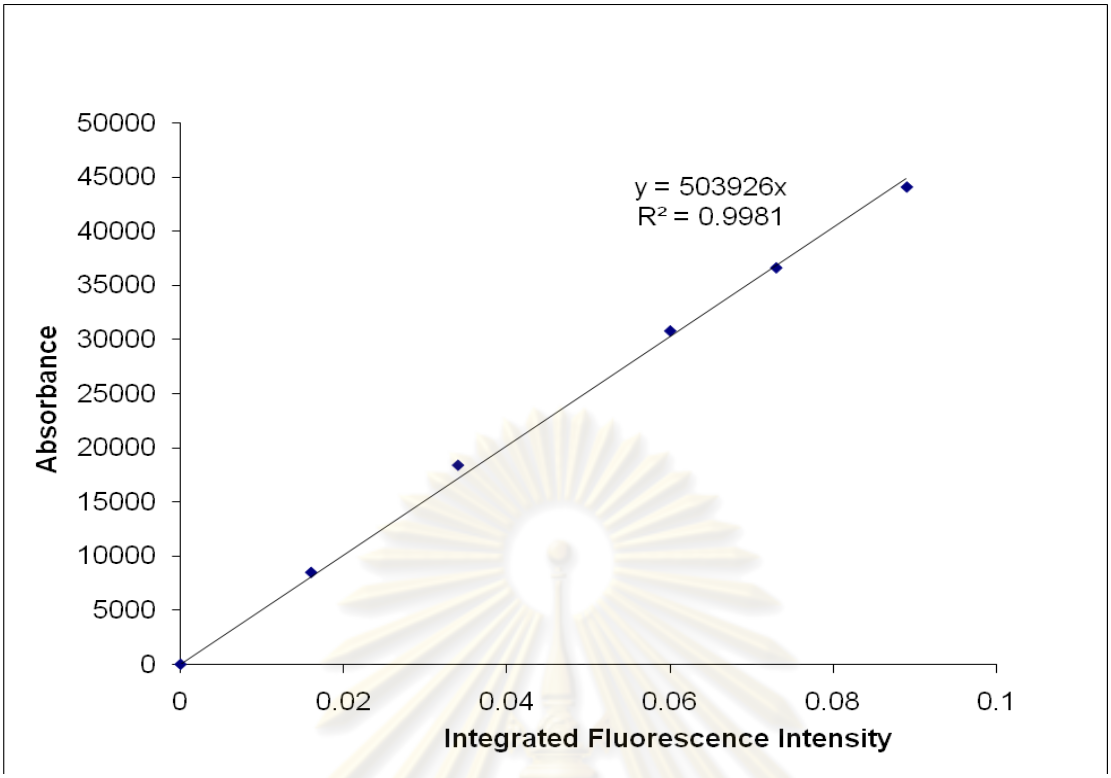

Figure A9 The linear plot between integrated fluorescence intensity (arbitrary units) and absorbance for **BF_2-OH** in CH_3Cl

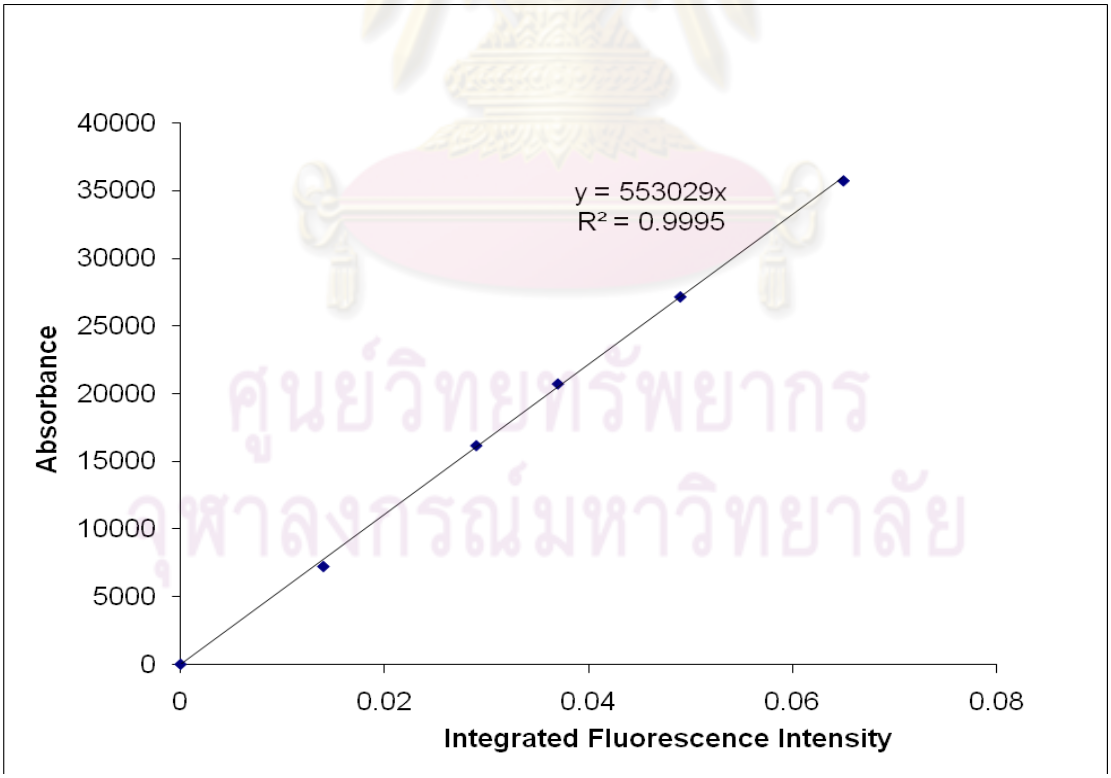

Figure A10 The linear plot between integrated fluorescence intensity (arbitrary units) and absorbance for **BF_2-OH** in toluene

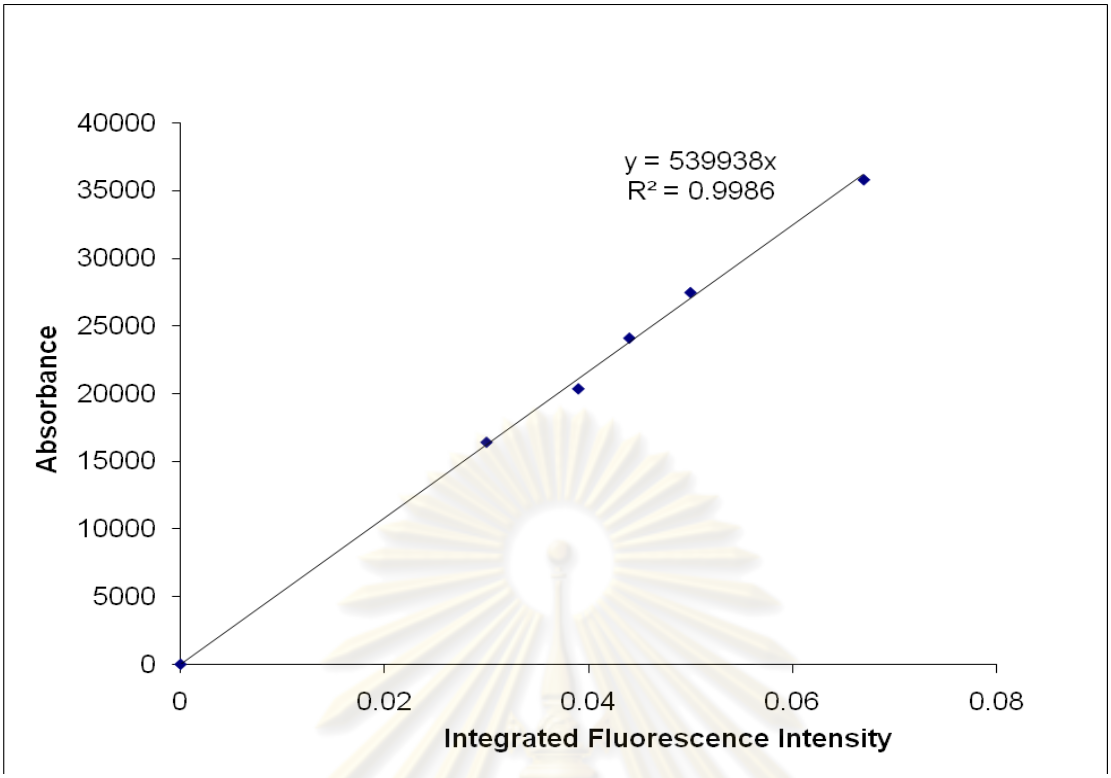

Figure A11 The linear plot between integrated fluorescence intensity (arbitrary units) and absorbance for **BF_2-OH** in benzene

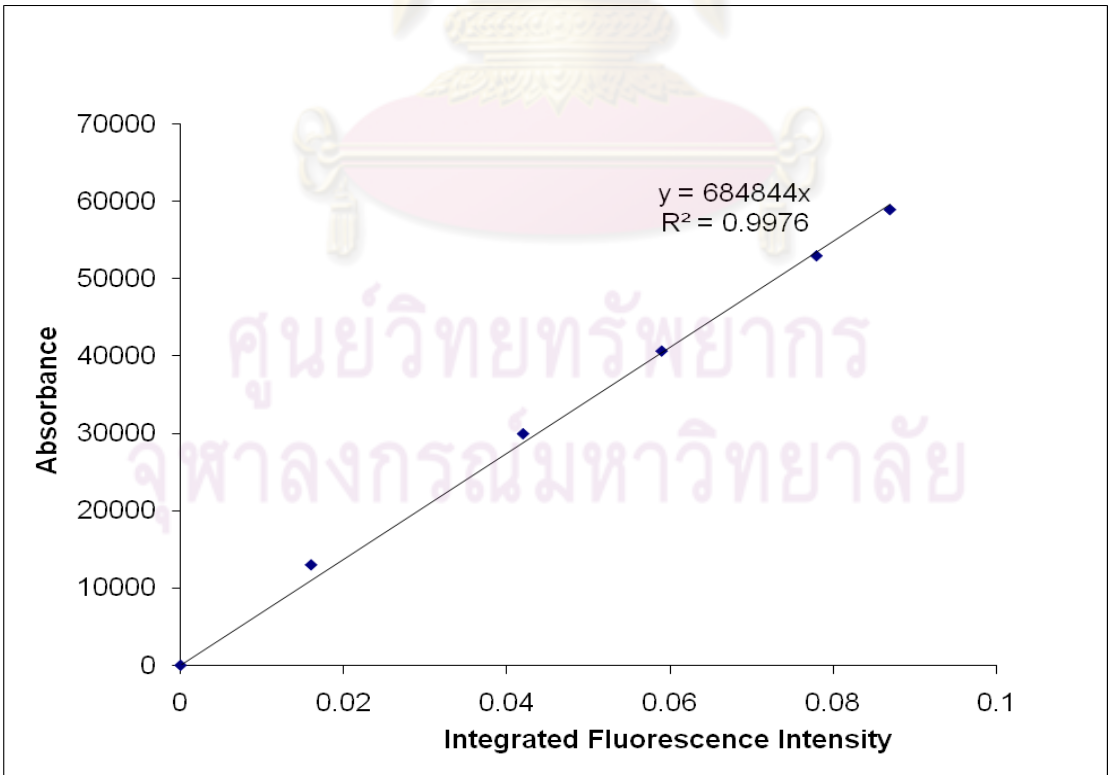

Figure A12 The linear plot between integrated fluorescence intensity (arbitrary units) and absorbance for **BF_2-OH** in diethyl ether

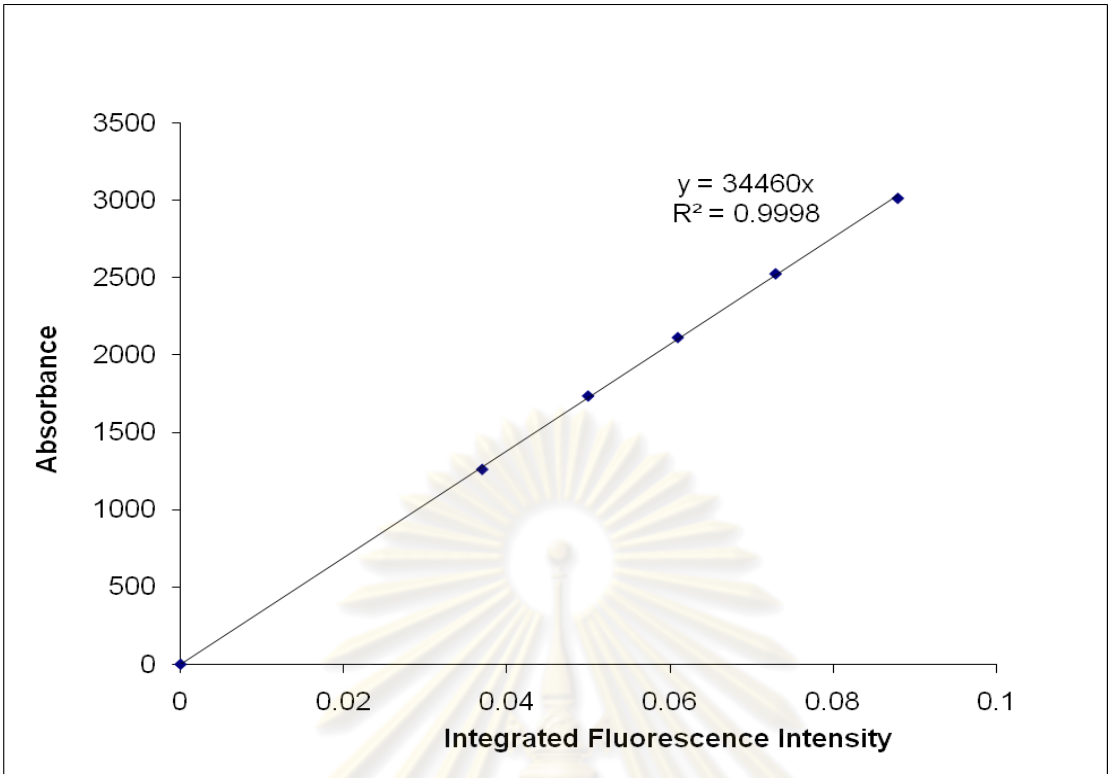

Figure A13 The linear plot between integrated fluorescence intensity (arbitrary units) and absorbance for **curcumin** in MeOH

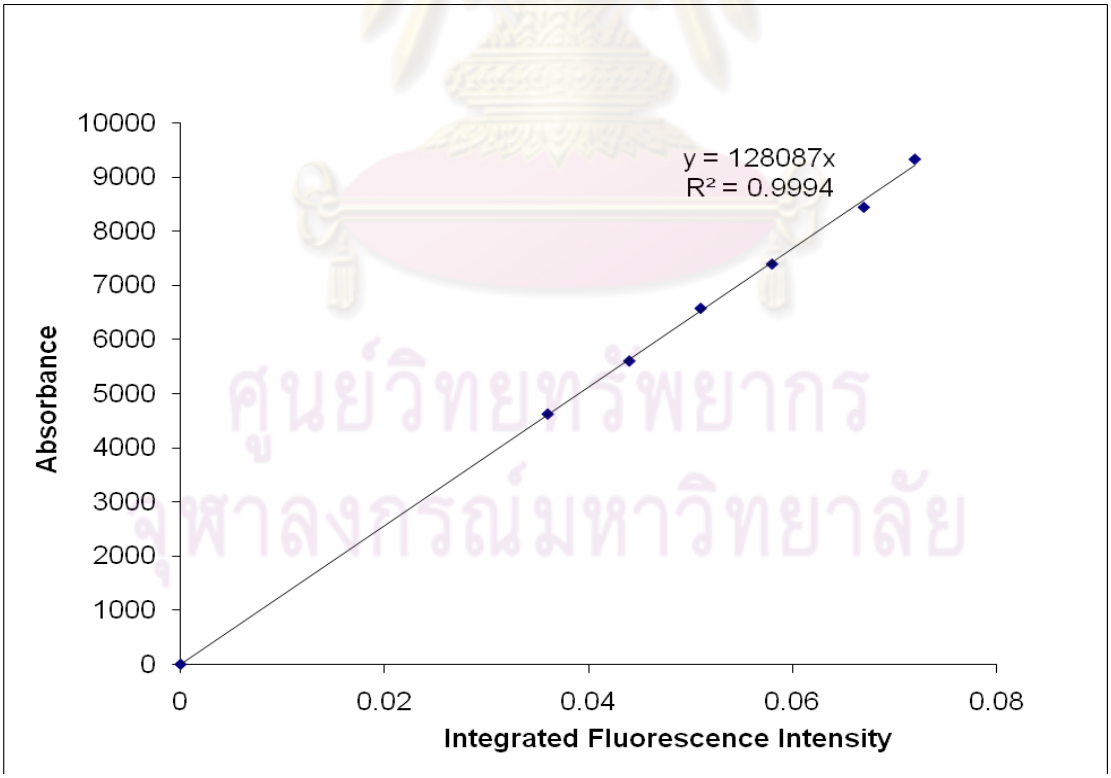

Figure A14 The linear plot between integrated fluorescence intensity (arbitrary units) and absorbance for **curcumin** in EtOH

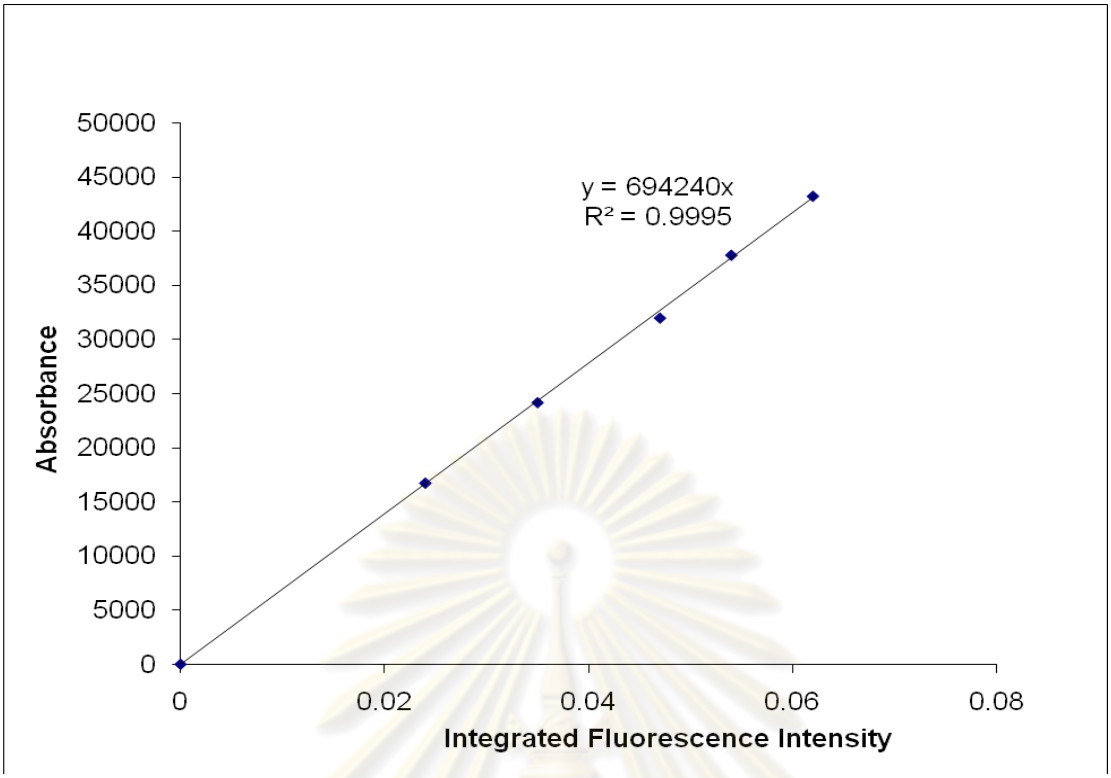

Figure A15 The linear plot between integrated fluorescence intensity (arbitrary units) and absorbance for **curcumin** in CH_3Cl

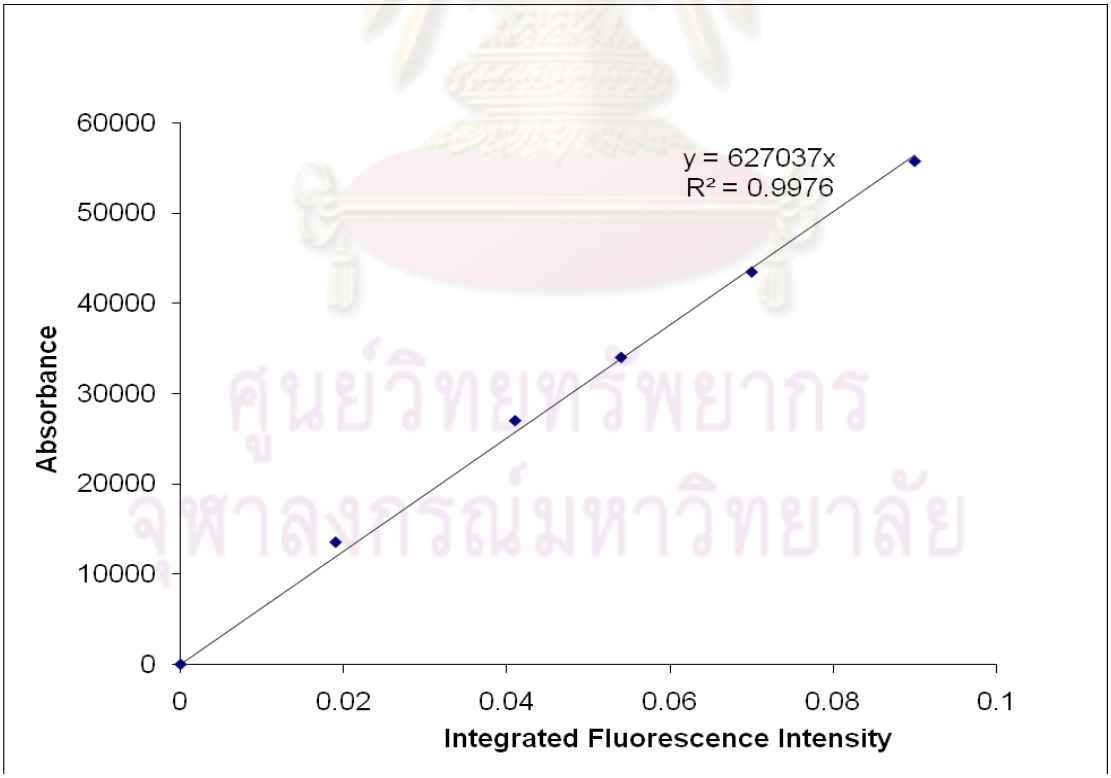

Figure A16 The linear plot between integrated fluorescence intensity (arbitrary units) and absorbance for **curcumin** in toluene

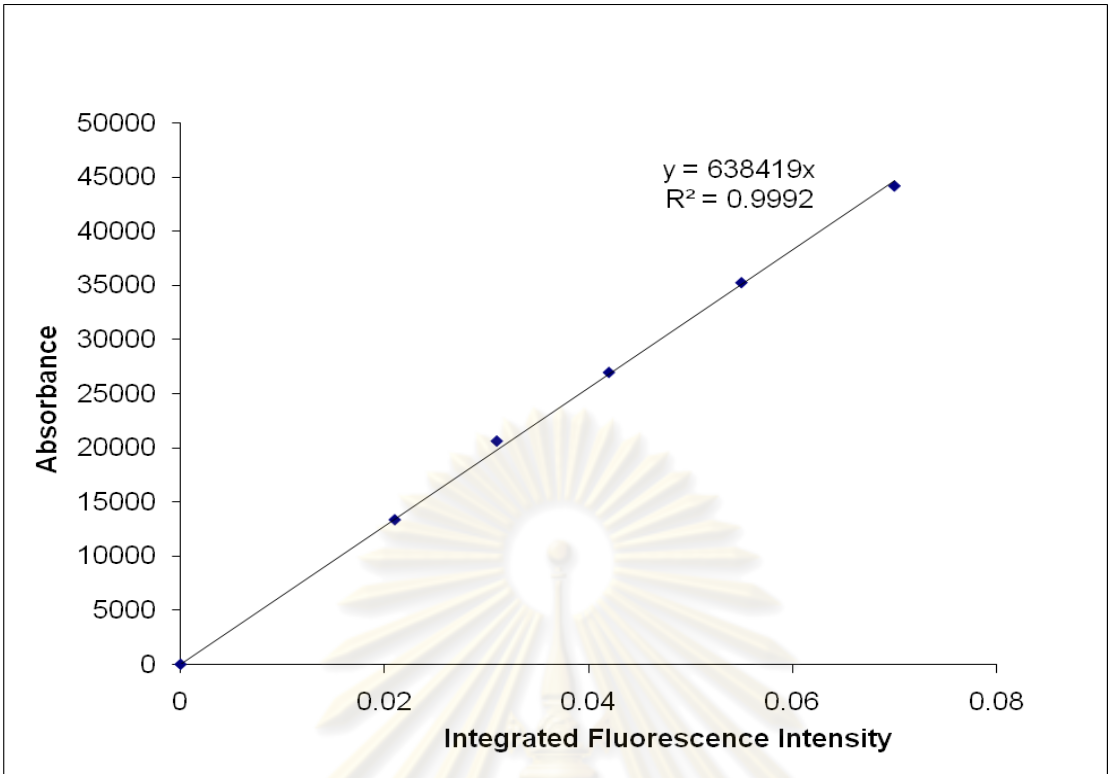

Figure A17 The linear plot between integrated fluorescence intensity (arbitrary units) and absorbance for **curcumin** in benzene

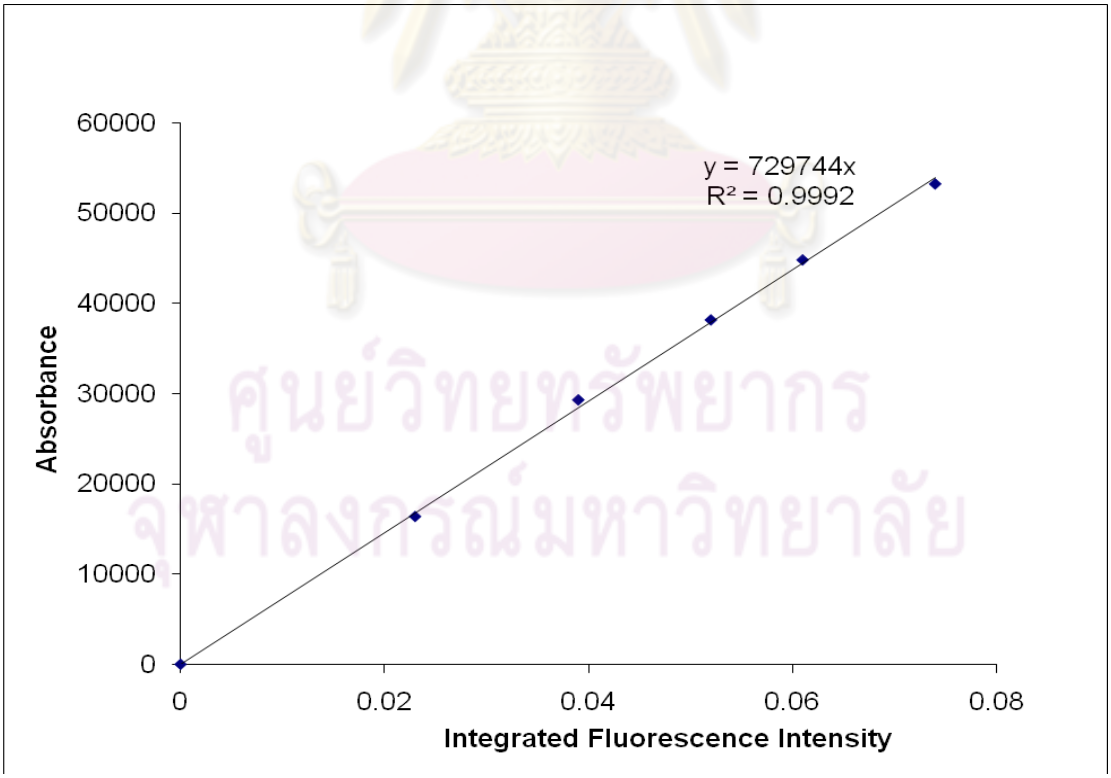

Figure A18 The linear plot between integrated fluorescence intensity (arbitrary units) and absorbance for **curcumin** in diethyl ether

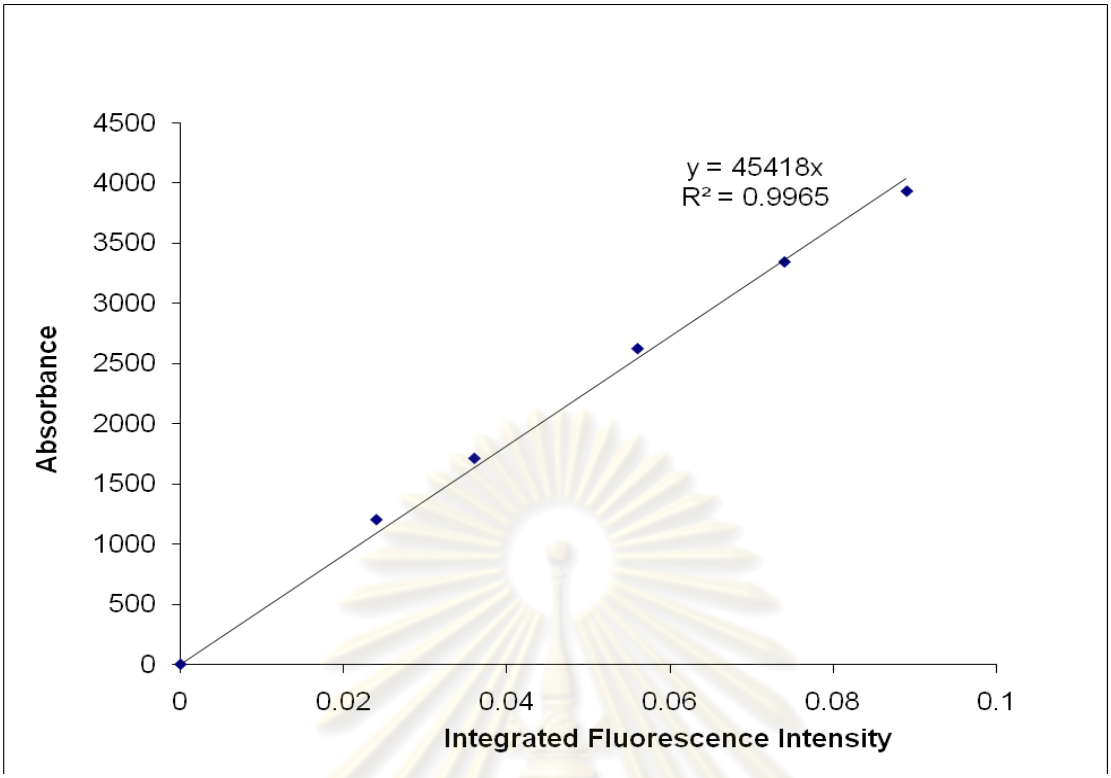

Figure A19 The linear plot between integrated fluorescence intensity (arbitrary units) and absorbance for **curcumin** in DMSO

VITA

Mister Anusak Chaicham was born on October 30, 1983 in Chaiyaphum, Thailand. He graduated with a high school diploma from Phukhieo, Chaiyaphum in 2001.He received his Bachelor's degree of Science in Chemistry from Khonkean University in 2005. Since 2006, he has been a graduate student at the Department of Chemistry, Chulalongkorn University and become a member of the Supramolecular Chemistry Research Unit under supervision of Assistant Professor Dr. Boosayarat Tomapatanaget. He finished his Master's degree of Science in the academic year 2009.